V. AIR QUALITY AND DEPOSITION

A. BACKGROUND ON MONITORING EFFORTS

The Shenandoah National Park (SHEN) air quality monitoring and research program has acquired information about key air pollutants that can degrade visibility, injure or impact growth and vitality of plant species sensitive to ground-level (tropospheric) ozone (O_3), acidify streams, impact aquatic biota, leach nutrients from soils, erode buildings and materials, or harm human health. Table V-1 summarizes the park's comprehensive visibility, ambient air quality, and deposition monitoring and research program.

Table V-1. Visibility, air quality and atmospheric deposition monitoring at SHEN.

Monitoring Parameter	Program	Location	Years
Visibility/Particulate Matter			
Teleradiometer and manual 35mm camera	National Park Service (NPS)	Loft Mountain (Rocky Mountain Vista)	1980-1986
Automatic 35 mm camera	NPS	Pinnacles (Laird's Knob Vista)	1986-1991
Transmissometer	Interagency Monitoring of Protected Visual Environments (IMPROVE)	Big Meadows	1987-1991
Transmissometer – Long	IMPROVE	Big Meadows	1991-present
Nephelometer	IMPROVE Research	Big Meadows	1991 summer
Nephelometer	IMPROVE Research	Big Meadows	1992 (July-Aug)
Nephelometer	IMPROVE	Big Meadows	1996-present
Time-lapse 8mm camera	NPS	Skyland (WNW Vista)	1991-1992
Automatic 35 mm camera	IMPROVE	Skyland (WNW Vista)	1991-1995
Automatic 35 mm camera and 8mm camera	IMPROVE	Dickey Ridge (SW Vista)	1991
Particulate Matter (PM_{10} & $PM_{2.5}$) – Stacked Filter Unit	IMPROVE	Big Meadows	1982-1987
Particulate Matter (PM_{10} & $PM_{2.5}$)	IMPROVE	Big Meadows	1988-1999
Particulate Matter (PM_{10} & $PM_{2.5}$) - Version II Sampler	IMPROVE	Big Meadows	2000-present
Ammonium	IMPROVE Research	Big Meadows	1997-present
Visibility Study – additional IMPROVE sampler, Ammonia & Ammonium	IMPROVE Research	Big Meadows	1991 (summer)
Comparison Study – additional IMPROVE sampler	IMPROVE Research	Big Meadows	1996 (summer)

Table V-1. Continued.

Monitoring Parameter	Program	Location	Years
Mass-Independent Sulfur Isotopic Compositions in Sulfate Aerosols	Special Research	Big Meadows	2001
Monitor and study aerosol optical properties	Aerosol Robotic Network	Big Meadows	2001-present
Ambient Air Quality			
Ozone	NPS	Big Meadows	1983-present
Ozone – Passive Samplers	NPS Research	Big Meadows	1995
Ozone, Sulfur Dioxide	NPS	Dickey Ridge	1983-1994 (summers)
Ozone	NPS	Sawmill Run	1983-1994 (summers)
Sulfur Dioxide	NPS	Sawmill Run	1984-1994 (summers)
Meteorology	NPS	Big Meadows	1988-present
Meteorology	NPS	Sawmill Run	1987-1994 (summers)
Meteorology	NPS	Dickey Ridge	1989-1994 (summers)
Low Level Sulfur Dioxide, Carbon Monoxide	Enhanced Ozone Monitoring Research	Big Meadows	1995-present
Volatile Organic Compounds, Nitrogen Oxides	Enhanced Ozone Monitoring Research	Big Meadows	1995-2000
Atmospheric Chlorofluorocarbons	US Geological Survey (USGS) Groundwater Studies	Big Meadows	1996-present
Volatile Organic Compounds, ozone, meteorology	Environmental Protection Agency (EPA) Funded Research	Big Meadows, Loft Mountain, Hogback Mountain	1998-1999
Ultraviolet Radiation	Park Research and Intensive Monitoring Network	Big Meadows	1997-present
Atmospheric Deposition			
Wet Acid Deposition	National Atmospheric Deposition Program	Big Meadows	1981-present
Wet Acid Deposition	University of Virginia	North Fork Dry Run (Pinnacles)	1986-present
Wet Acid Deposition	University of Virginia	White Oak Run	1980-present
Wet Acid Deposition	USGS	Weakley Hollow	1982-present
Dry Acid Deposition, Nitric Acid, Sulfate, Nitrate, Sulfur Dioxide	Clean Air Status and Trends Network	Big Meadows	1988-present
Cloud Chemistry	Cloud Water Project	Loft Mounain	1984-1985
Cloud Chemistry	EPA Mountain Cloud Chemistry Program	North Fork Dry Run Watershed – 3 locations	1986-1988
Cloud Chemistry	Shenandoah Cloud and Photochemistry Experiment	Pinnacles	1990
Mercury in Precipitation	Mercury Deposition Network	Big Meadows	2002-present
Precipitation Sulfur Isotopes	USGS Groundwater Studies	Big Meadows	1989-present

The purpose of this chapter is to characterize past, current, and future air quality and deposition within SHEN. Natural background conditions are estimated for O_3, visibility, and deposition of sulfur (S) and nitrogen (N). Current conditions and recent trends are summarized. Finally, modeled future changes in air quality and deposition are presented in response to each of the emissions control scenarios described in Section IV.

B. ESTIMATED NATURAL CONDITIONS

1. Ground-level Ozone

There are factors not controlled or influenced by human activity that contribute to a variable background concentration of ground-level O_3. There are also some O_3-enhancing human activities that are generally not considered subject to control. Thus, there may be both a "natural" background and a "practical" background level of O_3. Examples of indirect influences include hemispheric very-long-range transport of O_3 or its precursors, changes in land use, and changes in vegetation. There is some indication that O_3 background concentrations may have increased from near 5 to 10 ppb (parts per billion) in the nineteenth century (Beck and Grennfelt 1994, Kasibhatla et al. 1996) to an estimated 20 to 45 ppb during summer in the United States today (Fiore et al. 2002). Increases of a few ppb have likely occurred over the United States during the past two decades (Oltmans et al. 1998, Lin et al. 2000).

The spatial and temporal distribution of background O_3 varies with season, climate, landmass, elevation, vegetation, and latitude. Annual variation in O_3 concentration, with a maximum in spring, is the natural expected pattern. Only locations remote from anthropogenic emissions sources still exhibit this pattern. Continental areas are well known to have higher background O_3 than remote oceanic areas. This is partly due to deeper convective activity over the landmasses which transport stratospheric and lightning-produced O_3 from above the boundary layer down to the surface. The large amount of thunderstorm activity along the equator produces O_3 that is transported progressively towards the poles. Higher elevation sites are more likely to have higher background O_3 because they are more frequently above the surface mixing layer and are more likely to intercept free-tropospheric air that contains stratospheric O_3 and lightning-produced O_3. Thus, location will also affect the expected background.

Four techniques have been used to estimate background O_3 from observed data. Each is described below.

a. Average Observed Ground-level Ozone Concentrations at Remote Locations

The remote mid-latitude Atlantic Ocean has average O_3 concentrations of 15- 25 ppb (Ray et al. 1990, Kasibhatla et al. 1996). Especially in the summer, meteorology in the eastern United States is dominated by a circular flow around the Bermuda High that carries Atlantic air masses over the continent. This low background is sometimes observed in Florida and along the southeastern coastline, and SHEN is influenced by this oceanic flow periodically. An extreme case was observed during hurricane Hugo when O_3 concentrations of 19 ppb were observed at Big Meadows (Doddridge et al. 1991)

Aircraft and surface measurements indicate an average O_3 concentration from 5 to 20 ppb over the Pacific Ocean (Oltmans, et al. 1998). Measured concentrations at western coastal sites subject to clean air inflows from the ocean have been 10-20 ppb at Olympic NP and 21-23 ppb at Redwoods NP (Altshuller and Lefohn 1996).

Measurements from long-term National Oceanic and Atmospheric Administration (NOAA) monitoring stations located at high elevation and often influenced by free tropospheric air have mean annual O_3 values of 35-42 ppb at Whiteface Mountain, NY and about 40 ppb at Mauna Loa, HI. Both sites have seen small increases in O_3 since 1975 (Oltmans et al. 1998).

b. Probability Distribution Methods

The 25th percentile of the probability distribution (36 ppb) was used at Harvard Forest, MA to estimate the background O_3 level for the eastern United States, which was compared to other locations (45 ppb and 50 ppb in western Tennessee and at the Grand Canyon in Arizona, respectively; Lin et al. 2000, Fiore et al. 2002). Other percentiles could be chosen. For example, Altshuller and Lefohn (1966) summarized 10th and 30th percentile data from several inland monitoring stations (Table V-2). SHEN data for 1983-1990 are given in the table for comparison, as reported in the National Park Service (NPS) Quick Look Report, Volume II (Joseph and Flores 1993) for the 10th and 25th percentiles. There appears to be an elevational gradient in O_3 concentration in the park, based on results from the three monitoring sites. The 25th percentile values for background O_3 of 26 to 39 ppb were within the ranges for other remote locations and the Harvard Forest site.

Table V-2. Values for the 10th and 30th percentile O_3 measurements at remote inland locations compared with generally comparable data from SHEN.

Location	State	10th Percentile	30th Percentile
Badlands NP[a]	SD	20	24
Yellowstone NP[a]	WY	18	28
Theodore-Roosevelt NP[a]	ND	19	27
Great Sand Dunes NP[a]	CO	30	37
Arches NP[a]	UT	26	33
Montgomery Co.[a]	AR	5	15
		10th Percentile	25th Percentile
SHEN - Big Meadows [b]	VA	30	39
SHEN - Dickey Ridge[b]	VA	28	37
SHEN - Sawmill Run [b]	VA	17	26

[a] Altshuller and Lefohn (1966)

[b] Joseph and Flores (1993). Measurement elevations were: Big Meadows, 1074 m; Dickey Ridge, 610 m; and Sawmill Run, 445 m

c. Correlation Methods with Ground-level Ozone Precursors

Regression models for O_3 vs $[NO_y - NO_x]$ provide a useful context for the question of background O_3 concentration. The regression intercept provides an estimate of the background O_3 concentration because at zero nitrogen oxide (NO_x) concentration the photochemical formation of O_3 would cease. Using this approach, 1995 data from Harvard Forest suggested background O_3 of 30 ppb (Fiore et al. 2002). Typical values from Harvard Forest were 20 to 40 ppb for background O_3 (Hirsch et al. 1996). For a location in Giles County, TN, 110 km SSW of Nashville, a summer 1991 study estimated a background of 36 to 42 ppb (Olszyna et al. 1994).

Detailed studies of O_3 and reactive oxides of N (NO_y) have been conducted at Big Meadows in SHEN (Hallock-Waters 2000). A background intercept of 39 ppb was found for three years of O_3 and NO_y data, although it must be noted that the slope and correlation varied strongly by season. The summertime intercept estimate of background O_3 was about 20 ppb. This may reflect cleaner air from the Atlantic Ocean region that is carried in by the flow around the

Bermuda High that develops each summer. Back trajectory analysis indicated that highest O_3 values at SHEN occur when air flow is from the west and northwest. A weighted climatological average based on air flow would define the annual average background.

d. Computer Simulation Modeling

Ozone production in the North American boundary layer includes about 50% surface afternoon O_3. Most of the remainder is from tropospheric production outside the region. Stratospheric injection is not believed to contribute more than 2 ppb to the background. Mean summer afternoon O_3 concentrations derived from transportation from outside the boundary layer were estimated to range from 15 to 35 ppb, with the highest values in the western United States. The higher background in the West can be explained by the higher average O_3 lifetime of three to five days in the West as compared with less than two days in the East. The West also has a higher mixing layer (2 km) and lower average O_3 deposition (0.4 cm/sec) than the East (Fiore et al. 2002).

In a modeling study, Jacob et al. (1993) estimated that background North American O_3 concentration was regulated by horizontal transport and deposition and ranged from 30 to 40 ppb. For much of the eastern United States, the estimated background was 35 to 40 ppb. About half of the average summertime O_3 concentration at the surface over the continental United States was estimated to be background O_3 originating from outside the continent.

In summary, the background O_3 concentration is not known with a high degree of certainty, partly because of different ways of defining it and partly because it is not a measurable condition. Human activities now influence O_3 concentration throughout the Northern Hemisphere. Changes not normally associated with air pollution, such as widespread agriculture and landscape vegetation changes, have also altered the natural components of the background O_3. The O_3 background concentration over the eastern United States likely ranges from approximately 20 to 40 ppb.

2. Visibility

As was discussed in Section III.F, there are natural causes for visibility degradation. For example:

- The scattering of light by oxygen (O) and N molecules in the air limits visibility and causes the sky to appear blue.

- Particles associated with natural processes (e.g., biogenic emissions, volcanic activity, oceanic hazes, or windblown dust) can become suspended in the air, thus causing visibility impairment.

- If suspended particles are hygroscopic, their effect on visibility will be exacerbated by high relative humidity.

A simplified, general approach was used to establish a benchmark of natural visibility conditions for assessing current visibility conditions and trends throughout the United States and more specifically within SHEN. The approach relied on estimates of the natural concentrations of particulate matter that are known to contribute to visibility impairment and the calculated contribution to light extinction that can be attributed to these assumed background concentrations.

The estimates of annual average concentrations for natural levels presented in Table V-3 for the key particulate species were adapted from Trijonis (1990) and the U.S. EPA guidance document on estimating natural conditions (U.S. EPA 2001b). The calculated contribution to visibility degradation of each of these key species is based on the Interagency Monitoring of Protected Visual Environments Program (IMPROVE) algorithm (Appendix B) which applies the dry extinction efficiencies and appropriate adjustment for relative humidity to these

Table V-3. Estimated natural background particulate concentrations and light extinction.

	Annual Average Mass Concentrations (mg/m^3)		Dry Extinction Efficiencies (m^2/gm)	Estimated Average Annual Natural Conditions (Mm^{-1})	
	East	West		East	West
Fine Particles					
Ammonium Sulfate	0.23	0.11	3.0	2.83	0.73
Organic Material	1.4	0.47	4.0	5.60	1.88
Light-absorbing Carbon	0.02	0.02	10.0	0.20	0.20
Ammonium Nitrate	0.1	0.1	3.0	1.23	0.66
Soil	0.5	0.5	1.0	0.50	0.50
Coarse Mass	3.0	3.0	0.6	1.80	1.80
Clear Sky (Rayleigh)				10.00	10.00
Light Extinction Coefficient (Haziness)				22.2 (8.0 dv)	15.8 (4.6 dv)
Visual Range				176 km (109 miles)	248 km (154 miles)
Relative Humidity Factors				4.1 (87%RH)	2.2 (70%RH)

concentrations, to calculate the total light extinction due to assumed natural conditions. For concentrations, to calculate the total light extinction due to assumed natural conditions. For illustrative purposes, nominal relative humidity adjustments for the eastern and western United States of 4.1 and 2.2, respectively (Malm 2000), have been applied to give a rough comparison of the two geographical areas.

These estimates are generally accepted as reasonable first approximations to annual average background conditions. They are, however, rough estimates and could easily be off by a factor of two or more. The estimates are summarized graphically in Figure V-1. In the East, natural visual range is estimated to be 176 km (109 mi) whereas in the West it is 248 km (154 mi). Under natural conditions, carbon (C)-based particles are responsible for most of the non-Rayleigh visibility reduction, with all other particle species contributing significantly less. Clear sky scatter (Rayleigh) is the largest contributing factor to the reduction of visual range, at about 45% in the East.

Estimates have also been derived for the distribution of natural conditions at SHEN (U.S. EPA 2001b). The estimated average natural background standard visual range at SHEN is ~184 km (~115 mi) (U.S. EPA 2001b). The standard visual range is estimated to be ~270 km (~170 mi) for the best natural conditions (mean of the 20% best days) and ~125 km (~78 mi) for the mean of the worst 20% days. The corresponding light extinction values under natural conditions are 21.2, 14.5, and 31.2 Mm^{-1}, respectively; and the corresponding haziness values under natural conditions are 7.5, 3.7, and 11.4 dv, respectively.

3. Deposition

Historical levels of S and N deposition prior to about 1980 in and near SHEN are not well known. However, Shannon (1998) provided estimates of historical deposition during the period 1900 to 1990 at SHEN, as part of the Southern Appalachian Mountains Initiative (SAMI) assessment (Sullivan et al. 2002a). These estimates (Table V-4) were based on historical emissions data and were constructed with the Advanced Statistical Trajectory Regional Air Pollution (ASTRAP) model (Shannon 1981, 1985), including wet, dry, and cloud forms of deposition. Estimates of pre-industrial (i.e., pre-1850) deposition of S and N are not available, but are assumed to have been substantially lower than Shannon's (1998) estimates for 1900.

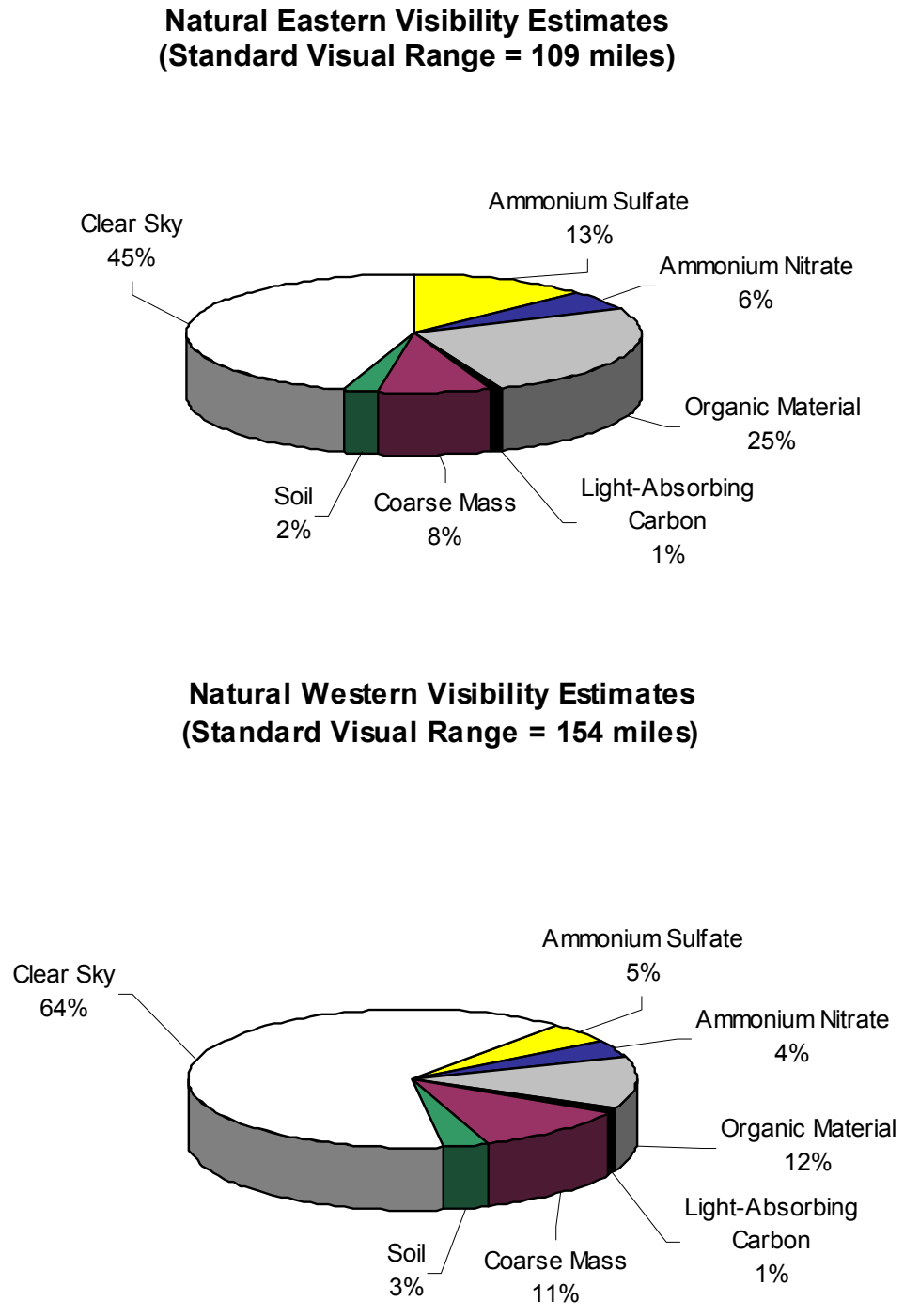

Figure V-1. Estimated natural background particle contributions to visibility reduction in the eastern and western United States.

Table V-4. Estimates of historical deposition in SHEN of sulfur and oxidized nitrogen at five year intervals, normalized to 1990 and expressed as a percentage of the 1990 values (Shannon 1998).

	S Deposition (Percent of 1990 Value)[a]				Nitrate-N Deposition (Percent of 1990 Value)[a]			
Year	Wet	Dry	Cloud	Total	Wet	Dry	Cloud	Total
1900	30	33	42	34	14	14	13	14
1905	42	47	60	47	18	18	18	18
1910	52	58	75	59	22	24	24	23
1915	62	69	90	70	25	27	28	26
1920	66	73	98	75	27	29	30	28
1925	72	79	106	81	36	36	35	36
1930	65	72	98	74	40	38	37	39
1935	53	58	82	60	32	31	30	31
1940	64	69	97	72	36	36	37	36
1945	83	90	132	96	48	46	48	48
1950	78	83	126	90	53	52	54	53
1955	78	83	114	87	60	60	61	61
1960	87	90	125	96	71	70	72	71
1965	92	102	102	96	79	78	72	77
1970	113	121	116	116	92	90	84	90
1975	116	118	102	113	98	94	86	94
1980	104	104	90	100	102	97	90	97
1985	97	96	86	95	97	96	96	97
1990	100	100	100	100	100	100	100	100

[a] For reference, five-year average values, centered on 1990, of total deposition of S and N were 13 and 7.6 kg/ha/yr, respectively

C. CURRENT CONDITIONS AND TRENDS

1. Air Quality

a. Ambient Conditions

The NPS maintains a network of O_3 monitors, using ultraviolet absorption photometric analyzers, at about 30 park units across the country. Monitoring has occurred in SHEN since 1983, although data collection was spotty prior to 1988. SHEN's monitoring locations are shown in Figure V-2. Two of the monitoring locations, Dickey Ridge and Sawmill Run, were closed after the 1994 O_3 season, but the Big Meadows site (U.S. EPA AIRS Site No. 51-113-0003, Madison County, Virginia) continues in operation. Meteorological parameters and O_3 measurements were collected at all three sites. Also shown in Figure V-2 are state O_3 monitoring locations near SHEN. Monitoring methods and quality assurance procedures used in the NPS monitoring network meet the applicable 40 CFR Part 58 EPA requirements, allowing

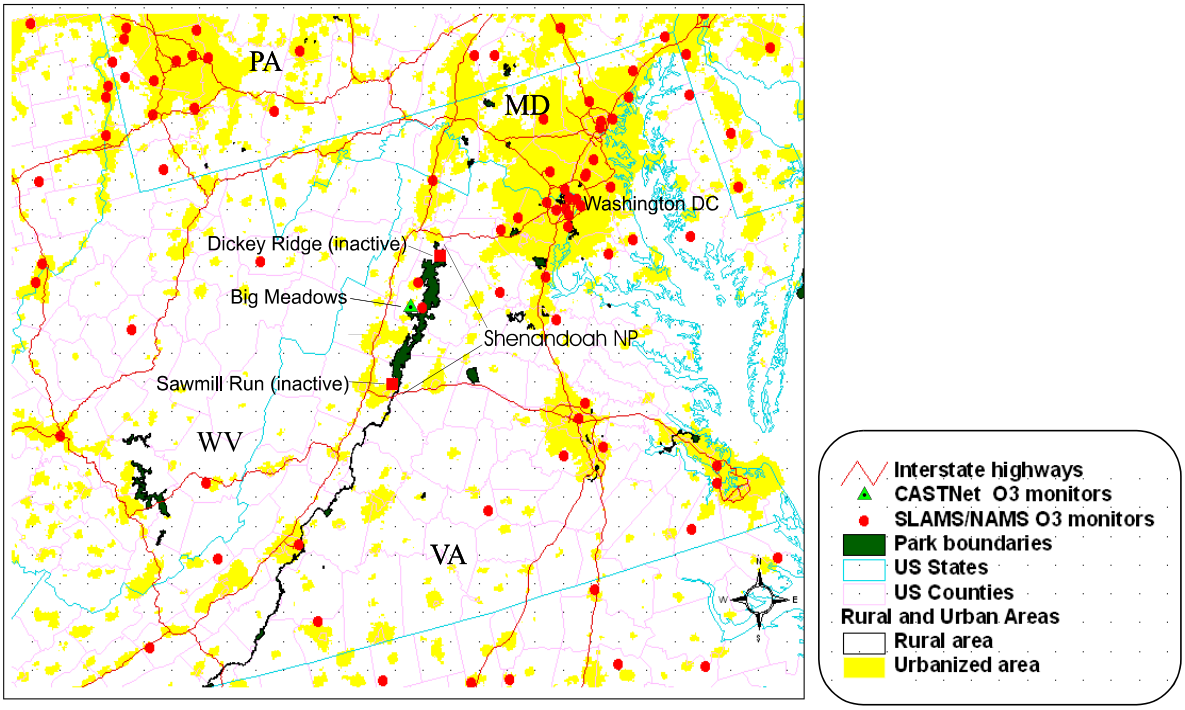

Figure V-2. Ozone monitoring locations in and near SHEN.

for the direct comparison of NPS-collected data with those collected by the EPA and state and local air pollution control agencies. Hourly average O_3 concentrations are recorded by on-site data loggers and transferred to a central database located at Air Resource Specialists, Inc., in Fort Collins, Colorado, where the data are validated.

Based on back trajectory modeling, Big Meadows is mostly removed from strong local anthropogenic sources of air pollution and is largely representative of regional O_3 levels (Poulida et al. 1991, Hallock-Waters 2000, Cooper and Moody 2000). It should be noted, however, that back trajectory models have limited capability to estimate the contributions of local sources to O_3 exposures at a given sensitive receptor (J. Moody, pers. comm., May 2003; K. Gebhart, pers. comm., April 2003). In addition to O_3, measurements of other trace gases have been made at the Big Meadows site from 1995 to 2000. These trace gases include sulfur dioxide (SO_2), carbon monoxide (CO), and NO_y. Reactive oxides of N encompass a range of compounds including NO, NO_2, NO_3, nitric acid (HNO_3), and peroxyacetylnitrate (PAN), as well as other oxides of nitrogen. Examination of the concentrations of trace gases can provide insight into the origins of these pollutants. More detailed analyses of these data can be found elsewhere (e.g., Hallock-

Waters 2000, Kang et al. 2001), so only the major conclusions from these analyses are summarized here.

High O_3 concentrations often occur during periods of warm temperatures, high atmospheric pressure, stagnant air masses, and high solar insolation. As a result, O_3 levels frequently exhibit strong seasonal trends. Two Virginia O_3 sites located outside the park in Frederick County (U.S. EPA AIRS site no. 51-069-0010) and Fauquier County (U.S. EPA AIRS site no. 51-061-0002) are included in the O_3 data analyses for illustrative purposes to compare high (SHEN-Big Meadows) and low elevation O_3 data. Figure V-3 shows the monthly maximum 1-hour O_3 concentrations measured at Big Meadows from 1995 through 1997. The higher values generally occurred in the summer season of May through September. Peak O_3 values were most often recorded in July or August. The lowest monthly maximum 1-hour concentrations generally occurred in November through January.

The three-year averages of the annual fourth-highest daily maximum 8-hour O_3 concentrations at Big Meadows, Frederick County, and Fauquier County are shown in Table V-5 and plotted in Figure V-4 for 1992-2000. Only April through October data were used to generate these averages. Three-year averages are shown for all periods that met the EPA's completeness criteria. Values not meeting the EPA standard are indicated in bold. The current primary NAAQS for O_3 provides that the fourth highest annual daily maximum 8-hour average O_3 concentration cannot exceed 0.08 ppm over three years. Thus, a site is in compliance if there are fewer than 4 days with a maximum daily 8-hour average O_3 concentration greater than, or equal to, 0.085 ppm (resulting in a rounded average of 0.08 ppm) over three years. An analysis of the monitoring data showed that the number of times that a maximum 8-hour average exceeded 0.085 ppm (85 ppb) in 1997-1999 were 6, 22, and 15, respectively. Based on this standard, Big Meadows was not in compliance during the study period. The previous primary and secondary NAAQS for O_3 was 0.125 ppm (rounded to 0.12), not to be exceeded more than once per year. Under this older standard, Big Meadows was not in compliance in 1998, but did not violate the standard in 1997, when the maximum monitored concentration was 0.104 ppm, or in 1999, when the maximum monitored concentration was 0.111 ppm. For comparison, the Fauquier County monitoring site exceeded the standard in 1993, 1999, and 2000, and the Frederick County site exceeded the standard in 1998-2000. Also shown in Table V-5 are the number of individual days at each site with a maximum 8-hour O_3 average greater than or equal to 85 ppb. At all three sites, at least one such day occurred in each year listed.

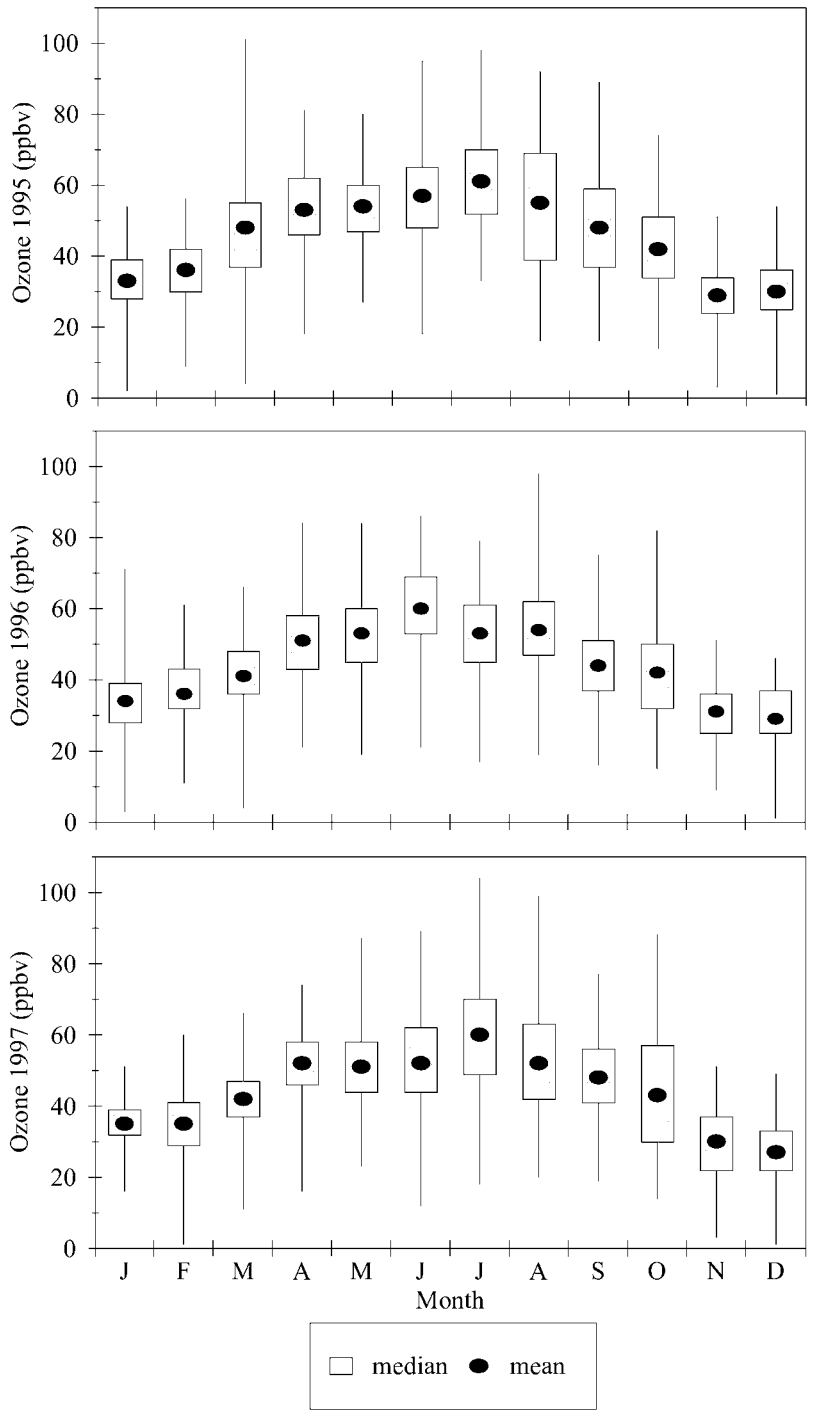

Figure V-3. Box and whisker plot showing the monthly maximum 1-hour ozone averages at Big Meadows for the period 1995 to 1997. The rectangle signifies the quartile values and the whiskers reflect the range. (Source: Hallock-Waters 2000)

Table V-5. Three-year averages of annual 4th highest daily maximum 8-hr ozone concentrations and annual exceedances. (Ozone season defined as April through October.) Values in bold exceed the level of the 1997 National Ambient Air Quality Standard for Ozone.

	SHEN--Big Meadows		Fauquier County		Frederick County	
	3-Year Average of the 4th High Daily Max 8-hr O_3 ppb [a]	Number of Days with Maximum 8-Hour Ozone Concentration ≥ 85 ppb	3-Year Average of the 4th High Daily Max 8-hr O_3 ppb [a]	Number of Days with Maximum 8-Hour Ozone Concentration ≥85 ppb	3-Year Average of the 4th High Daily Max 8-hr O_3 ppb [a]	Number of Days with Maximum 8-Hour Ozone Concentration ≥ 85 ppb
1992	b	1	84	2	c	1
1993	b	2	**85**	6	c	1
1994	81	2	82	2	80	2
1995	84	7	82	1	83	4
1996	83	1	79	2	82	1
1997	**85**	6	81	3	84	4
1998	**92**	22	84	12	**88**	10
1999	**96**	15	**88**	9	**90**	5
2000	**93**	1	**86**	1	**87**	2

[a] Year indicates the ending year of the 3-year average
[b] Did not meet EPA's completeness criteria for computing 3-year average
[c] Data collection began 1992

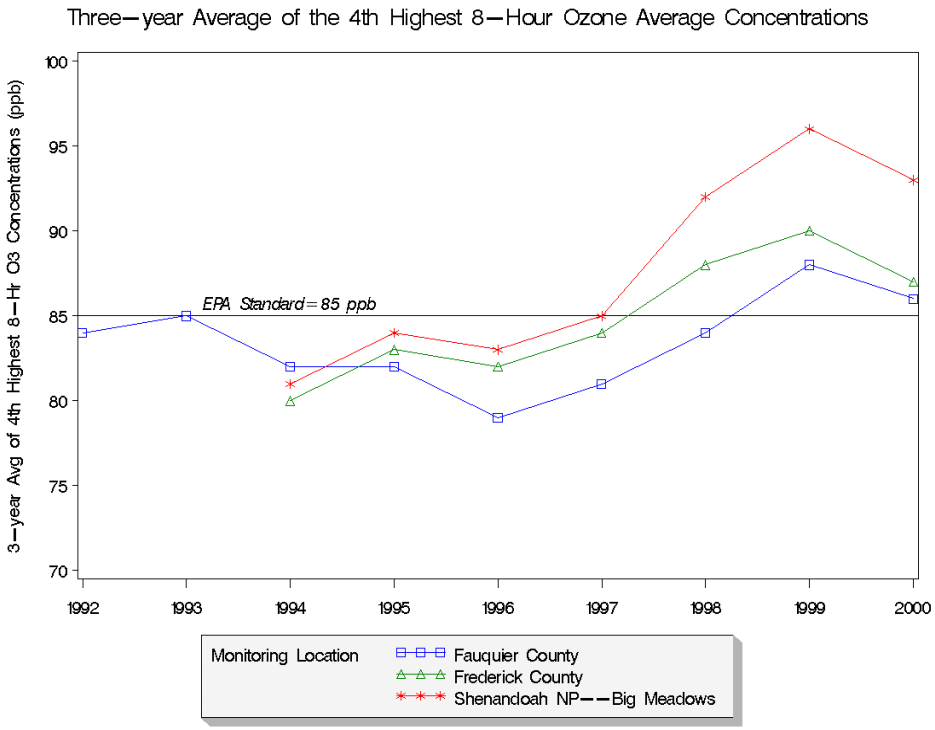

Figure V-4. Three-year average of the 4th highest 8-hour ozone average concentrations.

Urban areas typically experience strong diurnal trends in ambient O_3 concentrations. Ozone concentrations begin increasing after sunrise and peak in the late afternoon or early evening. At night, as photochemical activity ceases, O_3 reacts with fresh NO and is removed from the atmosphere. This is not the case, however, for Big Meadows. Situated at a relatively high elevation (1,073 m), it is generally above the inversion layers that trap nighttime pollution. It is also located in a rural setting and is mostly removed from strong local sources of fresh NO. As a result, removal of O_3 by NO at night does not occur to any significant degree and thus the diurnal pattern at this location does not exhibit the range of variation typical of urban areas. Figure V-5 shows hourly O_3 averages plotted against each hour of the day during each of the four seasons during the period 1995 to 1999. The mean 1-hour average varied only slightly during the course of the day. Maximum hourly values also exhibited relatively little diurnal variation, with the

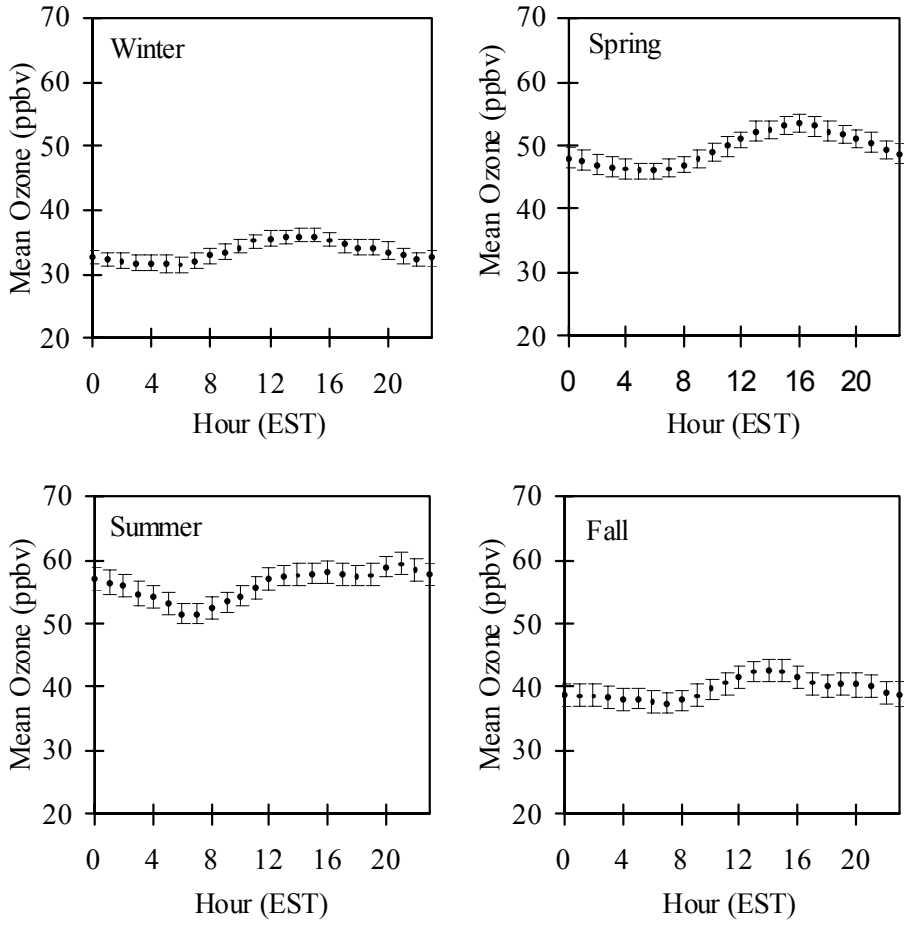

Figure V-5. Diurnal hourly ozone patterns at Big Meadows during each of the four seasons during the period 1995 to 1999. (Source: Hallock-Waters 2000)

highest values occurring during late afternoon or early evening for all seasons except summer, when the daily peak values tended to occur during evening or night time. This suggests that insufficient NO is generally available during the nighttime hours to significantly lower O_3 concentrations, or during the day to boost O_3 concentrations locally. This lack of strong diurnal variation contrasts with urban locations such as Washington, DC (Figure V-6), where peak hourly O_3 concentrations occur between noon and 1 p.m.

Table V-6 contains means, minima, and maxima of the annual May-September values of the SUM06 and W126 O_3 exposure indices, which are particularly relevant for vegetation, calculated for all three SHEN monitoring sites and the nearby monitoring sites in Frederick and Fauquier Counties. Because all O_3 values are added to the W126 index, and every O_3 value 0.06 ppm (60 ppb) and higher is added to the SUM06 index, these indices are particularly sensitive to missing data. Ozone data completeness during some years, particularly for Dickey Ridge and Sawmill Run, was less than during other years, making comparisons between years particularly difficult. For this reason, the raw index values were adjusted by dividing by the percentage of data completeness. For example, in 1991 at Dickey Ridge 76.6% of hourly values from 8 AM to 8

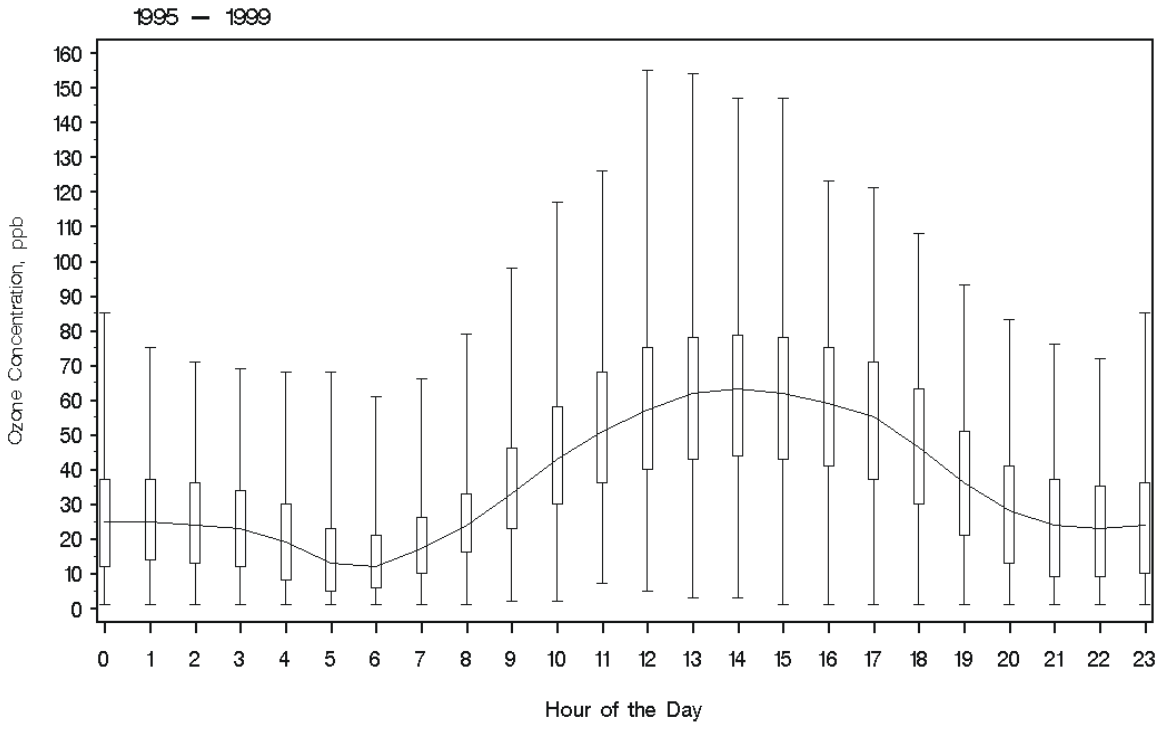

Figure V-6. May-September diurnal ozone patterns at Washington, DC for the period 1995 to 1999 (AIRS Site No. 11-001-0043). The range of concentration values is provided by hour.

Table V-6. May Through September SUM06 and W126 ozone exposure values, for the period 8AM-8PM, adjusted by percent of data completeness.

Site	May-Sep SUM06 Exposure (ppm-hr)			May-Sep W126 Exposure (ppm-hr)		
	Mean	Minimum	Maximum	Mean	Minimum	Maximum
Fauquier County 1990-2000	35.5	21.4	49.1	26.9	16.5	38.4
Frederick County 1992-2000	35.3	19.9	55.9	26.5	16.0	42.1
SHEN-Big Meadows 1990-2000	46.9	31.1	83.4	34.1	22.5	60.1
SHEN-Dickey Ridge 1989-1994	27.3	16.2	41.8	20.9	14.1	30.3
SHEN-Sawmill Run 1989-1994	25.5	13.2	36.4	20.2	11.6	28.7

PM during May through September were available, so the O_3 exposure indices were divided by 0.766. In no case was the percentage of data completeness less than 60%.

Adjusted SUM06 values from the Big Meadows, Fauquier County, and Frederick County monitoring locations are plotted in Figure V-7. The highest values generally occur at the Big Meadows site, which has the highest elevation, but all three sites follow similar patterns. Particularly noticeable is a large increase in the SUM06 index in 1998, followed in 1999 by much lower exposures, and in 2000 by the lowest values in the 11-year period. Adjusted W126 values are plotted in Figure V-8. Patterns here are similar to the SUM06 plot, and again the highest W126 exposures were recorded at Big Meadows.

b. Trends in Air Quality

The adjusted SUM06 and W126 index values were tested for trends using the method described by Theil (1950). In this analysis, slopes were first calculated between all possible pairs of points, where each point is the value of the May-September 8 AM-8 PM SUM06 or W126 exposure index in a given year. These slopes were then sorted from smallest to largest. The slope of the overall trend line was estimated to be the median of the individual slopes. The significance of the Theil slope is found by assuming that the "true" slope is zero, then calculating the probability that the estimated slope occurred by chance. The results obtained by this technique are not affected by unusually high or low values (Sisler and Malm 1998).

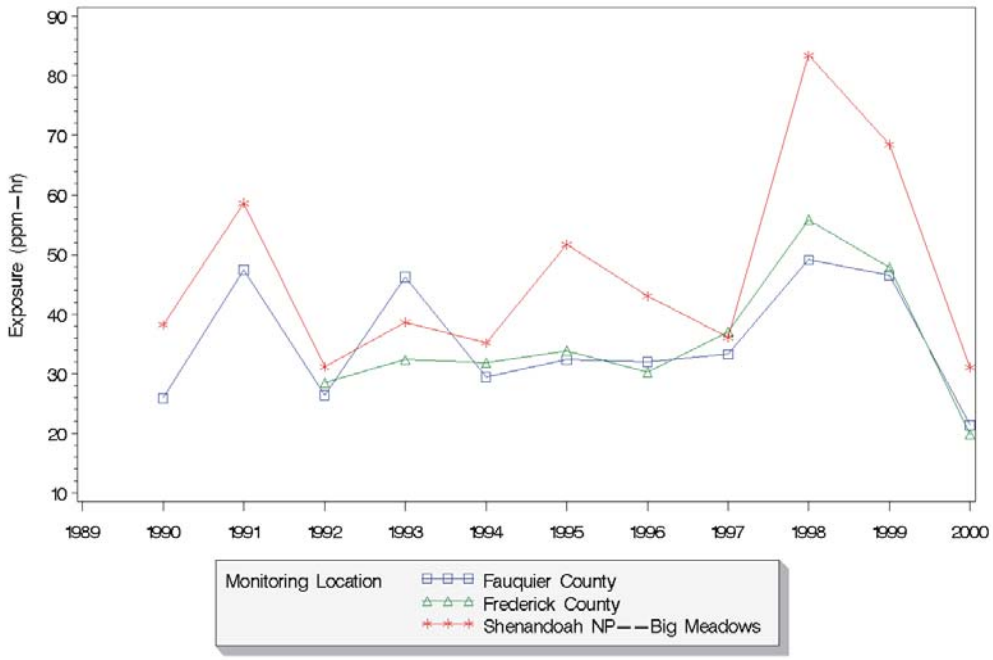

Figure V-7. Adjusted SUM06 values for Fauquier County, Frederick County, and Big Meadows monitoring sites for the period 1990 through 2000.

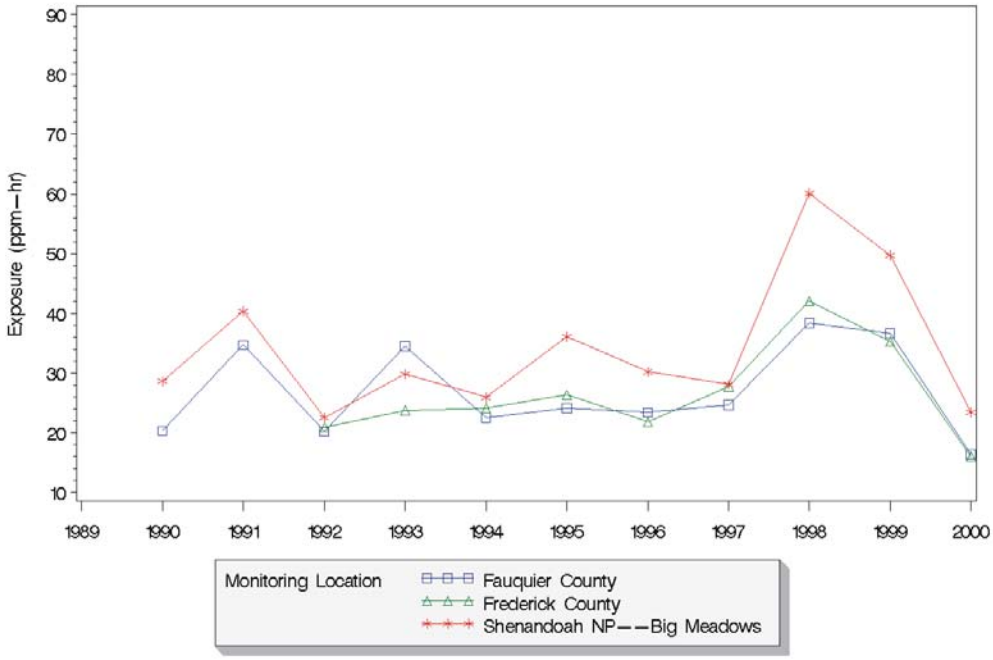

Figure V-8. Adjusted W126 values for Fauquier County, Frederick County, and Big Meadows monitoring sites for the period 1990 through 2000.

Trends in SUM06 and W126 at the Big Meadows, Frederick County, and Fauquier County monitoring sites are shown in Table V-7. Sawmill Run and Dickey Ridge are not included since they closed in 1994. Trends were calculated from 1990 (1992 for Frederick County) through 2000. A positive slope indicates increasing O_3 exposure, and thus deteriorating air quality; a negative slope indicates improving air quality. Slopes of the trend lines were all positive, but they were not statistically significant, with the exception of the Frederick County W126 index which had a positive slope of 1.29 ppm-hr/year ($p \leq 0.15$). A significance level of 0.15 is used in order to maintain consistency with NPS trend reporting under the Government Performance and Results Act (GPRA; www2.nature.nps.gov/ard/GPRA/index.html).

Table V-7. Trends in May through September (8 AM-8 PM) ozone exposure in and around SHEN during the period 1990-2000.

Site	SUM06		W126	
	Annual Slope (ppm-hr/yr)	p-value	Annual Slope (ppm-hr/yr)	p-value
SHEN--Big Meadows	+0.70	0.38	+0.74	0.32
Fauquier County	+0.68	0.27	+0.57	0.27
Frederick County	+1.56	0.18	+1.29	0.13

Trends in O_3 concentration are routinely calculated by the NPS for all of its monitoring locations for reporting under GPRA. The O_3 statistic used for this purpose is the average daily maximum 1-hour O_3 value from May through September, where each day's maximum is the maximum of all 24 1-hour values (as opposed to using only those from 8 AM to 8 PM). The resulting trends are shown in Table V-8. For purposes of GPRA reporting, a sliding ten-year window is used. The trend estimate for Big Meadows over 1991-2000 was not statistically significant ($p=0.36$). Also included in the table for comparison are the same trends for Fauquier and Frederick Counties. The slope determined for Frederick County was 0.80 ppb/yr ($p=0.13$); the slope for Fauquier County was not statistically significant.

GPRA trends for the previous 10-year sliding window are also included in the table. The period 1990-1999 was used to estimate trend, except for the Frederick County site where the period was 1992-1999. The trend estimates for this time period were statistically significant and increasing at Big Meadows and the Frederick County site ($p=0.08$ and $p=0.01$, respectively),

Table V-8. Trends in May through September daily maximum 1-hour average ozone concentration.

Site	Time Period	Average Daily Maximum	
		Annual Slope (ppb/yr)	p-value
SHEN--Big Meadows	1991-2000	+0.43	0.36
Fauquier County	1991-2000	-0.29	0.30
Frederick County	1992-2000	+0.80	0.13
SHEN--Big Meadows	1990-1999	+0.94	0.08
Fauquier County	1990-1999	+0.31	0.24
Frederick County	1992-1999	+0.99	0.01

with slopes of almost 1 ppb per year at both locations. The 1990-1999 trend estimate for Fauquier County was not statistically significant. Overall, the available data suggest that the May through September average daily maximum 1-hour average O_3 concentration appears to have been increasing at Big Meadows and Frederick County through 1999, but not at the Fauquier County site. The trend estimate was sensitive to the low O_3 in 2000 and the 10-year period of evaluation that was selected.

c. Ground-level Ozone Formation

The relationship between O_3, NO_x, and volatile organic compound (VOC) concentrations is non-linear. It is possible, depending upon the initial concentrations of these gases, that decreases in either NO_x or VOC concentrations will not decrease O_3 concentrations, and may actually increase them. Production of O_3 may be limited by the availability of either NO_x or VOCs, depending upon the NO_x to VOC ratio. Research by Hallock-Waters (2000) using 1995-1997 Big Meadows data indicated that O_3 production is NO_x-limited over SHEN during the summertime, when production of VOCs by vegetation is high, and VOC-limited during the winter. Autumn is a period of transition from NO_x-limited to VOC-limited O_3 production. These results confirm earlier modeling work by Jacob et al. (1995).

Nitrogen oxides are emitted in large quantities from anthropogenic sources such as industrial processes, coal-fired utilities, and vehicles. These emissions are generally in the form of NO, which is rapidly oxidized to NO_2. The sum of these two compounds is generally referred to as NO_x. Hallock-Waters (2000) found that NO concentrations at SHEN were generally below detection limits at night, when the lack of sunlight prevented photolysis of NO_2 to create NO.

NO concentrations were highest during the winter, when photochemical activity and O_3 concentrations were lowest. Based on the oxidation rate of NO to NO_2, Hallock-Waters (2000) concluded that most NO_x in air parcels at SHEN resulted from long-range transport.

Similarly, the NO_x/NO_y ratio is also indicative of the degree of photochemical aging experienced by an air parcel. NO_x represents the most photochemically active fraction of NO_y. For relatively fresh emissions, nearly all of the nitrogen oxides would be in the form of NO_x, since time is required for NO_x to convert to other nitrogen oxide compounds. This would result in a NO_x/NO_y ratio near one. Ratios of one were, in fact, observed at times, suggesting fresh plumes arrived on those occasions. More often, however, the ratio was much lower—around 0.25 to 0.5 in summer, and 0.45 to 0.6 in winter. This is consistent with the idea that Big Meadows is mainly removed from strong local sources of NO_x, and generally receives air parcels that have undergone photochemical processing during long-range transport before arriving at the site (Hallock-Waters 2000).

Cooper and Moody (2000) examined back trajectories for air masses arriving at Big Meadows from 1989-1994 during periods of relatively high and relatively low O_3. They found that in springtime, air masses associated with low O_3 concentrations were more likely to arrive from the north, whereas air masses associated with higher O_3 concentrations were more likely to arrive from the southwest. During the summertime, air masses associated with low O_3 concentrations were more likely to have originated to the south of Big Meadows, while air masses associated with high O_3 concentrations were most likely to have come from the west. In addition, air masses arriving at Big Meadows with high O_3 concentrations during both seasons were generally associated with high pressure systems and often descended from higher altitudes. In contrast, air masses arriving at Big Meadows with lower O_3 concentrations were generally associated with low pressure systems and approached the site from low elevations.

Sources of NO_x include both stationary and mobile sources. Sulfur dioxide and CO can be used as tracers of these sources, since stationary sources emit large quantities of SO_2 but relatively little CO, while mobile sources emit large amounts of CO but little SO_2. Stehr et al. (2000) used two approaches to examine the relationship between NO_x, CO, and SO_2 at Big Meadows. Data used in the study were collected from September through December, 1996. The first approach involved using U.S. EPA emissions data to estimate the SO_2/NO_y ratio for stationary sources and the CO/NO_y ratio for mobile sources. These ratios were used along with the measured concentrations of CO and SO_2 at Big Meadows to estimate the fraction of NO_y

attributable to mobile and point sources. The second approach used linear regression to fit the concentrations of NO_y as functions of SO_2 and CO. Both approaches yielded similar results. Based upon the results of these two analysis methods, Stehr et al. (2000) estimated that approximately 34% of NO_y at SHEN resulted from point sources. Hallock-Waters (2000) also examined the correlation between NO_y and both CO and SO_2, finding NO_y correlated reasonably well with both; this also suggested that sources of NO_y at Big Meadows include both stationary and mobile sources.

The observed O_3 concentration at Big Meadows is the result of several atmospheric processes, including horizontal transport, vertical mixing, and local O_3 production. During transport, both formation and destruction of O_3 occurs; the extent of each is dependent on the source regions and transport path. VOC and CO measurements at Big Meadows can help infer the local O_3 production component. Biogenic emissions of isoprene and other very reactive VOCs typically constitute the dominant precursors for O_3 formation in rural environments (Goldan et al. 2000). At Big Meadows, the measured biogenic fraction of VOC accounted for approximately 70% of the O_3 formation potential. However, air mass aging, dilution, and prior O_3 formation have reduced the overall anthropogenic VOC concentration to fairly low O_3 formation potential at SHEN. Based on model projections, the local production of O_3 accounts for only about 43% of the observed O_3, whereas 50% of daytime O_3 in SHEN is attributable to transport from other areas (Kang et al. 2001). Several VOCs have been measured at SHEN at concentrations greater than those often reported in urban areas. In addition, there is evidence for an anthropogenic VOC source to the southwest of the park that emits several chlorinated organics (Zika 2001).

Often overlooked in the discussion of O_3 formation is the contribution of CO, which is a precursor of relatively low reactivity, but which often occurs at high concentrations (160 to 180 ppb average during summer) compared to the other VOC species. Thus, when more reactive VOC species are not available and when O_3 formation occurs over periods of several days, the O_3 formed from CO can be important to the total observed. Overall, 29% of the variance in summer season O_3 at SHEN is associated with CO (Hallock-Waters 2000). At Big Meadows, CO has weak diurnal and weak seasonal variation. However, the O_3 to CO correlation has a seasonal variation that is positive in summer (O_3 formation) and negative in winter (O_3 destruction). Over the period from 1988 to 1997, CO concentrations were observed to decrease by 5 ppb/year (-22.9% change) at Big Meadows (Hallock-Waters et al. 1999). This is similar to

the 18.3% decrease in emissions reported by EPA for the entire United States (U.S. EPA 1998b) and the 21% decrease reported at Big Meadows in 1999. Thus, the Big Meadows site appears to be regionally representative. The fact that O_3 showed little or no statistical decrease at Big Meadows during this period, yet both CO and VOC emissions decreased in the 1995-1999 period, suggests that NO_x is more likely to be controlling in summertime O_3 events (Hallock-Waters 2000, Poulida et al. 1991).

Computer Modeling of VOC Photochemical Reactions and Ozone Formation

Computer modeling was used to assess the effects of VOC concentrations at SHEN on local production of O_3. Extensive data were collected over a five year period at SHEN (Big Meadows) and at locations in two other eastern parks (Great Smoky Mountains [GRSM] and Mammoth Cave [MACA]) that can be used for comparison and model evaluation. Observational data were compared to output from the Multiscale Air Quality Simulation Platform (MAQSIP) model, an emissions-based comprehensive Eulerian grid model (Kang et al. in review, Mathur et al. in review).

The modeling domain was chosen so as to adequately represent conditions at the three subject eastern national parks (Kang et al. 2001). The subdomain of this modeling system consisted of 35 x 43 cells using 36-km horizontal resolution. The vertical domain varied from the surface to the stratosphere and was separated into layers. Only concentration fields in the lower 12 layers nearest the surface were extracted from the model output for this evaluation. The time period chosen for the model exercise was 12:00 pm July 14 to 12:00 pm July 29, 1995, to take advantage of the greater VOC sampling frequency during that period and because photochemical activity is at a maximum in July (Kang et al. 2001). Several scenarios were run with different emissions levels to estimate the effects of emissions changes on O_3 formation. Since our primary concerns were rural areas and the characteristics of biogenic hydrocarbons, represented by isoprene, rather than anthropogenic hydrocarbons, emissions of isoprene were varied in the scenarios more than other VOCs.

The model provided an estimate of the overall O_3 production and the extent to which the observed O_3 at Big Meadows was produced locally. Input to the model included emissions inventory and meteorological data plus emissions levels of biogenic isoprenes, which were estimated using the Biogenic Emissions Inventory System (BEIS3) model. Model output was compared to measured O_3, anthropogenic VOC, and isoprene concentrations at the three parks.

The observed O_3 at Big Meadows was a combination of transported and locally-produced O_3, as described in the previous section.

The mean daily total O_3 production (P_{O3}) through photochemical reactions within the model domain is shown in Figure V-9. This parameter was evaluated as the average of hourly O_3 production from 10 AM to 5 PM for each day during the modeling period. Of the three locations, MACA consistently was simulated to have the largest P_{O3}, GRSM the least, and SHEN intermediate. Ozone production rates at SHEN and GRSM were substantially (about one-fourth) less than those in and immediately downwind of urban areas. Variations across the scenarios suggested that O_3 production is significant when total VOC levels increase up to the highest VOC level observed at MACA, but simulated O_3 production was not sensitive to VOC emissions increases at GRSM and SHEN.

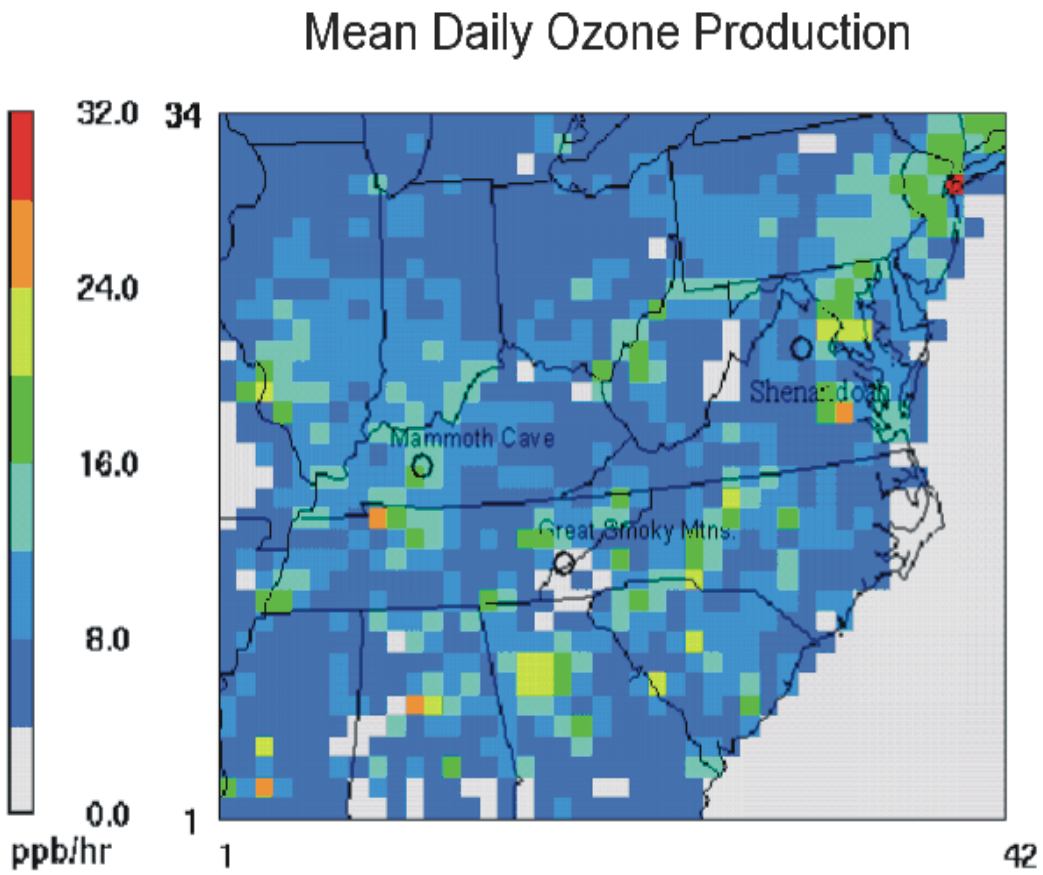

Figure V-9. Mean daily ozone production rates during the modeling period in 1995. Production rates are coded for each cell in the modeling domain. Largest production rates are near urban centers. The area around SHEN had a fairly low simulated ozone production rate.

The average simulated VOC loss (L_{VOC}) due to photochemistry during the photochemically active period of each day over the entire modeling period is presented in Figure V-10. It is interesting to note that, unlike O_3 chemistry in which MACA was always simulated to have the largest P_{O3}, the largest simulated L_{VOC} always appeared at SHEN. Reactive VOCs react not only with hydroxide (OH^-) to produce O_3, but also directly with O_3 as well. One possible explanation for the simulated higher VOC photochemistry but lower O_3 production due to photochemistry at SHEN lies in the fact that reactive VOC species (i.e., isoprene) constitute a larger share of total VOCs at this location. The reactive part of the VOCs reacts with O_3 readily, leading to O_3 removal rather than O_3 formation. Isoprene concentrations at SHEN (mean mid-day concentration: 3.36 ppbv) were much higher than those at MACA (mean mid-day concentration: 0.78 ppbv). Thus, although more VOC is undergoing reaction at SHEN, the net O_3 production is lower than at MACA.

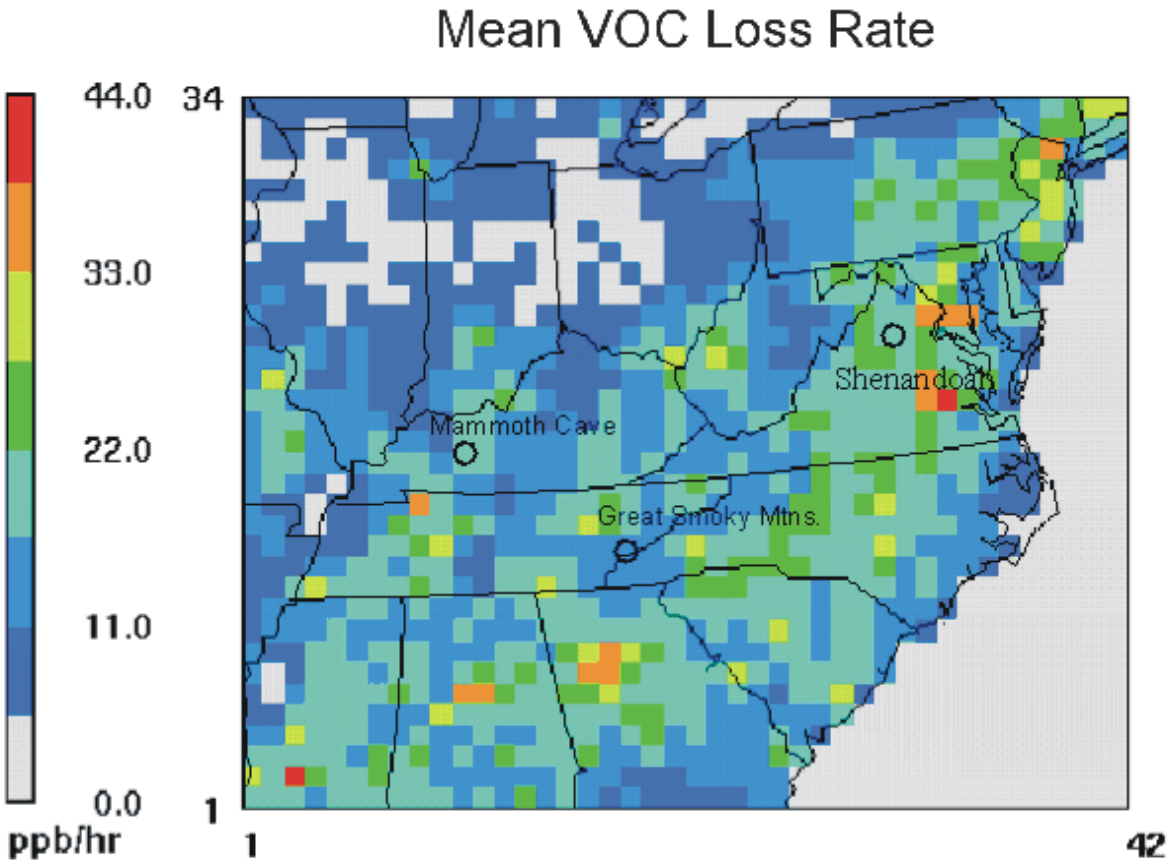

Figure V-10. Domain plot of the simulated average VOC loss (L_{VOC}) due to photochemistry.

The relationship between net O_3 production (P_{O3}) and VOC loss by reaction (L_{VOC}) at the three locations is presented in Figure V-11. Note that VOCs are consumed as O_3 is produced by the photochemical reactions. (For convenience's sake, the negative sign of the VOC chemistry term is changed to positive). Model output suggested that the consumption of VOCs contributed to an approximately linear production of O_3 at all three locations, but the actual relationship between simulated O_3 production and VOC consumption varied from location to location.

The ozone production efficiency can be expressed by the ratio of the ozone production to the VOC loss. Thus the potential for O_3 production (VPOP) is defined as:

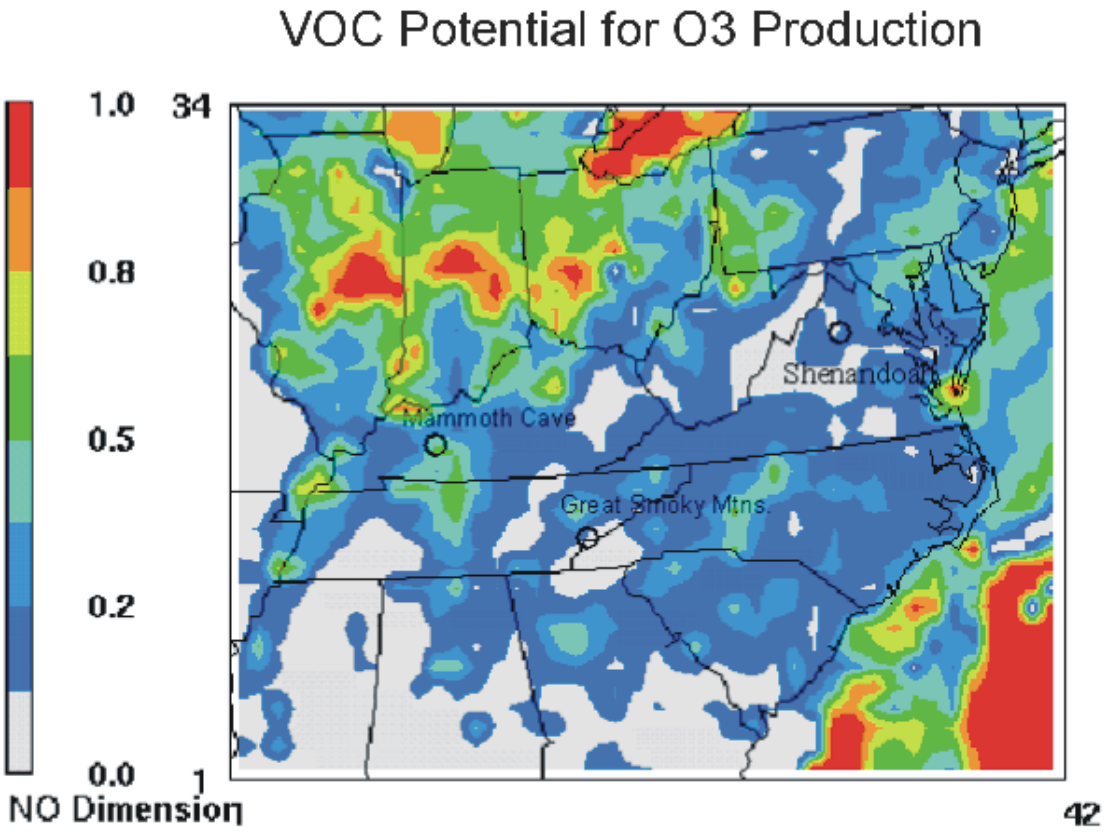

Figure V-11. Simulated values of VPOP, the O_3 production efficiency of VOC photochemistry. Areas in the Midwest were simulated to have high VPOP and therefore may be more sensitive to changes in VOC concentration. SHEN is located in a region that appears to be relatively insensitive to VOC change.

$$VPOP = \frac{d\,[O_3\ chemistry]}{d\,[VOC\ chemistry]}$$

VPOP is a measure of how much O_3 is produced per unit of VOCs consumed or, in other words, the O_3 production efficiency of VOC chemistry.

As shown in Figure V-11 for the modeling domain, the ratios (in ppbv) of O_3 production to VOC consumption, were 0.065 (GRSM), 0.11 (SHEN), and 0.36 (MACA). The model output suggested that local O_3 production from VOC photochemistry is inefficient at SHEN during summer. It is interesting to note that if VOC chemistry is set to zero, values for O_3 production due to photochemistry are similar at all three locations (3.1 to 4.4 ppbv/hr). These values may represent background O_3 production from inorganic reactions such as, for example, with CO and methane (CH_4) plus contributions from very-long range transport and from stratospheric exchange.

The sensitivity of net O_3 production to additional VOC can be expressed relative to the base scenario which was selected to represent existing conditions. If we define the maximum VOC capacity point (MVCP; the point at which any further addition of VOCs reduces O_3 concentrations) as:

$$\text{MVCP = VOC emission (kgC/km}^2\text{hr) when } \frac{d\,[O_3]}{d\,[VOC]_e} = 0$$

where $[O_3]$ is O_3 concentration, and $[VOC]_e$ is VOC emissions (kgC/km^{2}hr), then the simulated MVCPs are 1.59 (GRSM), 2.61 (MACA), and 2.02 (SHEN) kgC/km^{2}hr (Figure V-12). Both MACA and SHEN in the base scenario have not reached their MVCPs, so any additional VOC emissions at these two locations may increase O_3 concentrations. Therefore, the MVCP, combined with the emissions data, can be used as a measure to determine if a location is NO_X-limited. In older models that used O_3 isopleths, when VOC concentrations are increased within a NO_X-limited area, the O_3 concentration usually levels off, with no such capacity points as MVCP. However, at all three locations, the model results reported here suggested the existence of MVCP. This condition is expected to occur primarily during summer when biogenic organic emissions produce a local abundance of VOC in rural areas. When isoprene emissions are increased by three-fold in the model, the estimated increase in O_3 at SHEN is relatively small (0-5%). In contrast, the estimated increases at GRSM are up to 10% and at MACA up to 15%.

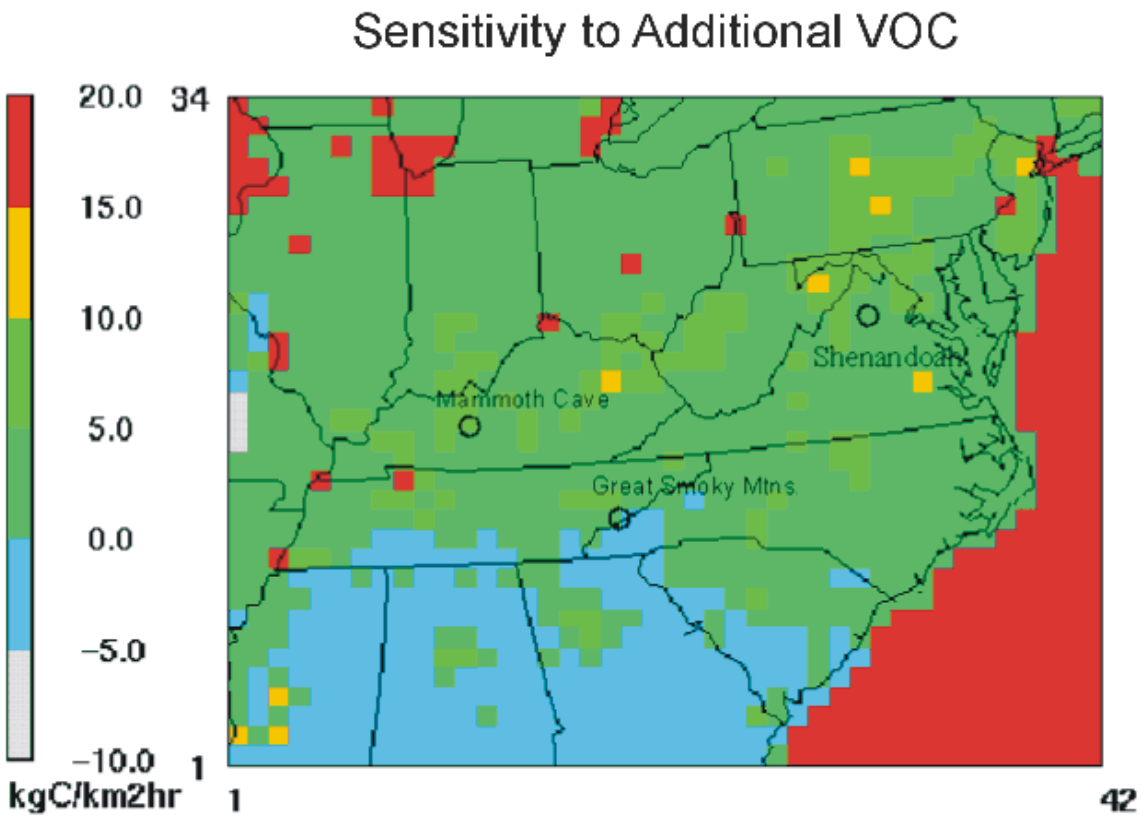

Figure V-12. Sensitivity to added VOC. Positive values suggest that with an increase of VOC emissions above the Base Scenario, O_3 concentrations will increase. Negative values suggest that the MVCP point has been reached before the emissions level for the Base Scenario, and at the Base Scenario emissions rate O_3 concentration will decrease. The MVCP points are never reached within the designed emissions perturbation scheme in the red areas.

The results of this analysis suggest that there are distinctive characteristics of O_3 distribution, transport, and production at different locations, perhaps partly in response to different elevations. At SHEN, the model output suggested that reducing anthropogenic VOC emissions will not reduce O_3 concentrations. Since transport dominates local O_3 concentrations at high-elevation sites, the most effective O_3 reduction strategy is to reduce O_3 levels in the source areas from which it is transported. The apparent existence of MVCP implies that the large amounts of reactive biogenic VOCs that are often found in densely vegetated environments during summer may help moderate local production of O_3 under NO_X-limited conditions.

2. Visibility

Visitors come to national parks in part to experience the breathtaking views of mountains, valleys, clear skies, and unique geologic features. Air pollution interferes with this experience to some degree in virtually all national parks, particularly in the eastern United States. Visibility is an especially important resource at SHEN. The Southern Appalachian National Park Committee's Report to Congress of 1924 emphasized the importance of the views from a "possible sky-line drive along the mountain top" in evaluating the suitability of the Shenandoah area for establishment of a national park. Shenandoah's Skyline Drive is on the National Register of Historic Places and features 69 historic overlooks that span the Park's 170-km length. Skyline Drive and the nearby Appalachian National Scenic Trail are designated SHEN cultural landscapes. Skyline Drive is also a designated Virginia State Scenic Highway. SHEN is one of three parks that are considered "regionally representative parks" where visibility is considered an important preservation value by the public (Chestnut and Rowe 1990). However, the views that gave the Blue Ridge its name are often obscured by human-caused haze.

The following sections describe first the current visibility conditions and recent trends throughout the United States and then the conditions and trends within SHEN. The visibility metric most often used in this discussion will be the light extinction coefficient (b_{ext}) , with parenthetical references to the corresponding visual range (VR). The reader is referred to Section III.F.1c and Appendix B for the definitions and relationships among visibility metrics.

a. National Conditions and Trends

In 1987, the IMPROVE visibility monitoring network was established as a cooperative effort between EPA, NPS, USDA Forest Service, Bureau of Land Management, U.S. Fish & Wildlife Service, NOAA, and state governments. The objectives of the network are to establish current conditions, to track progress toward the national visibility goal by documenting long-term trends, and to provide information for determining the types of pollutants and sources primarily responsible for visibility degradation.

Current National Conditions

Chemical analysis of particle measurements provides ambient concentrations and associated light extinction for PM_{10}, $PM_{2.5}$, sulfates, nitrates[1], organic and light absorbing carbon (LAC), soil, and a number of other elements. The data summaries from EPA, NPS, and IMPROVE that follow are based on data from the IMPROVE network. Figure V-13 provides a graphic view of all the IMPROVE deployed sites in operation as of December 1999 (Malm et al. 2000). The network has undergone a significant expansion in 2001 and these data will be available for future assessments.

Figure V-14 shows isopleths of current annual average visibility conditions calculated from March 1996 - February 1999 IMPROVE particle data (CIRA 2001). The same data are presented on all three maps but are represented in terms of the indices: b_{ext} (Mm^{-1}), haziness

Figure V-13. IMPROVE Monitoring Sites.

[1] In May 2001, the NPS and other participants of the IMPROVE Program identified technical concerns about measured nitrate concentrations at all IMPROVE sites prior to June 1996, and about estimates of sulfate, primarily at eastern IMPROVE sites prior to 1995. A discussion of the technical concerns can be found on the IMPROVE Web site, http://vista.cira.colostate.edu/IMPROVE/Data/QA_QC/issues.htm.

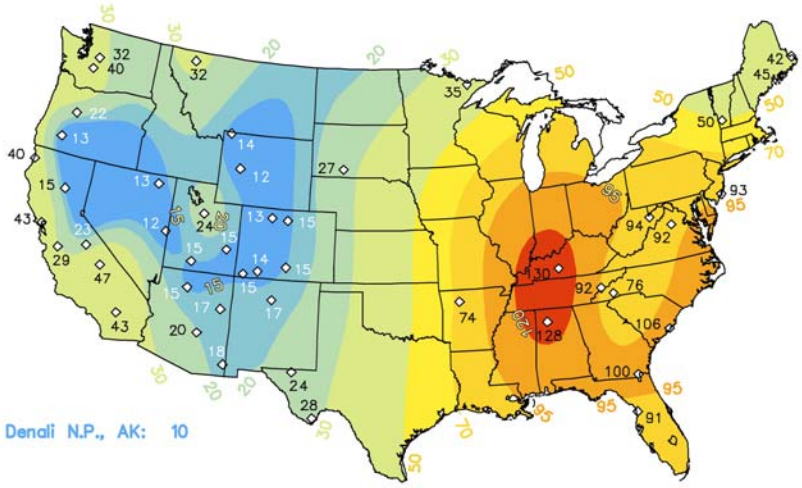

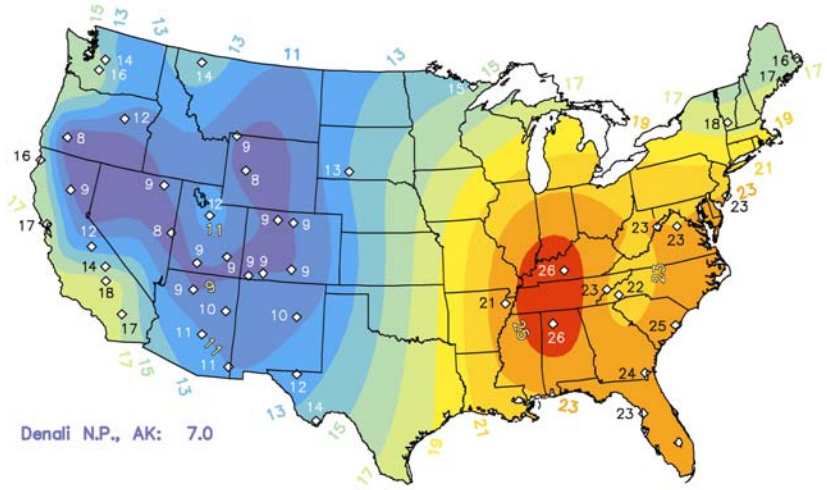

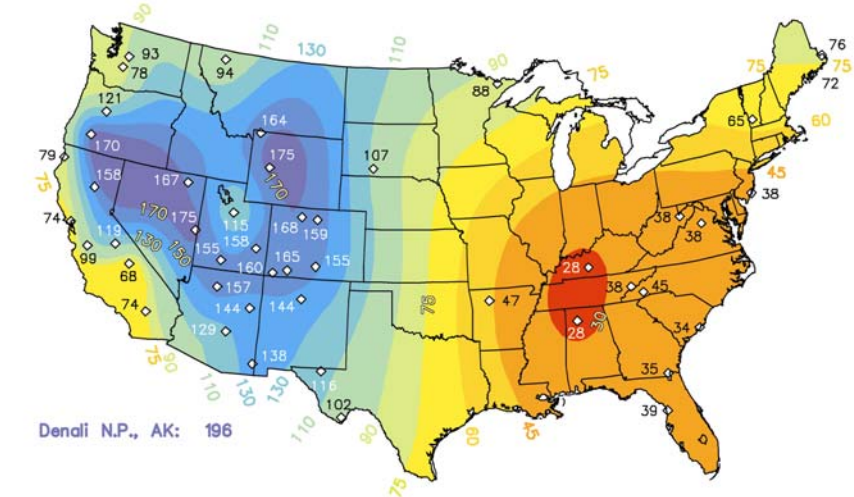

Figure V-14.

Average 3-year visibility (March 1996 - February 1999) reconstructed from IMPROVE aerosol data and represented as:

(a) Light extinction coefficient (Mm^{-1})

(b) Haziness (deciview)

(c) Standard visual range (km)

(deciview [dc]), and standard visual range (SVR; km). Because only a few IMPROVE monitoring sites exist in the eastern United States, isopleths cannot be drawn with a high degree of accuracy. The poorest visibility, highest light extinction (more than 120 Mm^{-1}, about 25 dv, or 33 km SVR) occurs in the eastern United States, whereas the best visibility, lowest light extinction (less than 22 Mm^{-1}, about 8 dv, or 178 km SVR) occurs in the Great Basin, central Rocky Mountains, and non-urban southwest. Comparison of current conditions with the natural conditions given in Section V.B (8.1 dv and 4.7 dv for the East and West, respectively) indicates a high degree of current degradation.

In order to remedy existing visibility impairment, the EPA promulgated the Regional Haze Regulations that require states to adopt plans that achieve progress toward a national goal of no human-caused impairment. The regulations specifically call for improvement of the haziest days (mean of the "worst" 20%) and no degradation of the clearest days (mean of the "best" 20%). Figures V-15a to V-15c (U.S. EPA 2001c) illustrate current levels of visibility impairment, in terms of deciviews, for the clearest, middle (typical), and haziest 20% days based on IMPROVE data from 1997-1999.

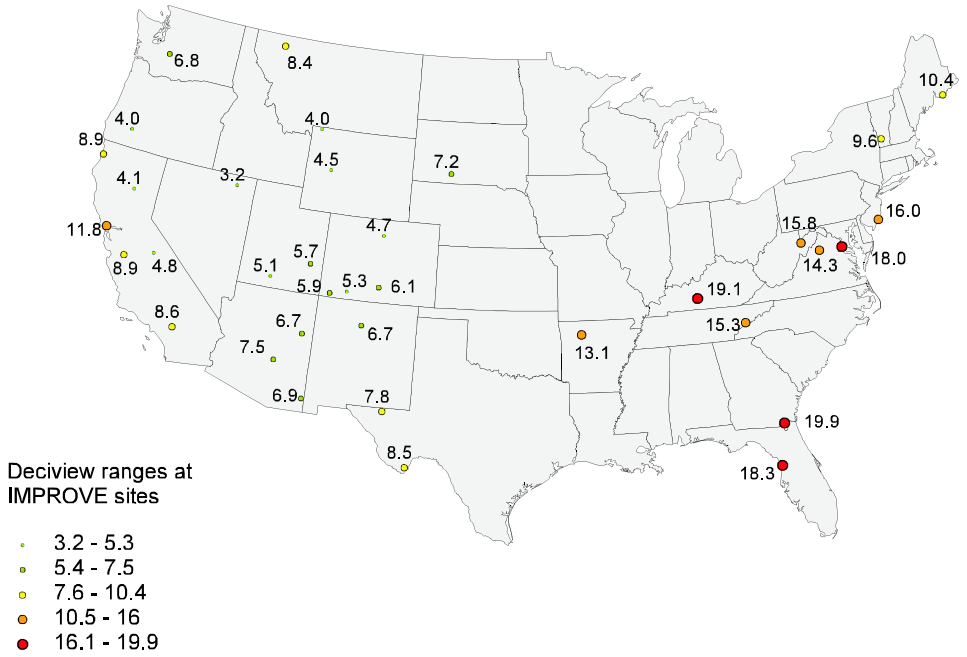

Figure V-15a. Current visibility impairment expressed in deciviews for the clearest 20 percent days based on 1997-1999 IMPROVE data.

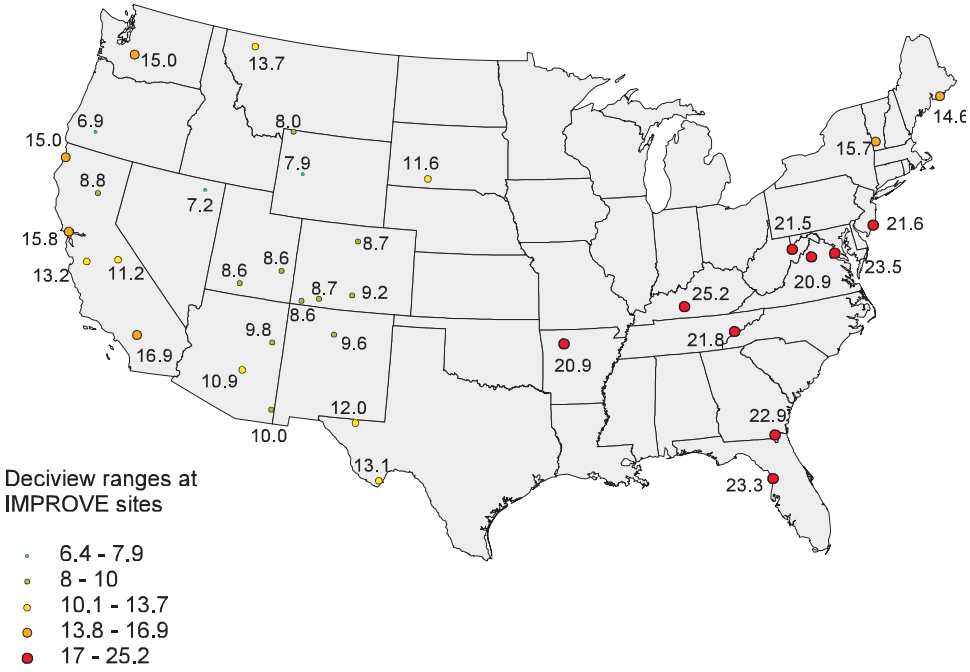

Figure V-15b. Current visibility impairment expressed in deciviews for the middle 20 percent days based on 1997-1999 IMPROVE data.

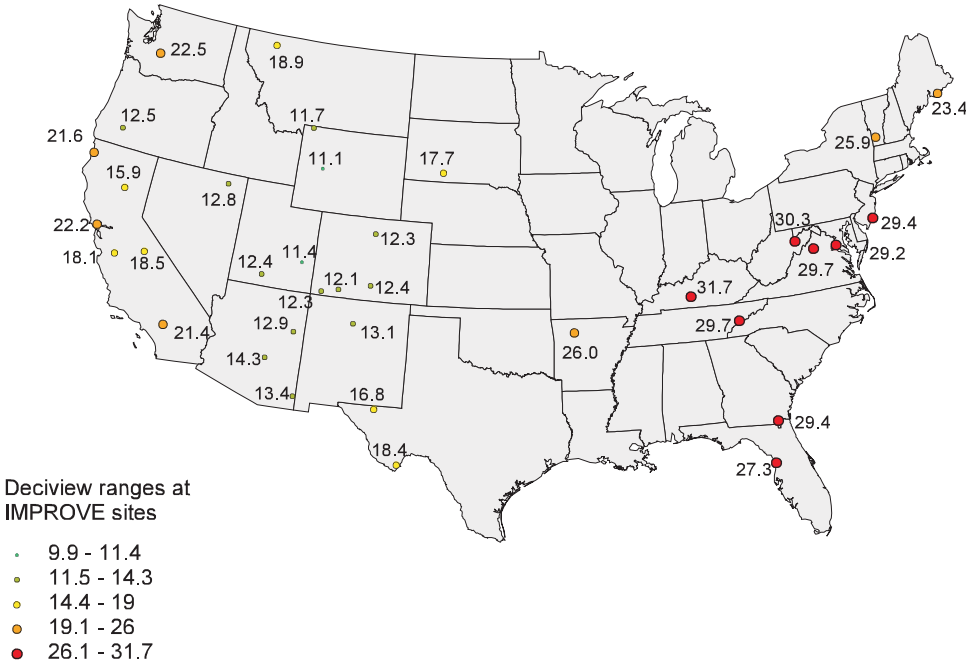

Figure V-15c. Current visibility impairment expressed in deciviews for the haziest 20 percent days based on 1997-1999 IMPROVE data.

Historical Trends

Since the late 1940s, there have been a number of particle and visibility monitoring programs implemented in the United States, most notably the National Weather Service (NWS) and IMPROVE Programs. Trends in visibility degradation can be inferred from these long-term records of visual range. Figures V-16 through V-19 describe long-term visibility degradation trends derived from such data.

Airport Observations

The isopleths of the 75th percentile visual range, shown in Figure V-16, were derived from airport data from 1950 through 1994 (Schichtel et al. 2001). Winter includes January, February, and March; spring includes April, May, and June; summer includes July, August, and September; and autumn includes October, November, and December. The reference scale

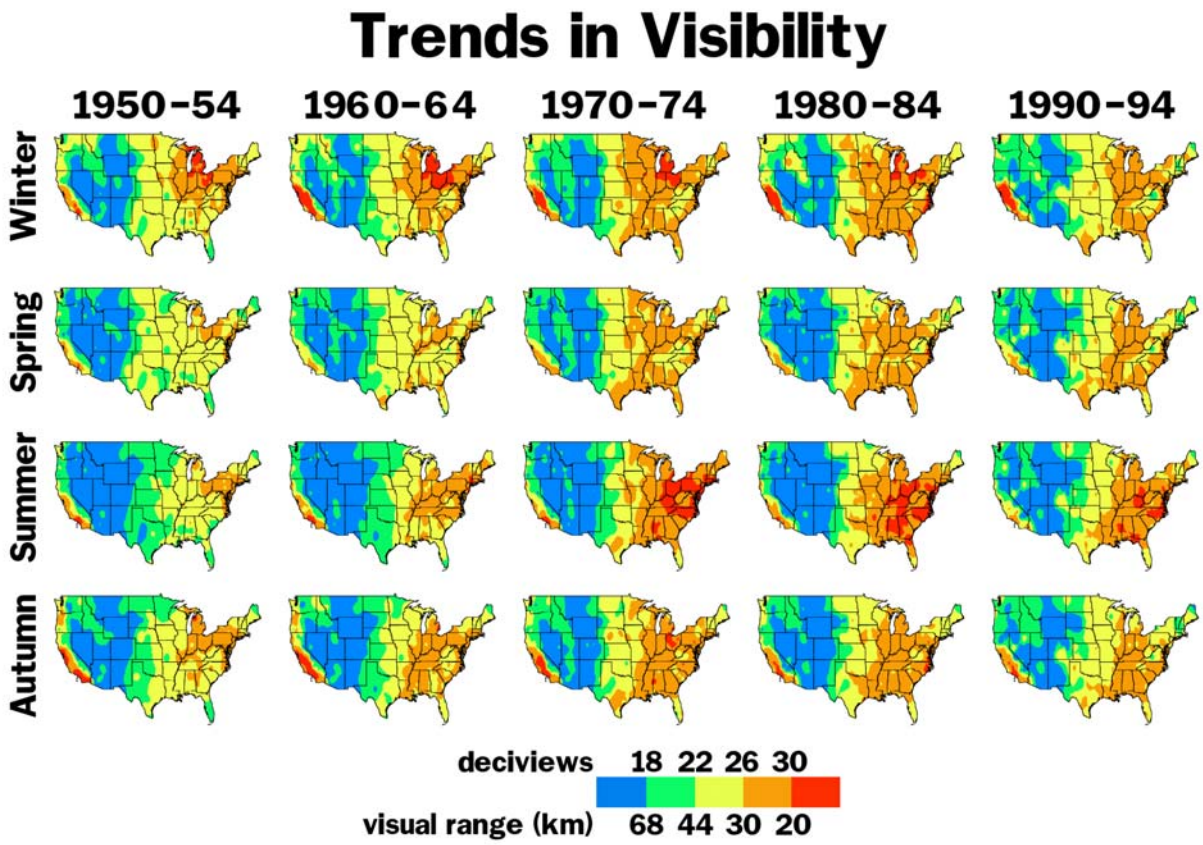

Figure V-16. Trends in 75th percentile visual range over the United States from 1950 through 1994. These data have been filtered for weather and adjusted to a relative humidity of 60% (Schichtel et al. 2001).

takes into account site-specific target considerations and human-eye sensitivity (red being worst, blue being best). The prominent nationwide features are fairly apparent. For example, visibility is generally better in the west (southern California excepted) and poorer in the East and the summer season provides the worst visibility in the East and the best in the West. Historical trends of generally decreasing visibility in the eastern portion of the country are quite evident in Figure V-16. The poorest visibility occurs in summer, and the winter months have somewhat better visibility. There have also been changes observed over time:

- In winter, there was some improvement in visibility in the north-central United States from the period 1950-54 to the period 1990-1994. However, during the 1960s and 1970s, the winter season showed decreased visibility in the Southeast.
- The spring season showed a degradation of visibility throughout the entire eastern United States, especially along the Gulf Coast and the south and central East Coast.
- In summer, a region of poor visibility in the eastern United States during 1950 to 1954 steadily expanded and became worse, until the entire eastern United States was substantially degraded. By the 1970s, summer was the haziest season in the eastern United States.
- The autumn season showed some improvement in the north central industrial areas in recent years, with little change in the remainder of the east.

IMPROVE Data

IMPROVE seasonal patterns are graphically portrayed in Figure V-17 (Malm et al. 2000). (Note that this figure includes only particle extinction and does not include the Rayleigh scattering effect.) The summer extinction coefficient is the greatest in the East, with the greatest seasonal differences also occurring in the East. In the West, the worst visibility conditions can occur in any season, and the seasonal differences are not as pronounced as they are in the East. These East-West differences are due in part to the greater pollutant emissions (particularly SO_2) and high relative humidity in the East. Annually, SO_4^{2-} species comprise over 70% of the measured visibility impacts in the East.

IMPROVE data from the 36 Class I area monitoring sites across the United States that have a minimum of 10 years of monitoring data each, were analyzed for upward and downward light extinction trends using nonparametric regression methodology (U.S. EPA 2001c). Table V-9 summarizes the trends analysis performed on these 36 sites for haziness (expressed in deciviews)

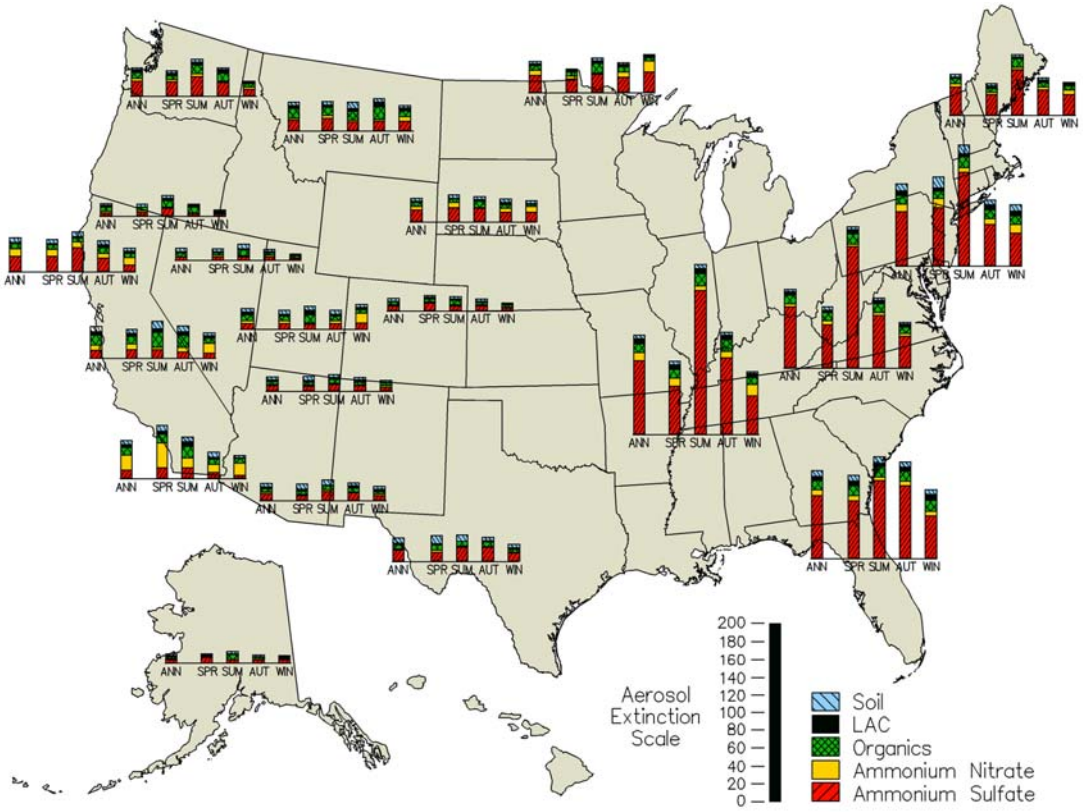

Figure V-17. Summary plot of calculated light extinction and the fractional contribution of each species for the 20 monitoring regions in the IMPROVE network (Washington, D.C. is not shown).

Table V-9. Summary of Class I area extinction trend analysis[a].

Parameter	Number of Sites With Significant[b] Upward Haziness (Deteriorating Visibility) Trends		Number of Sites With Significant[b] Downward Haziness (Improving Visibility) Trends	
	West	East	West	East
Deciviews, worst 20% [c]	4	0	1	2
Deciviews, middle 20% [c]	0	0	6	2
Deciviews, best 20% [c]	0	0	9	1
Light extinction due to sulfate, worst 20%	4	0	4	2
Light extinction due to sulfate, middle 20%	1	1	6	4
Light extinction due to sulfate, best 20%	0	1	14	0

[a] Based on a total of 36 monitored sites with at least 10 years of data in the West and eight years of data in the East: 26 sites in the West, 10 sites in the East.
[b] Statistically significant at the 5-percent level.
[c] For deciview trends changes in nitrate concentrations were not considered in the trend analysis. A constant value based on mean 1997 – 1999 extinction associated with nitrates was substituted for all years.

and light extinction due to sulfates on an area-by-area basis. Figures V-18 and V-19 graphically depict the significant trends for the Class I areas as summarized in Table V-9. A solid dot indicates the IMPROVE monitoring site location. An up-arrow indicates increasing haziness and therefore a deteriorating visibility trend, and a down-arrow indicates an improving visibility trend. The different color arrows represent the cleanest 20% of days, middle 20% of days, and haziest 20% of days. As shown in Figure V-18, several sites in the eastern United States with improving trends show improvement in more than one of the three quintiles. Figure V-19 also shows there are improving trends associated with aerosol b_{ext} due to SO_4^{2-} in the East.

b. Current Conditions and Trends in SHEN

As part of the IMPROVE monitoring network, visual air quality at SHEN has been monitored using an aerosol sampler, nephelometer, transmissometer, and camera. The aerosol sampler has operated from 1982 through the present. The IMPROVE network upgraded the

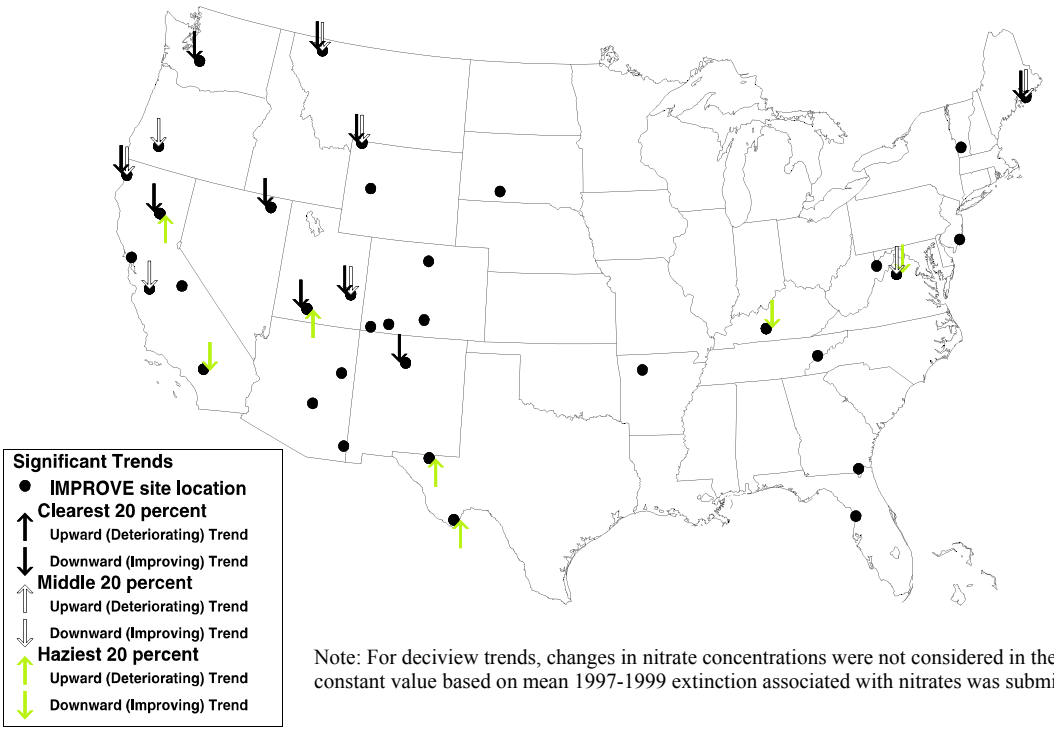

Note: For deciview trends, changes in nitrate concentrations were not considered in the trend analysis. A constant value based on mean 1997-1999 extinction associated with nitrates was submitted for all years.

Figure V-18. Class I area significant trends in haziness for the clearest 20%, middle 20%, and haziest 20% days, as summarized in Table V-9.

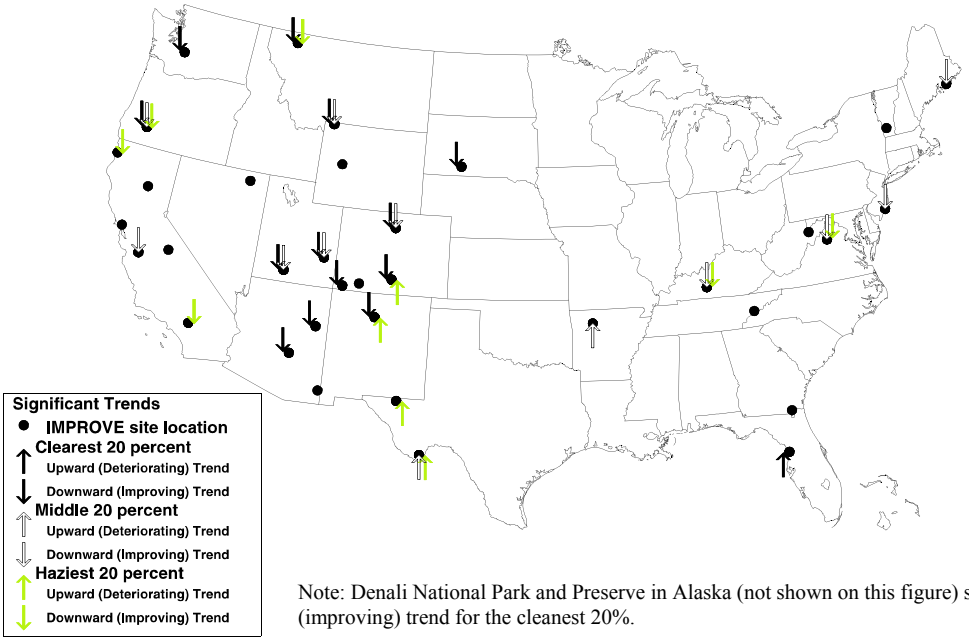

Note: Denali National Park and Preserve in Alaska (not shown on this figure) showed a downward (improving) trend for the cleanest 20%.

Figure V-19. Class I area significant trends in light extinction due to sulfate for the clearest 20%, middle 20%, and haziest 20% days as summarized in Table V-9.

SHEN sampler to an IMPROVE Version II sampler in January 2000. The transmissometer has been operating from December 1988 to the present. The nephelometer has been operating from September 1996 to the present. An automatic 35mm camera was operated at Skyland from July 1991 through April 1995, viewing west-northwest. Another automatic 35mm camera was operated at Dickey Ridge as part of an intercomparison study from July of 1991 through November 1991, viewing southwest.

Particle Monitoring

Particle data from the SHEN IMPROVE site have been summarized to characterize the full range of visibility conditions for March 1988 through February 2000, based on seasonal periods (spring: March, April, May; summer: June, July, August; autumn: September, October, November; and winter: December, January, February) and annual periods (March through February of the following year, (e.g., the annual period of 1998 includes March 1998 through February 1999).

The composition and concentration of visibility-reducing pollutants are generally quantified by aerosol sampling. Aerosol sampling provides a time-integrated (generally 24-hour average) measurement of the size, concentration, and chemical composition of visibility-related aerosols.

Prior to the calculation of multi-year average, yearly aerosol sampler data were checked for completeness using the criteria that:

- No more than nine samples in a row were missing at any time; and
- No less than 75% of all possible samples during a year had at least some data available.

SHEN data for 1995 did not meet these criteria, but because all missing data occurred in the winter, the other three seasons are displayed. No annual data are reported for this year.

Observed Concentrations

Table V-10 shows the mass concentrations ($\mu g/m^3$) of fine and coarse aerosol, and the chemical composition (mass budgets) of the fine aerosol for SHEN for the period March 1988 through February 2000. Note that these concentrations, particularly ammonium sulfate, exceed the natural conditions estimates given in Table V-3. Fine mass budgets for the mean of the cleanest, middle, and haziest 20 percent days are presented in Figure V-20.

Table V-10. Measured fine and coarse aerosol mass concentrations (in $\mu g/m^3$) for SHEN (March 1988 - February 2000).

Season	Fine Mass	Ammonium Sulfate	Ammonium Nitrate	Organics	Light Absorbing Carbon	Fine Soil	Coarse Mass
Spring	9.3	5.8	0.5	2.0	0.4	0.5	4.8
Summer	17.1	11.9	0.5	3.6	0.4	0.7	5.8
Autumn	9.9	6.2	0.5	2.3	0.4	0.4	4.9
Winter	5.7	3.1	0.5	1.5	0.3	0.2	3.0
Annual	10.5	6.8	0.5	2.4	0.4	0.5	4.7

Calculated Light Extinction Coefficients

Atmospheric b_{ext} (see Appendix B) generated from aerosol sampler data apportion the extinction at SHEN to specific aerosol species, Rayleigh scattering (the natural scattering of light by atmospheric gases), ammonium sulfate ($[NH_4]_2SO_4$) , ammonium nitrate (NH_4NO_3), organics, elemental (light absorbing) C, and coarse mass. The effects of relative humidity on extinction by $(NH_4)_2SO_4$ and NH_4NO_3 were based on monthly climatological averages. Common sources contributing to each aerosol species are as follows:

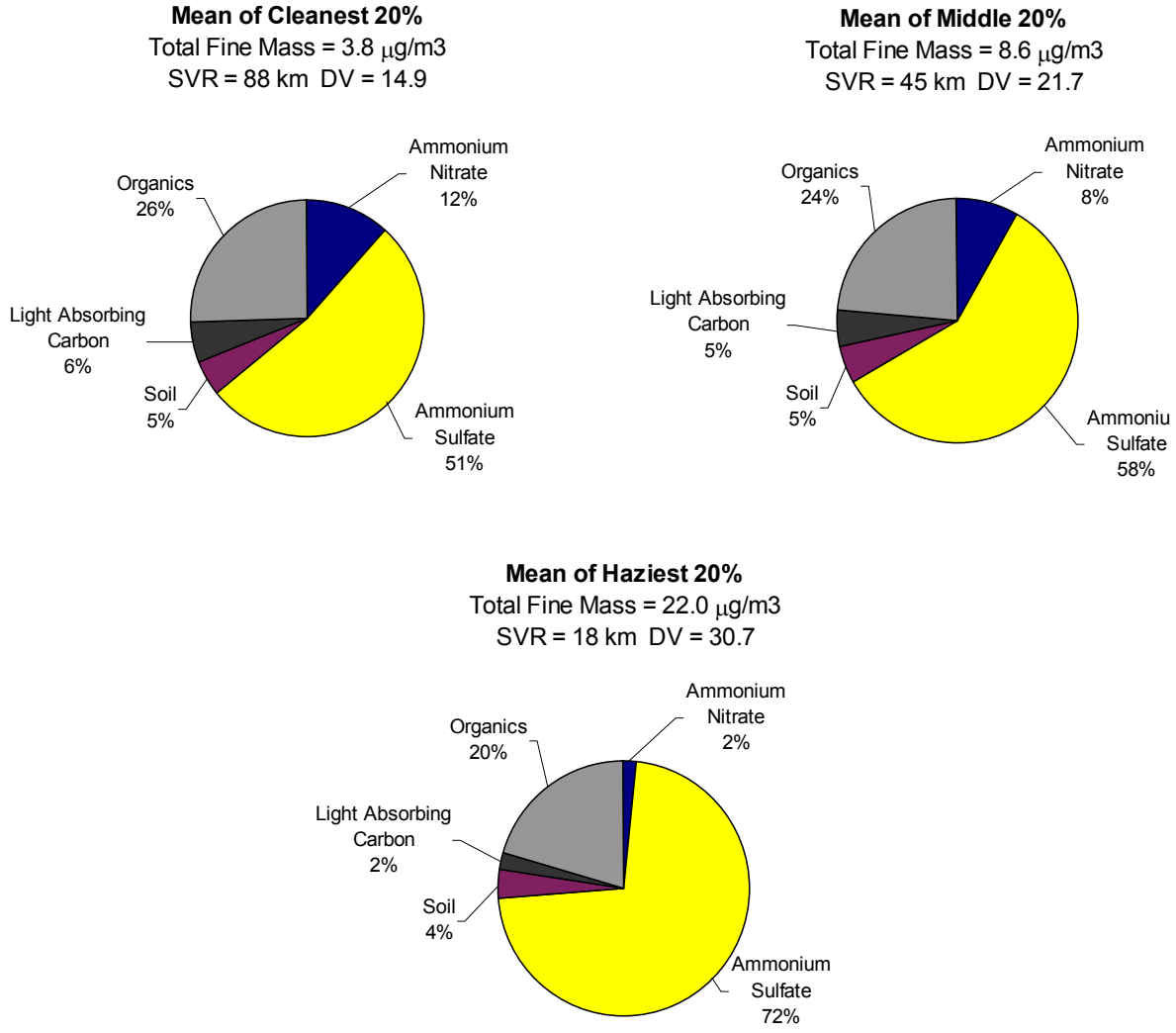

Figure V-20. Fine mass budgets (in percent) for the mean of the cleanest, middle, and haziest 20% of days for SHEN (March 1988 - February 2000). SVR refers to standard visual range and DV refers to the haziness index in deciviews.

Sulfate: Coal/oil fired power plants, refining and smelting activities;

Nitrate: Automobiles, combustion sources;

Organics: Biogenics (natural emissions), smoke, industrial solvents;

Light absorbing carbon: diesel exhaust, smoke;

Fine soil: Wind-blown dust, agricultural activities, off-road traffic;

Coarse particles: Dust, smoke, pollen.

This list is not complete and does not necessarily represent sources of pollution at SHEN. The sum of these species accounts for the majority of non-weather related visibility degradation. Figure V-21 depicts graphically the seasonal and annual variation in extinction budgets for the mean of the cleanest, middle, and haziest 20 percent. The "cleanest" and the "haziest" signify lowest fine mass concentrations and highest fine mass concentrations respectively, with "middle" representing the 20% of days with fine mass concentrations in the middle of the distribution. Each budget includes the corresponding b_{ext}, SVR, and dv. The segment at the bottom of each stacked bar in Figure V-21 represents Rayleigh scattering, which is assumed to be a constant 10 Mm^{-1} at all sites during all seasons. Higher fractions of extinction due to Rayleigh scattering indicate cleaner conditions. Comparisons of calculated extinctions for the 1988-2000 period (Figure V-21) to estimated natural conditions discussed in Section V.B.2 demonstrate that visibility in and near the park has been severely degraded. The average visual range for the cleanest days (Figure V-21) is presently about 90 km, or about 30% of what it was estimated to have been in the absence of anthropogenic air pollution (270 km). Figure V-22 further identifies average contributions of SO_4^{2-}, NO_3^-, organics, LAC, and coarse particles (including fine soil) by month for the period 1996-1998.

A tabular and graphic summary of average calculated extinction coefficient values by season and year for the March 1988 - February 2000 period are provided in Table V-11 and Figure V-23, respectively.

Trends

Data from other IMPROVE visibility sites around the country have been presented graphically (Section V.C.2.a) so that spatial, historical, and seasonal trends in visual air quality for SHEN can be understood in perspective. Figures V-20 through V-21, as well as Tables V-10 and V-11, have been provided to summarize visual air quality in SHEN during the March 1988 - February 2000 period. Seasonal variability in the mean of the haziest 20% fractions is driven primarily by $(NH_4)_2SO_4$ extinctions. Non-Rayleigh atmospheric light extinction at SHEN is largely due to organics and $(NH_4)_2SO_4$. Historically, visibility varied with patterns in weather, wind (and the effects of wind on coarse particles), and smoke from fires.

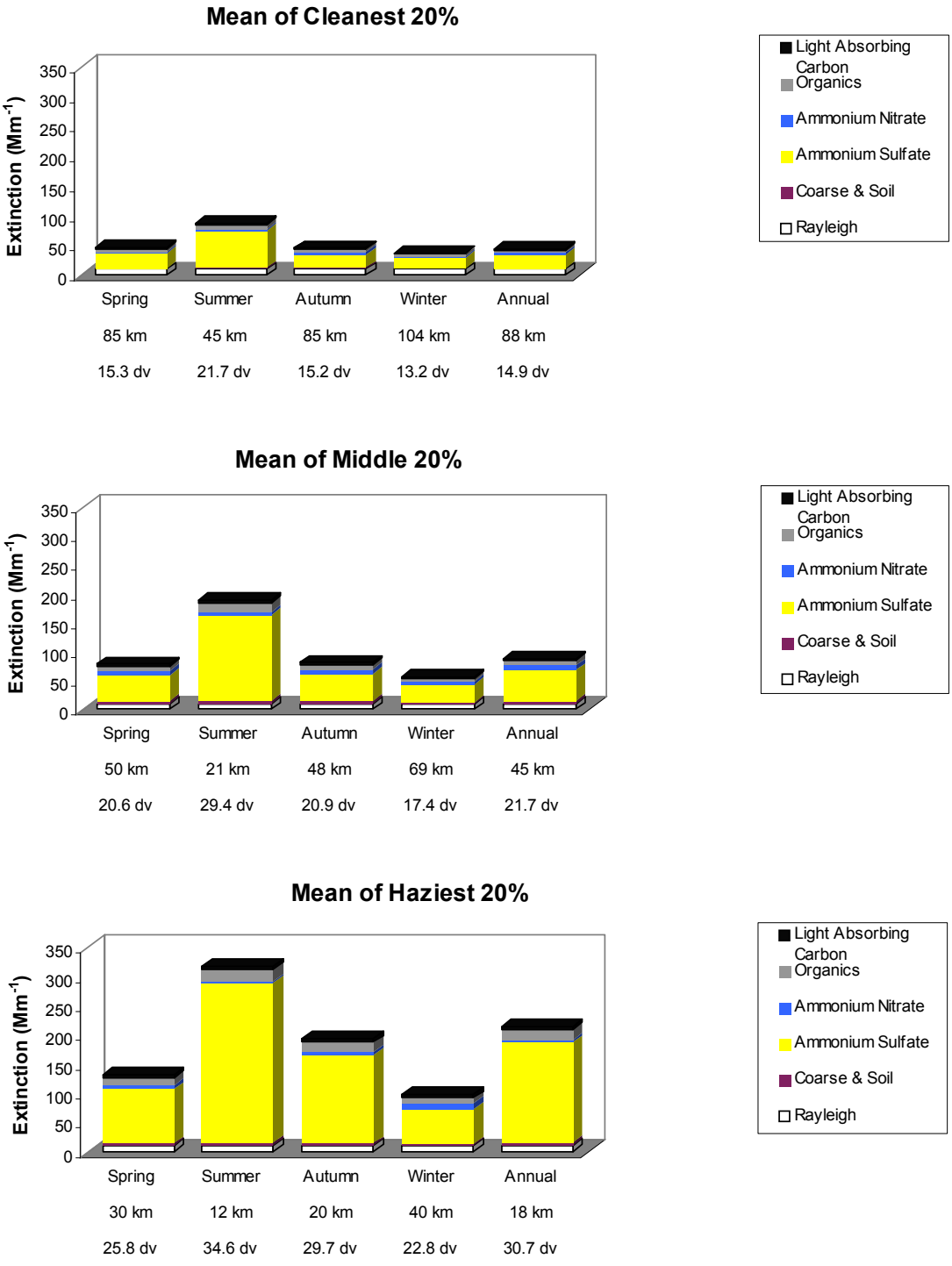

Figure V-21. Calculated extinction coefficient budgets for SHEN, March 1988-February 2000.

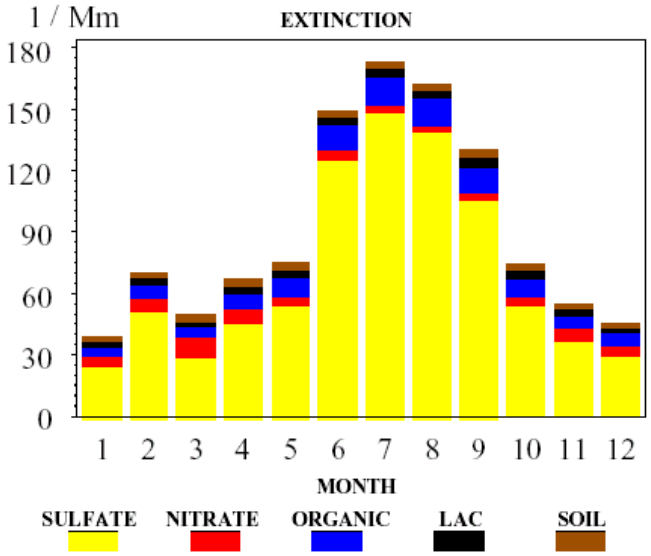

Figure V-22. Monthly contributions of total light extinction (excluding Rayleigh) contributed by sulfate, nitrate, organics, light absorbing carbon (LAC), and soil for SHEN (1996 – 1998).

Table V-11. Seasonal and annual average standard visual range (SVR; km) and calculated extinction (Mm^{-1}) at SHEN, March 1988 - February 2000.

Year	Spring (Mar, Apr, May)		Summer (Jun, Jul, Aug)		Autumn (Sep, Oct, Nov)		Winter (Dec, Jan, Feb)		Annual (Feb-Mar)[a]	
	SVR (km)	b_{ext} (Mm^{-1})	SVR (km)	b_{ext} (Mm^{-1})	SVR (km)	b_{ext} (Mm^{-1})	SVR (km)	b_{ext} (Mm^{-1})	SVR (km)	b_{ext} (Mm^{-1})
1988	40	98.1	30	132.4	39	100.7	70	56.1	39	100.2
1989	43	90.1	20	192.6	37	105.7	56	70.0	36	108.7
1990	44	88.6	19	202.2	38	104.3	67	57.9	35	110.8
1991	41	95.3	17	236.3	31	124.8	63	61.6	31	124.8
1992	45	87.5	20	199.0	36	107.5	54	72.4	34	113.7
1993	46	85.8	17	235.1	35	113.0	67	58.5	33	119.4
1994	54	73.0	17	223.9	40	98.1	75	52.0	36	108.9
1995	48	81.7	19	201.1	43	90.5	NA[c]	NA[c]	NA[c]	NA[c]
1996	54	72.3	21	181.9	46	84.7	59	66.2	40	98.0
1997	55	70.6	22	174.1	40	98.1	76	51.4	39	99.6
1998	51	76.7	23	173.0	39	101.5	63	61.7	39	101.4
1999	56	69.6	23	170.2	45	86.0	62	63.3	43	91.2
Mean[b]	47	82.4	20	193.5	39	101.2	64	61.0	36.8	107.0 [d]

[a] Annual period data represent the mean of all data for each March through February annual period.
[b] Combined season data represent the mean of all seasonal means for each season of the March 1988 through February 2000 period.
[c] Winter and annual average values are not available for 1995 because of missing data.
[d] Combined annual period data represent the mean of all combined season means.

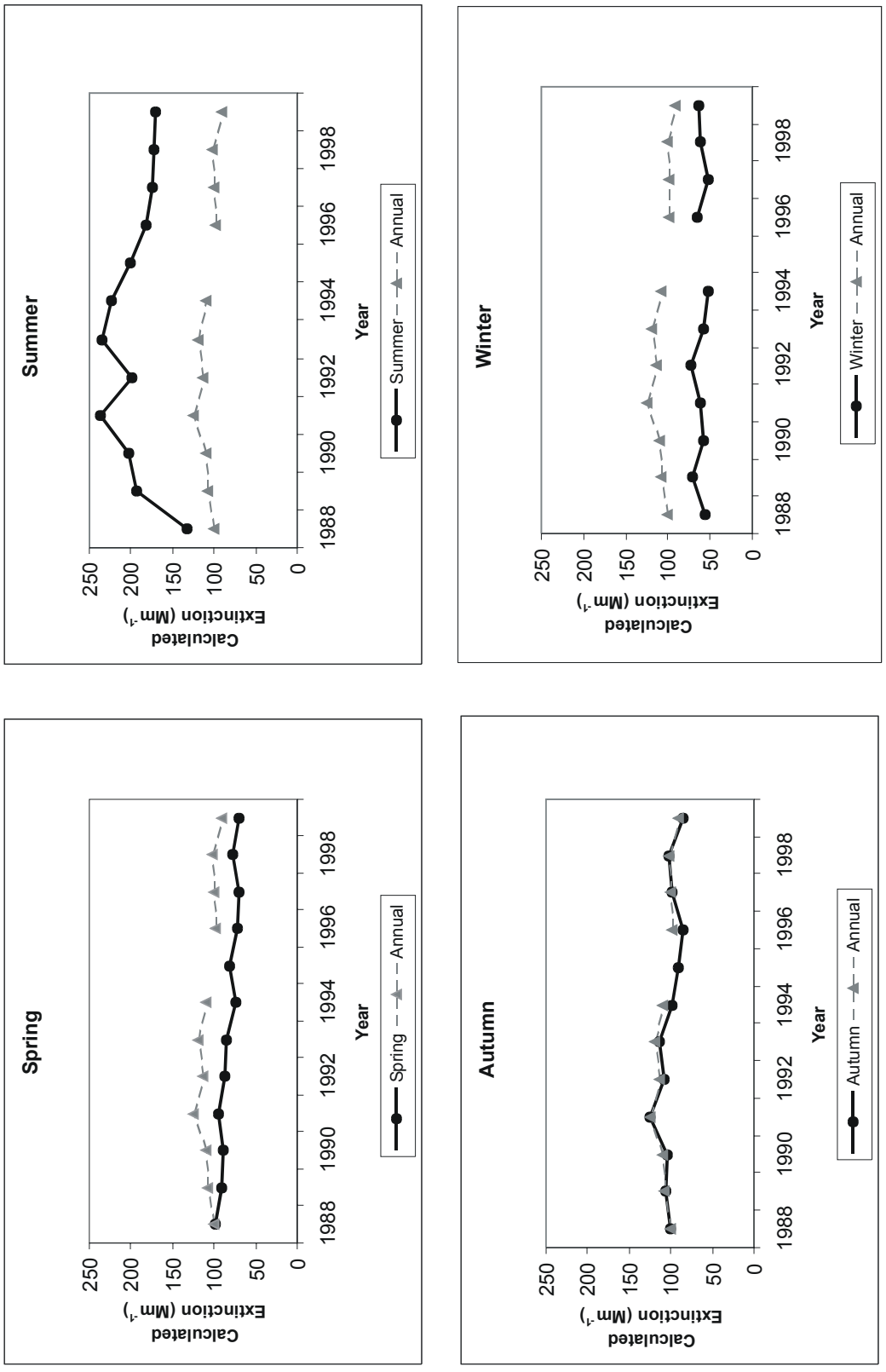

Figure V-23. Seasonal and annual average calculated extinction (Mm^{-1}) for SHEN, March 1988 – February 2000.

The characterization of long-term trends can be a highly subjective exercise in that slopes and their significance can vary depending on the technique employed. Recently the IMPROVE aerosol network, initiated in March 1988, matured to a point where long-term trends of average ambient aerosol concentrations and calculated extinction can be assessed. In the IMPROVE report (Malm et al. 2000), the Theil (1950) approach was applied to describe trends for IMPROVE sites with 11 years of data. The distribution of $PM_{2.5}$ mass concentrations, calculated extinction expressed as dv, and associated constituents were examined for each site. The data were sorted into three groups based on the cumulative frequency of occurrence of $PM_{2.5}$: lowest fine mass days, 0%-20%; median fine mass days, 40%-60%; and highest fine mass days, 80%-100%. After sorting each group's average concentrations of $PM_{2.5}$ and selecting the associated principal aerosol species, scattering and/or absorption of each species, calculated light extinction and dv were estimated.

Figure V-24 plots the relative contribution to aerosol light extinction by the five principal particulate matter constituents for the cleanest 20%, middle 20%, and haziest 20% groups at SHEN from 1988 to 2000. Figure V-25 shows plots of the trends in annual average calculated light extinction for the cleanest 20%, middle 20% and haziest 20% groups at SHEN. Extinction is also presented in units of SVR (km) and dv.

Optical/View Monitoring

IMPROVE optical monitoring provides a continuous quantitative ambient measurement (generally hourly averages) of light extinction or its components. Optical data document the dynamics of the visual air quality, including diurnal variation or specific events. Optical data cannot identify the cause (pollutant composition) of visibility degradation. However, if optical and aerosol data are taken at the same location, measured visibility and aerosol-based estimates of visibility (calculated extinction) can be compared to refine and/or verify the assumptions applied to compute visibility parameters from aerosol measurements.

SHEN is one of three national parks that use both transmissometer and nephelometer monitoring instruments to measure light extinction or its components. As described in Section III.F, light extinction represents the attenuation of light per unit distance of travel in the atmosphere, due to scattering and absorption of light by particles and gases in the air (aerosols). The transmissometer instrument measures light extinction over a short path length (~5km). The nephelometer instrument measures light scattering (b_{scat}) at a given point. Nephelometers are

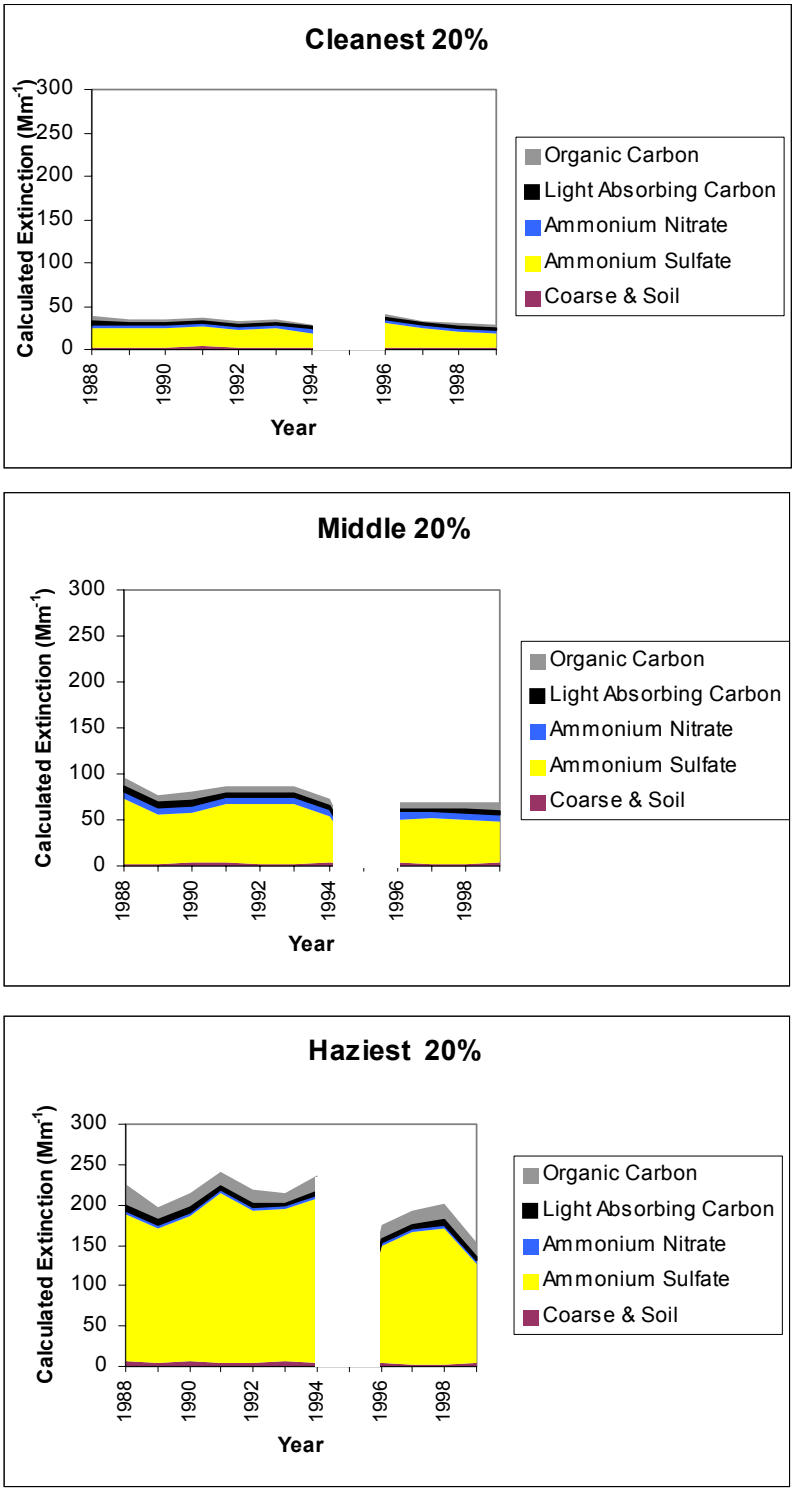

Figure V-24. Calculated aerosol light extinction in SHEN for the cleanest 20%, middle 20%, and haziest 20% of the days in the distribution, February 1988 - March 2000.

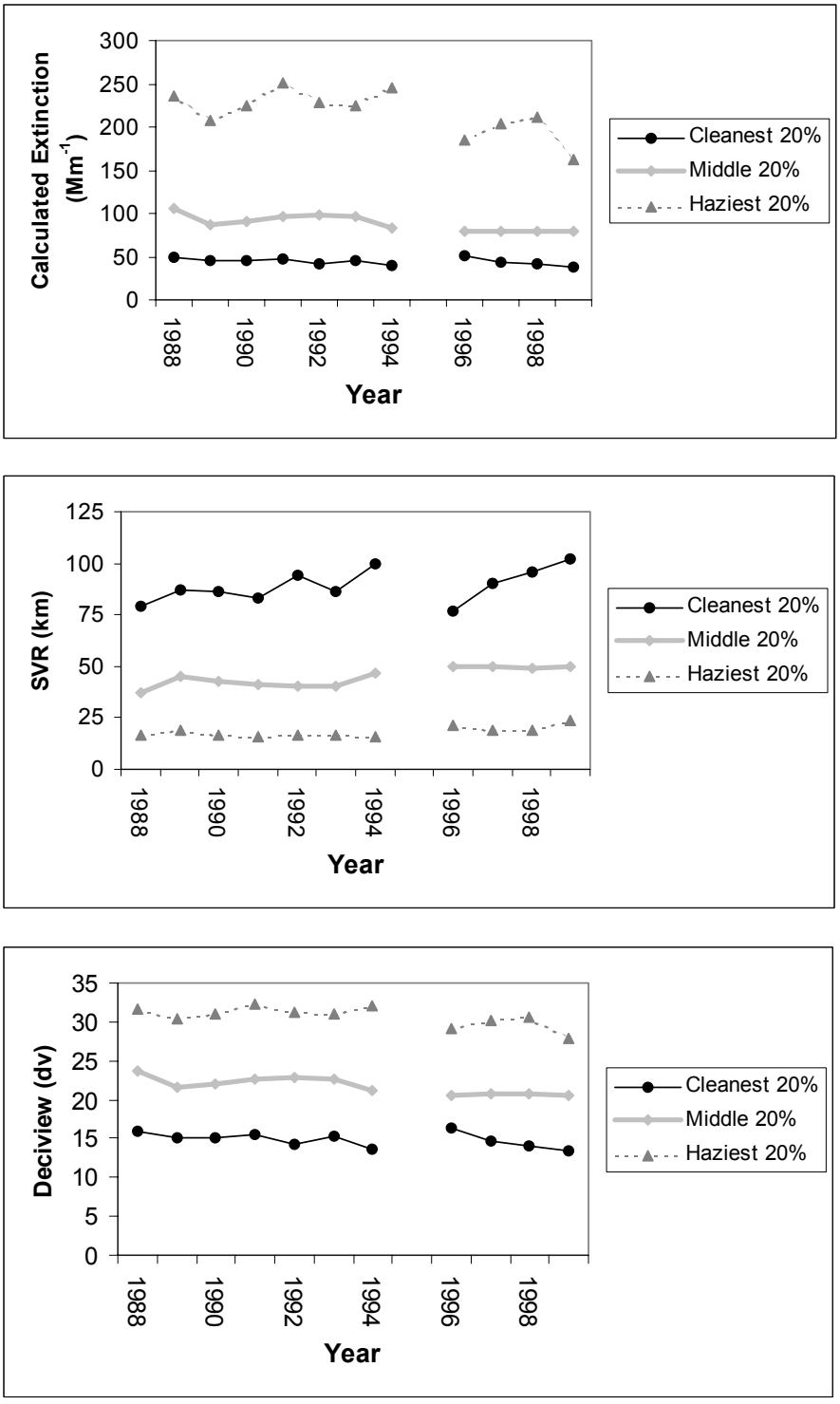

Figure V-25. Trends in annual averages for aerosol extinction (Mm^{-1}), standard visual range (SVR; km), and dv, February 1988 - March 2000.

often co-located with aerosol samplers, which provide the absorption component needed to calculate b_{ext} for the point location. By incorporating both types of optical monitoring instrumentation, SHEN includes both continuous path measurements of atmospheric extinction and continuous point measurements of the scattering component of extinction, for comparison to co-located aerosol measurements. Having both forms of optical monitoring provides a greater understanding of the temporal dynamics of visibility and additional cross checks of measured extinction (from transmissometers) and calculated extinction measurements (from aerosol samplers).

The goal of view monitoring is to use still-frame or time-lapse imagery to provide a qualitative representation of the visual quality of a scene of interest under a variety of air quality and illumination conditions at different times of day throughout the year. View monitoring images can be used to document how vistas appear under various air quality, meteorological, and seasonal conditions; record the frequency that various visual conditions occur, provide a quality assurance reference for collocated aerosol or optical measurements, and provide quality media for visually presenting program goals, objectives, and results to decision-makers and the public.

Transmissometer Data

The transmissometer system consists of two individually housed primary components: a transmitter (light source) and a receiver (detector). The b_{ext} can be calculated based on the intensity of light emitted from the source and the amount of light measured by the receiver (along with the path length between the two). Transmissometers provide continuous, hourly b_{ext} measurements. Meteorological or optical interference factors (such as fog, rain, or a dirty optical surface) can affect transmissometer measurements. Collected data that may be affected by such interferences are flagged, and the resultant data are designated "filtered". Detailed descriptions of the transmissometer system and data reduction and validation procedures used can be found in Standard Operating Procedures and Technical Instructions for Optec LPV-2 Transmissometer Systems (ARS 1996a).

Caution should be used when relying on transmissometer data without examining concurrent co-located nephelometer and/or speciated aerosol data. Relying solely on transmissometer data to represent visibility-related trends can often result in misleading conclusions, due to the following concerns: sight path interference (such as rain, airborne insect swarms, fogged or dirty optical surfaces), inadequate transmissometer calibration methods, and

insufficient manual and automatic hourly data validation analysis. Caution should also be used when comparing calculated (aerosol and/or nephelometer) and measured (transmissometer) extinction. Given differences in measurement periods and averaging methods, as well as relative humidity filtering methods and effects on light extinction efficiencies, the ratio of calculated extinction to measured extinction is seldom greater than 0.8.

Table V-12 provides a tabular summary of the "filtered" seasonal and annual mean extinction values. Combined season data represent the mean of all valid data for the combined seasons. Extinction values are also presented in units of SVR (in km) and dv. Tables V-13 and V-14 summarize the 20% cleanest and 20% haziest visibility metric statistics respectively. Data are represented according to the following conditions:

- No data are reported for seasons when the percentage of valid hourly averages (including weather) compared to total possible hourly averages was less than 50%.
- Annual data represent the mean of all valid data for each March through February annual period. No data are reported for years that had one or more invalid seasons.
- Combined season data represent the mean of all valid data for each season (spring, summer, autumn, winter) of the December 1988 through February 2000 period.
- Combined annual period data represent the mean of all combined data values for the period December 1988 through February 2000.

Figure V-26 provides a graphic representation of the "filtered" seasonal and annual means. No data are reported for annual periods with one or more invalid seasons.

Nephelometer Data

The nephelometer consists of a sampling chamber and a light source confined to a small volume so that the instrument may directly measure the light scattered by aerosols and gases at a fixed point. Nephelometers provide continuous, five-minute measurements of particle scattering (b_{sp}). The atmospheric scattering coefficient, b_{scat}, can be directly estimated from this measurement. Nephelometer measurements can be influenced by weather-related factors such as fog. Therefore, the data are "filtered" by flagging data points with relative humidities greater that 95%. Detailed descriptions of the nephelometer system and data reduction and validation procedures used can be found in Standard Operating Procedures and Technical Instructions for Nephelometer Systems (ARS 1996b).

Table V-12. Seasonal and annual arithmetic means, SHEN, transmissometer data (filtered), December 1988 through February 2000.

YEAR	Spring (Mar, Apr, May)			Summer (Jun, Jul, Aug)			Autumn (Sep, Oct, Nov)			Winter (Dec, Jan, Feb)			Annual (March - February)[a]		
	SVR[b] (km)	b_{ext} (Mm^{-1})	dv	SVR (km)	b_{ext} (Mm^{-1})	dv	SVR (km)	b_{ext} (Mm^{-1})	dv	SVR (km)	b_{ext} (Mm^{-1})	dv	SVR[b] (km)	b_{ext} (Mm^{-1})	dv
1988							---	---	---	65	61	18.1	***	***	***
1989	21	185	29.2	--	--	--	--	--	--	--	--	--	***	***	***
1990	--	--	--	19	202	30.1	42	93	22.3	--	--	--	***	***	***
1991	--	--	--	18	221	31.0	37	107	23.7	57	69	19.3	***	***	***
1992	49	80	20.8	--	--	--	45	88	21.7	43	92	22.2	***	***	***
1993	38	104	23.4	23	170	28.3	47	84	21.3	82	48	15.7	37	107	23.7
1994	49	80	20.8	24	166	28.1	43	92	22.2	73	54	16.9	45	88	21.7
1995	41	95	22.5	24	162	27.9	33	119	24.8	--	--	--	***	***	***
1996	56	70	19.5	26	152	27.2	46	85	21.4	39	102	23.2	40	98	22.8
1997	60	66	18.9	28	140	26.4	40	99	22.9	47	83	21.2	41	96	22.6
1998	30	132	25.8	18	219	30.9	28	138	26.2	31	128	25.5	26	153	27.3
1999	42	94	22.4	29	137	26.2	46	85	21.4	40	98	22.8	39	101	23.1
Mean[c]	40	98	22.8	22	176	28.7	40	98	22.8	44	89	21.9	35[d]	111[d]	24.1[d]

-- No data are reported for seasons with <50% valid data.
*** No annual data are reported for periods with one or more invalid seasons.
a Annual period data represent the mean of all valid data for each March through February annual period.
b The estimated natural visual range is about 185 km (115 mi; U.S. EPA 2001b).
c Combined season data represent the mean of all valid data for each season of the December 1988 through February 2000 period.
d Combined annual period data represent the mean of all combined valid data between December 1988 and February 2000.

Table V-13. Seasonal and annual 20% cleanest visibility metric statistics, SHEN, transmissometer data (filtered), December 1988 through February 2000.

YEAR	Spring (Mar, Apr, May)			Summer (Jun, Jul, Aug)			Autumn (Sep, Oct, Nov)			Winter (Dec, Jan, Feb)			Annual (March - February)[a]		
	SVR (km)	b_{ext} (Mm^{-1})	dv	SVR (km)	b_{ext} (Mm^{-1})	dv	SVR (km)	b_{ext} (Mm^{-1})	dv	SVR (km)	b_{ext} (Mm^{-1})	dv	SVR[b] (km)	b_{ext} (Mm^{-1})	dv
1988							---	---	---	191	21	7.4	***	***	***
1989	32	122	25.0	--	--	--	--	--	--	--	--	--	***	***	***
1990	--	--	--	49	81	20.9	133	30	11.0	--	--	--	***	***	***
1991	--	--	--	63	63	18.4	64.7	61	18.1	87.9	45	15.0	***	***	***
1992	102	39	13.6	--	--	--	91	43	14.7	76	52	16.5	***	***	***
1993	63	63	18.4	57	69	19.3	127	31	11.4	150	27	9.8	107	37	13.1
1994	108	37	13.0	61	64	18.6	120	33	12.0	179	22	8.1	129	31	11.2
1995	102	39	13.5	55	71	19.6	62	64	18.5	--	--	--	***	***	***
1996	104	38	13.4	67	59	17.8	129	31	11.3	85	46	15.4	100	39	13.7
1997	118	34	12.1	75	53	16.6	91	44	14.7	97	41	14.1	101	39	13.7
1998	46	86	21.5	35	114	24.3	51	78	20.5	45	87	21.6	46	86	21.5
1999	71	56	17.2	81	49	15.9	105	38	13.3	90	44	14.8	87	45	15.1
Mean[c]	94	42	14.4	63	63	18.4	102	39	13.6	110	36	12.8	94[d]	42[d]	14.4[d]

-- No data are reported for seasons with <50% valid data.
*** No annual data are reported for periods with one or more invalid seasons.
a Annual period data represent the mean of all valid data for each March through February annual period.
b The estimated natural visual range is about 185 km (115 mi; U.S. EPA 2001b).
c Combined season data represent the mean of all valid data for each season of the December 1988 through February 2000 period.
d Combined annual period data represent the mean of all combined valid data between December 1988 and February 2000.

Table V-14. Seasonal and annual 20% haziest visibility metric statistics, SHEN, transmissometer data (filtered), December 1988 through February 2000.

YEAR	Spring (Mar, Apr, May)			Summer (Jun, Jul, Aug)			Autumn (Sep, Oct, Nov)			Winter (Dec, Jan, Feb)			Annual (March - February)[a]		
	SVR (km)	b_{ext} (Mm^{-1})	dv	SVR (km)	b_{ext} (Mm^{-1})	dv	SVR (km)	b_{ext} (Mm^{-1})	dv	SVR (km)	b_{ext} (Mm^{-1})	dv	SVR[b] (km)	b_{ext} (Mm^{-1})	dv
1988							---	---	---	28	142	26.5	***	***	***
1989	15	259	32.5	--	--	--	--	--	--	--	--	--	***	***	***
1990	--	--	--	11	344	35.3	18	217	30.8	--	--	--	***	***	***
1991	--	--	--	8	478	38.7	19	202	30.1	37	105	23.5	***	***	***
1992	28	142	26.5	--	--	--	23	171	28.4	24	161	27.8	***	***	***
1993	22	182	29.0	12	340	35.3	22	179	28.8	49	80	20.8	17	234	31.5
1994	25	156	27.5	12	324	34.8	22	181	29.0	38	103	23.3	21	190	29.4
1995	21	184	29.1	13	310	34.3	16	241	31.8	--	--	--	***	***	***
1996	31	127	25.4	13	298	34.0	22	175	28.6	17	234	31.5	18	220	30.9
1997	32	121	24.9	13	292	33.7	19	202	30.1	25	159	27.7	19	208	30.3
1998	19	209	30.4	11	361	35.9	15	262	32.6	20	199	29.9	14	277	33.2
1999	26	149	27.0	15	258	32.5	25	160	27.7	23	170	28.3	21	185	29.2
Mean[c]	21	187	29.3	11	351	35.6	20	198	29.9	23	173	28.5	17[d]	237[d]	31.7[d]

-- No data are reported for seasons with <50% valid data.
*** No annual data are reported for periods with one or more invalid seasons.
a Annual period data represent the mean of all valid data for each March through February annual period.
b The estimated natural visual range is about 185 km (115 mi; U.S. EPA 2001b).
c Combined season data represent the mean of all valid data for each season of the December 1988 through February 2000 period.
d Combined annual period data represent the mean of all combined valid data between December 1988 and February 2000.

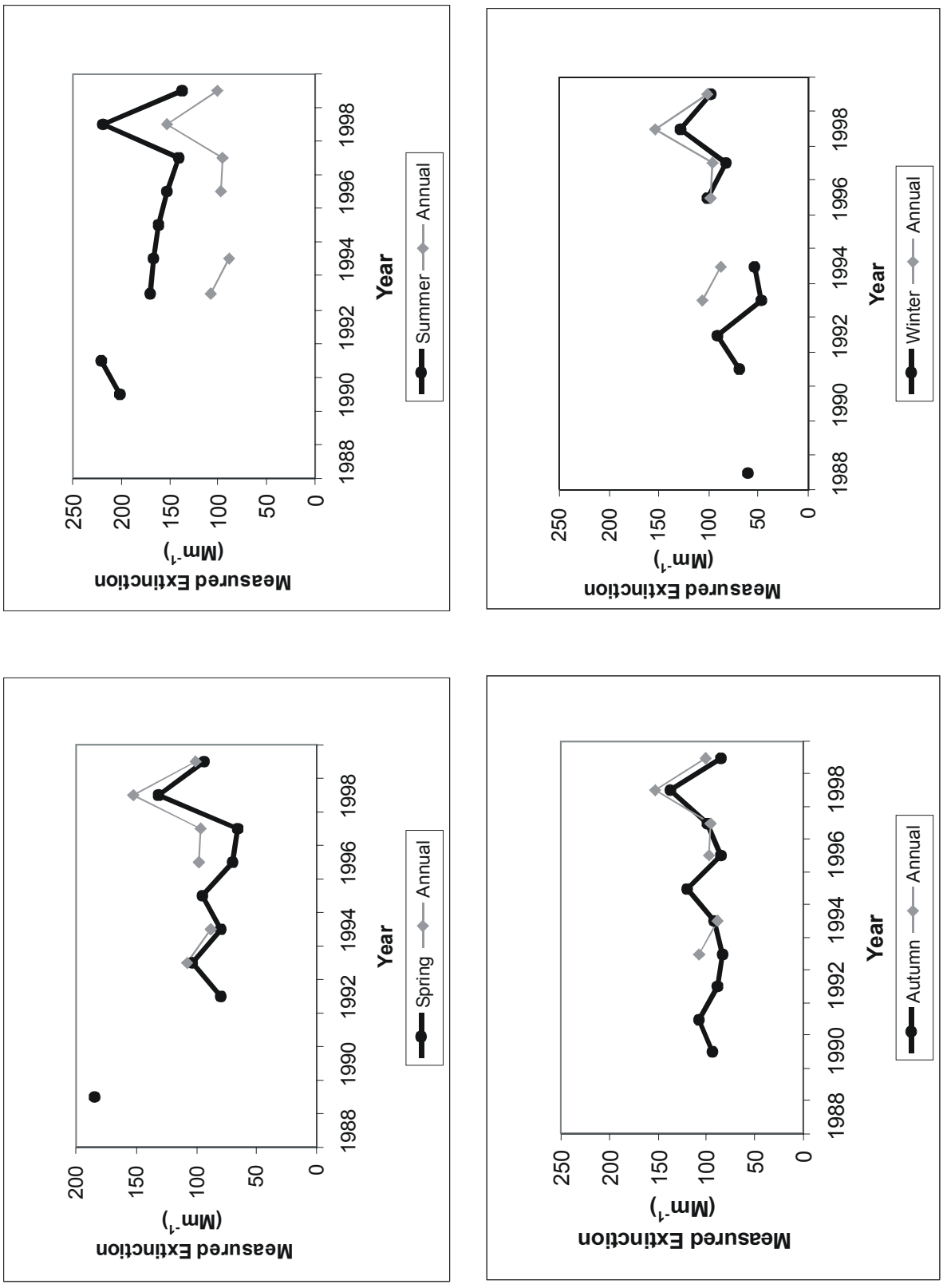

Figure V-26. Seasonal and annual arithmetic means for transmissometer data (filtered) at SHEN during the period 1988 to 2000.

Measurements of nephelometer b_{scat} are combined with estimates of aerosol absorption (b_{abs}) obtained from IMPROVE aerosol sampler measurements to calculate the total light extinction. Table V-15 provides a tabular summary of the "filtered" seasonal and annual mean scattering, absorption and extinction values. Extinction values are also presented in units of SVR (in km) and dv. Since nephelometer data rely on seasonal mean aerosol measurements of b_{abs} in order to reconstruct b_{ext}, no 20% cleanest or 20% haziest visibility metric statistics are provided. No data are reported for seasons when the percentage of valid hourly averages (including weather) compared to total possible hourly averages, was less than 50%. Figure V-27 provides a graphic

Table V-15. Seasonal and annual arithmetic means, SHEN, nephelometer data (filtered), September 1996 through February 2000.

Season	Year	b_{scat} Mean	b_{abs} Mean	b_{ext} [a]	dv	SVR
Spring	1996	--	--	--	--	–
	1997	43	3.1	46	15.3	85
	1998	47	3.5	51	16.2	78
	1999	38	4.3	42	14.4	94
Summer	1996	--	--	--	--	–
	1997	101	3.5	104	23.5	38
	1998	97	4.4	102	23.2	39
	1999	90	3.9	93	22.4	42
Autumn	1996	49	3.6	53	16.7	75
	1997	61	4.1	65	18.8	60
	1998	85	4.8	90	21.9	44
	1999	46	3.5	49	15.9	81
Winter	1996	43	3.1	46	15.3	86
	1997	40	2.8	43	14.6	92
	1998	43	3.4	47	15.4	85
	1999	39	2.8	42	14.4	94
Annual	1996	***	***	***	***	***
	1997	61	3.5	65	18.7	61
	1998	66	4.0	70	19.5	56
	1999	50	3.6	54	16.9	73

[a] Estimation based on the combined b_{scat} measurement (mean) and mean aerosol absorption coefficient (b_{abs}).
-- No data are reported for seasons with <50% valid data.
*** No annual data are reported for periods with one or more missing or invalid seasons.

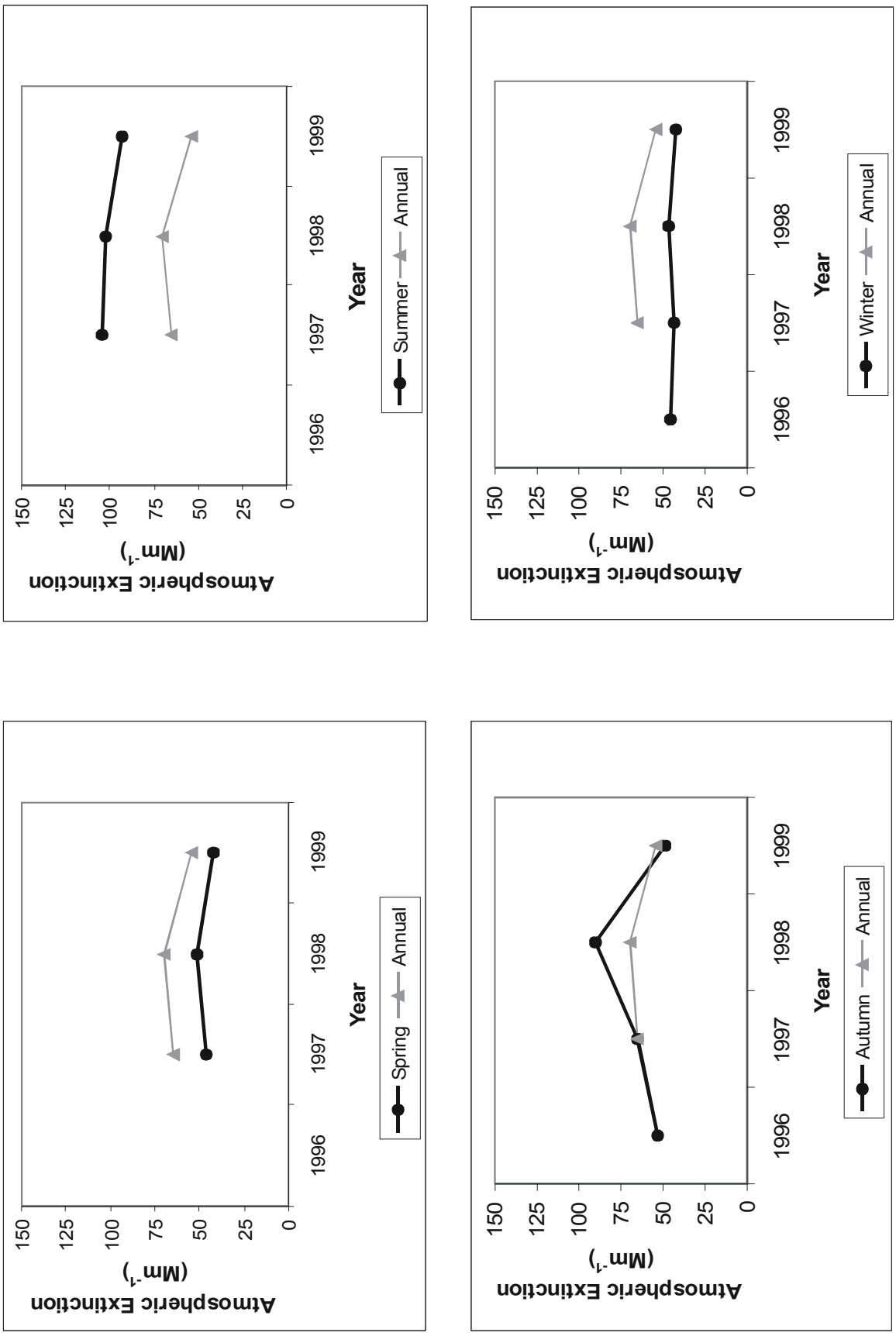

Figure V-27. Seasonal and annual arithmetic means, SHEN, nephelometer data (filtered), 1996 to 1999.

representation of the "filtered" seasonal and annual means of the nephelometer data. No data are reported for annual periods with one or more invalid seasons.

Camera Data

The NPS operated an automatic 35mm camera system at the Skyland-WNW vista in the Central District from July 1991 through April 1995. Color 35mm photographs of New Market Gap in the Massanutten Mountain were taken three times per day at 9:00 a.m., 12:00 p.m., and 3:00 p.m. In the summer of 1991, a second camera was temporarily set up at the Dickey Ridge-SW vista in order to do an intercomparison study of the Shenandoah Valley. This camera operated from July 1991 through November 1991. Color 35mm photographs were taken daily at 9:00 a.m., 12:00 p.m., and 3:00 p.m., and hourly from 7:00 am to 5:00 pm for a short time. The Skyland and Dickey Ridge vista photographs presented in Figures V-28 and V-29 were chosen to provide a feel for the range of visibility conditions possible and to help relate extinction, SVR, and deciview (haziness) data to the visual sense.

Optical/View Summary

Aerosol data at SHEN were presented in Section V-C.2.a so that the composition and concentrations of visibility reducing pollutants could be understood. For comparison, Figures V-24 and V-25 and Tables V-12 through V-15 have been provided to summarize optical data (measured and calculated extinction) at SHEN during the December 1988 through February 2000 period.

Caution should be used when comparing calculated (aerosol and nephelometer) extinction (Tables V-11 and V-15) with measured (transmissometer) extinction (Table V-12). The following differences and similarities should be considered:

- Data Collection - Calculated aerosol extinction measurements represent 24-hour samples collected twice per week from 1988 through 1999 and every three days since January 2000. Nephelometer scattering and transmissometer extinction estimates represent continuous measurements summarized as hourly means, 24 hours per day, seven days per week.

- Point versus Path Measurements - Calculated aerosol and nephelometer extinction represents an indirect measure of extinction at a fixed point. The transmissometer directly measures the irradiance of light (which calculated gives a direct measure of extinction) over a finite atmospheric path.

SHEN
on an "Excellent" day

Estimated Visibility Conditions:
Visual Range: 275-325 km
B_{ext}: 14-12 Mm^{-1}
Haziness: 4-2 dv

(a)

SHEN
on an "Average" day

Estimated Visibility Conditions:
Visual Range: 100-110 km
B_{ext}: 39-36 Mm^{-1}
Haziness: 14-13 dv

(b)

SHEN
on a "Poor" day

Estimated Visibility Conditions:
Visual Range: 20-25 km
B_{ext}: 156-196 Mm^{-1}
Haziness: 30-28 dv

(c)

Figure V-28. Photographs illustrating visibility conditions at Skyland in SHEN.

SHEN
on an "Excellent" day

Estimated Visibility Conditions:
Visual Range: 275-325 km
B_{ext}: 14-12 Mm^{-1}
Haziness: 4-2 dv

(a)

SHEN
on an "Average" day

Estimated Visibility Conditions:
Visual Range: 70-80 km
B_{ext}: 17-16 Mm^{-1}
Haziness: 56-49 dv

(b)

SHEN
on a "Poor" day

Estimated Visibility Conditions:
Visual Range: 5-6 km
B_{ext}: 782-652 Mm^{-1}
Haziness: 44-42 dv

(c)

Figure V-29. Photographs illustrating visibility conditions at SHEN, Dickey Ridge vista.

3. Deposition

a. Ambient Deposition

Some data are available regarding all forms of deposition in SHEN. An NADP/NTN wet deposition monitoring station has been in operation at Big Meadows (elevation 1,074 m) since 1981. Precipitation volume and the concentrations of major ions in precipitation are reported. Wet deposition of each ion is calculated as the product of the precipitation volume and ionic concentration in precipitation.

Annual wet deposition measurements and interpolated isopleths of SO_4^{2-}, NO_3^-, and inorganic N (NH_4^+ plus NO_3^-, as N) for the year 2001 are shown for the eastern United States in Figures V-30 to V-32. These are the most recent annual data available from the NADP/NTN monitoring program. Compared with other locations in the eastern United States, SHEN and the rest of western Virginia receive relatively high wet deposition of S (expressed on the map as SO_4^{2-}), and moderately high wet deposition of NH_4^+ and NO_3^-. Among Class I national parks, SHEN and GRSM receive the highest S and NO_3-N deposition. In general, S and N wet deposition values tend to be higher to the west and north of SHEN, but lower to the southeast of the park.

The concentrations of major ions measured in precipitation and measured precipitation amounts within SHEN are given in Table V-16. Data are available for three monitoring stations within the park: Big Meadows (1981-2000), White Oak Run (1980-2000) and North Fork Dry Run (1987-2000). Locations are shown in Figures II-1 and VI-1. Annual average precipitation at the monitoring stations, over the period of record, ranged from 91 cm at White Oak Run to 135 cm at Big Meadows. The Big Meadows site generally showed lower concentrations of major ions in precipitation than did the other two sites, with average SO_4^{2-}, NO_3^-, and sum of base cation concentrations equal to 31, 14, and 9 μeq/L, respectively (Table V-16).

Wet deposition fluxes (kg/ha/yr) were determined at each of the three wet deposition monitoring stations in the park for each year of available data. Annual average wet S deposition at Big Meadows varied over the period of record from about 2 to 10 kg/ha/yr, with an average of 6.7 kg/ha/yr (Table V-17). Both NH_4^+ and NO_3^- wet deposition varied during most years between 1 and about 3 kg N/ha/yr, with averages of 2.0 and 2.6 kg N/ha/yr, respectively at Big Meadows. The annual average total wet N deposition levels at Big Meadows, White Oak Run, and North Fork Dry Run during the periods of record were generally similar: 4.6, 3.8, and 4.8,

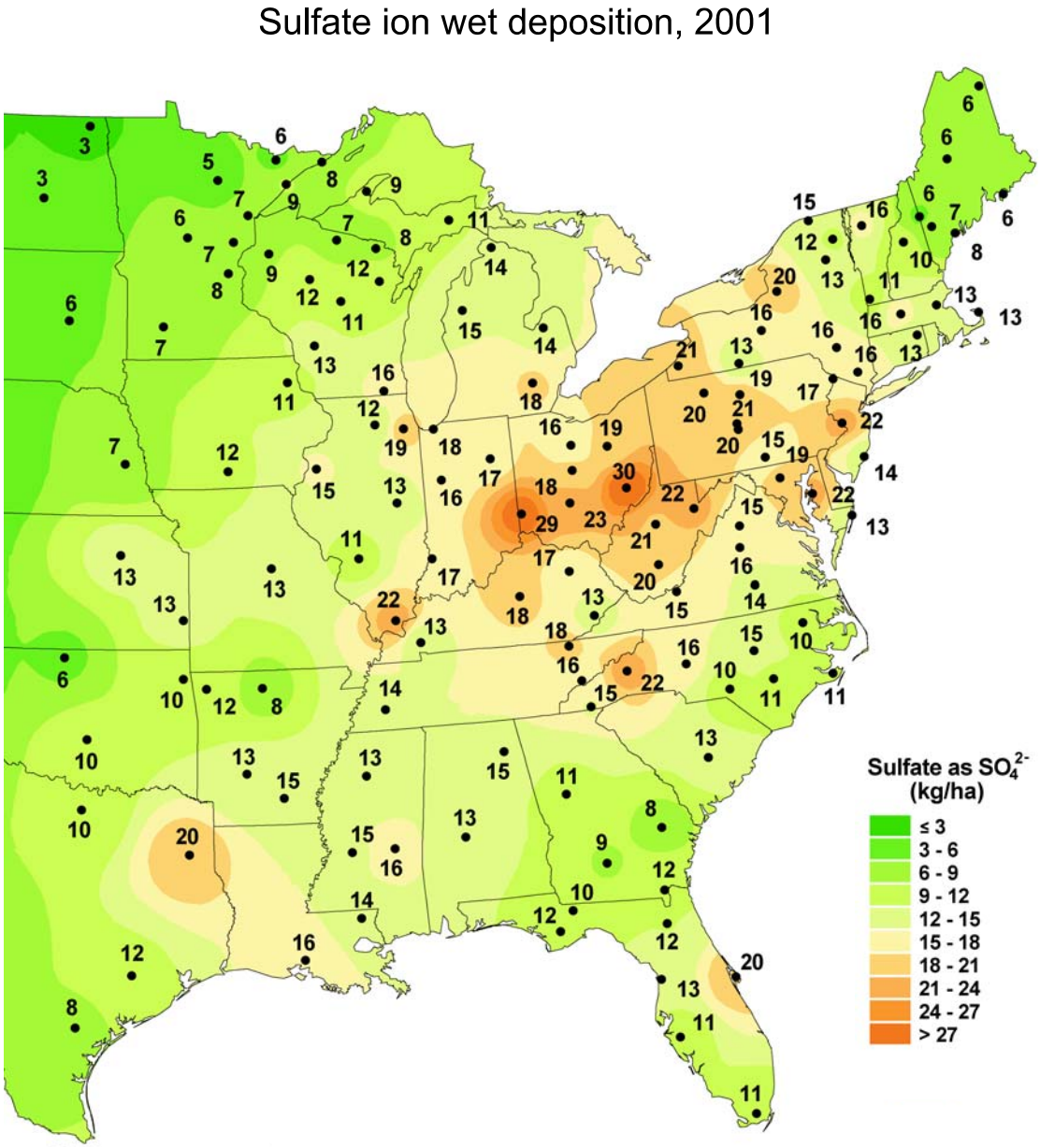

Figure V-30. Annual wet deposition of sulfate throughout the eastern United States during the most recent year of record. Note that sulfur deposition (as used elsewhere in this report) is one-third of sulfate deposition (as shown on this map). Source: http://nadp.sws.uiuc.edu

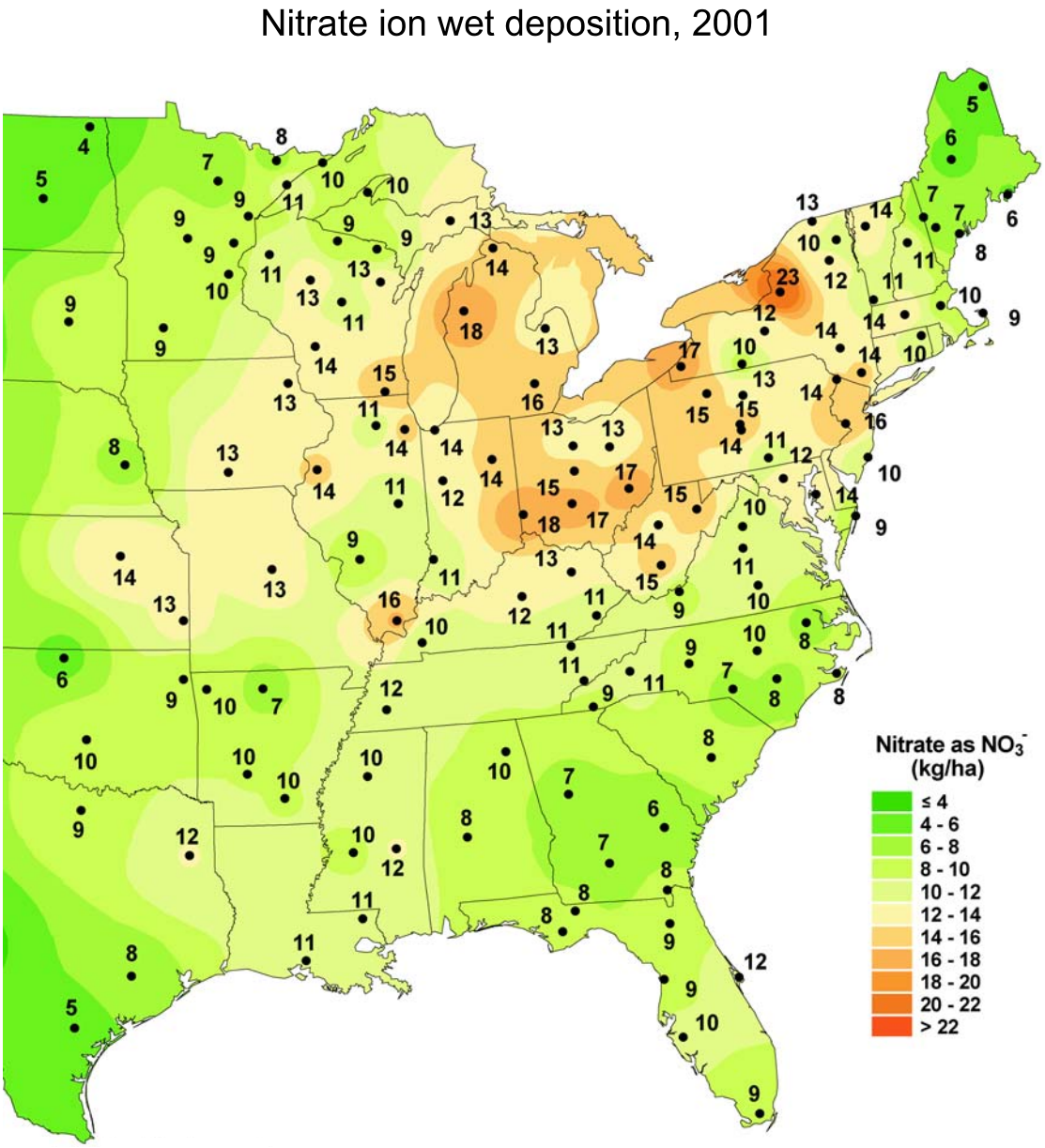

Figure V-31. Annual wet deposition of nitrate throughout the eastern United States during the most recent year of record. Note that nitrogen deposition as nitrate-nitrogen is equal to 22.58% of nitrate deposition (as shown on this map). Source: http://nadp.sws.uiuc.edu

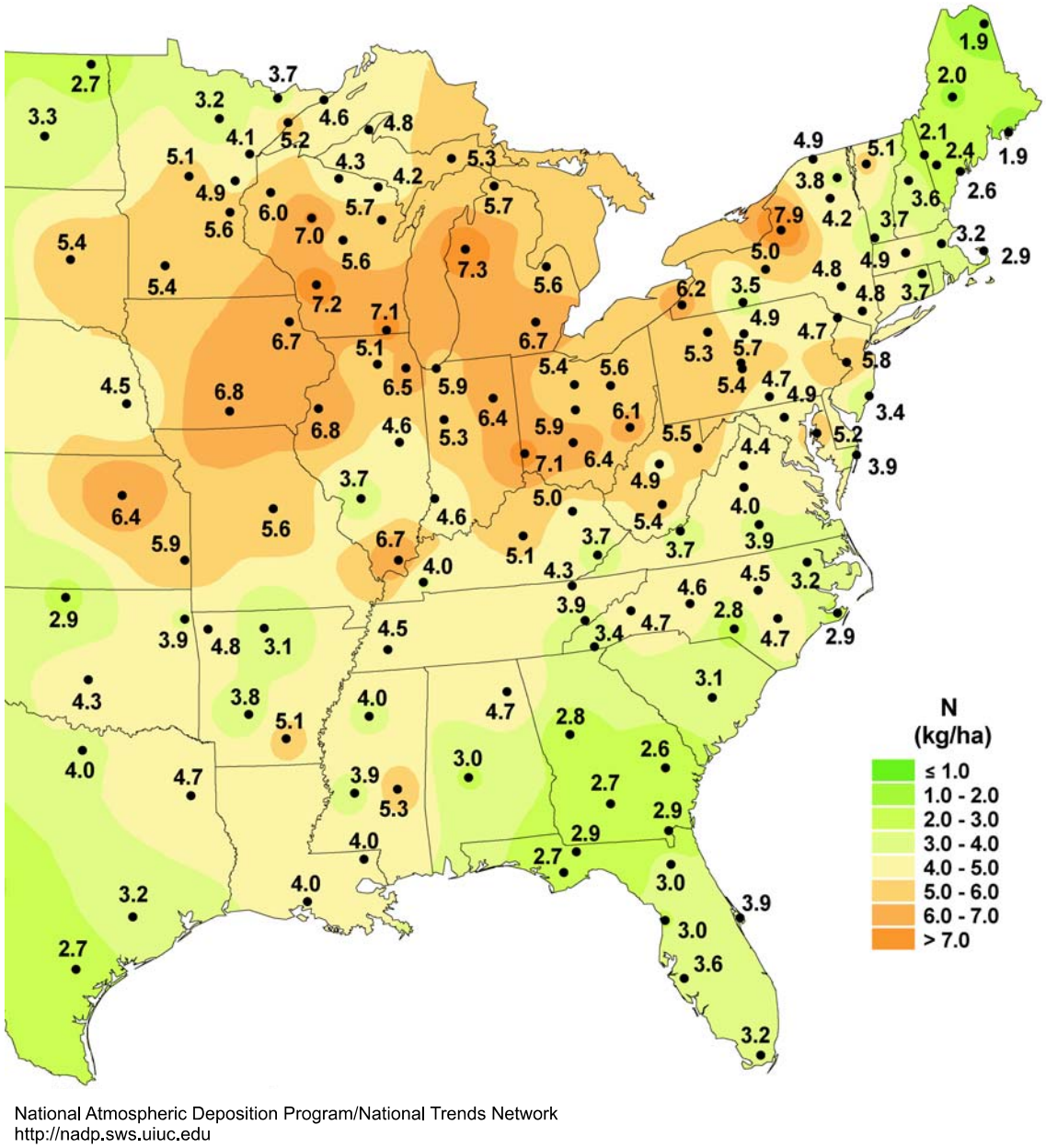

Figure V-32. Annual wet deposition of inorganic nitrogen throughout the eastern United States during the most recent year of record. Source: http://nadp.sws.uiuc.edu

Table V-16. Precipitation volume and measured concentrations of major ions in precipitation at monitoring sites within SHEN.

Year	Precipitation Amount (cm)	Concentration of Ion in Precipitation (μeq/L)								pH
		Ca	Mg	Na	K	NH_4	SO_4	NO_3	Cl	
Big Meadows[a] (Center of Central District, 1074 m)										
1981	93.3	6.1	4.2	5.6	0.7	10.7	40.2	13.7	5.3	4.5
1982	122.6	6.1	2.6	5.8	1.4	13.0	49.6	18.5	4.3	4.4
1983	183.4	3.1	2.0	5.2	0.5	8.7	29.4	11.9	7.1	4.6
1984	144.2	3.6	1.6	3.4	2.2	16.6	37.0	13.1	4.9	4.6
1985	151.0	3.0	1.6	2.2	0.3	6.5	34.0	11.5	3.0	4.5
1986	104.5	2.7	1.3	2.6	0.3	9.6	40.1	15.4	2.9	4.4
1987	51.7	2.5	1.1	3.0	0.2	4.6	19.6	9.9	3.4	4.7
1988	108.2	3.4	1.6	3.0	0.3	7.0	31.2	14.3	3.4	4.6
1989	150.7	3.1	1.5	4.3	0.4	13.9	40.4	17.5	5.9	4.4
1990	157.5	2.6	1.4	4.2	0.4	10.9	31.2	12.9	5.4	4.6
1991	107.5	2.6	0.9	2.6	0.7	12.1	34.5	15.0	3.8	4.5
1992	169.1	1.7	1.1	4.3	0.3	8.0	23.0	9.9	4.9	4.7
1993	150.8	1.8	0.7	2.0	0.2	10.9	30.9	13.2	2.5	4.5
1994	137.6	3.1	1.0	2.6	0.4	12.0	29.2	14.0	3.0	4.6
1995	193.5	2.1	2.1	11.4	0.3	8.1	17.0	10.1	9.6	4.8
1996	171.2	2.9	1.2	4.4	0.3	11.5	28.4	15.9	4.8	4.5
1997	126.5	2.3	0.8	2.3	0.2	11.2	29.3	14.7	2.9	4.6
1998	131.6	2.5	0.9	2.7	0.4	12.3	27.0	13.6	3.5	4.6
1999	141.1	3.4	1.7	4.1	0.4	10.4	27.7	12.7	5.2	4.6
2000	110.7	2.9	0.9	2.1	0.3	11.2	26.3	13.8	2.9	4.6
Average	135.3	3.1	1.5	3.9	0.5	10.5	31.3	13.6	4.4	4.6
White Oak Run[a] (South District, 387 m)										
1980	75.1	11.8	3.7	4.3	1.5	16.1	60.2	27.0	7.0	4.2
1981	71.9	10.2	3.2	6.1	1.8	11.1	55.6	21.7	8.1	4.3
1982	109.6	5.4	1.9	3.0	1.1	10.9	49.0	19.5	4.1	4.2
1983	106.5	6.0	1.5	5.2	1.3	15.1	61.8	21.2	5.9	4.3
1984	103.7	6.9	10.2	3.9	1.5	12.9	64.9	19.5	4.2	4.3
1985	102.1	6.1	2.4	6.1	2.4	13.3	42.3	19.6	7.7	4.3
1986	66.5	9.1	3.0	7.1	3.4	11.3	51.4	21.7	12.0	4.3
1987	88.9	7.7	2.2	2.9	2.0	14.4	74.2	26.1	6.0	4.1
1988	79.1	13.2	3.7	4.1	4.5	5.1	49.3	19.9	7.0	4.3
1989	125.3	7.4	2.3	2.2	1.8	5.1	48.3	16.0	5.1	4.3
1990	89.9	8.1	3.1	4.9	2.9	7.1	41.2	16.2	7.9	4.3

Table V-16. Continued.

Year	Precipitation Amount (cm)	Concentration of Ion in Precipitation (μeq/L)								pH
		Ca	Mg	Na	K	NH_4	SO_4	NO_3	Cl	
White Oak Run (continued)										
1991	97.0	8.0	2.0	2.3	1.8	12.4	48.4	20.3	4.6	4.3
1992	105.2	4.7	2.1	4.5	1.6	8.3	40.6	17.1	6.7	4.3
1993	95.6	5.6	1.9	2.6	2.0	7.6	43.5	17.6	5.0	4.3
1994	68.1	7.1	2.5	3.2	2.6	10.9	45.1	21.3	5.8	4.3
1995	70.5	7.1	3.4	8.4	1.9	6.8	28.8	14.8	11.4	4.5
1996	105.3	8.5	2.8	6.0	1.8	9.9	32.9	24.4	8.5	4.4
1997	86.9	7.1	2.2	4.0	2.3	10.9	36.7	15.6	5.6	4.4
1998	100.1	6.0	1.8	1.9	1.4	9.3	28.9	16.1	4.1	4.5
1999	86.9	8.5	2.6	4.1	1.5	9.2	39.2	19.7	7.3	4.3
2000	79.0	9.1	2.7	2.4	2.5	9.3	36.9	20.0	4.0	4.4
Average	91.1	7.8	2.9	4.2	2.1	10.5	46.8	19.9	6.6	4.3
North Fork Dry Run[a] (North End of Central District, 1014 m)										
1987	121.8	4.6	2.3	4.1	4.3	17.4	52.8	19.6	5.7	4.4
1988	88.4	9.2	3.9	3.9	3.6	17.5	52.3	20.8	5.2	4.4
1989	132.3	5.7	3.1	3.0	3.1	11.9	29.2	18.8	4.9	4.5
1990	135.5	6.4	2.5	4.5	5.3	15.0	36.2	15.9	5.9	4.5
1991	85.9	7.2	2.2	3.1	5.0	15.8	51.1	19.6	5.3	4.3
1992	129.5	4.3	2.4	4.9	3.9	8.0	30.6	13.0	6.6	4.5
1993	100.6	9.1	3.1	3.5	7.0	11.8	49.1	21.7	6.0	4.3
1994	97.6	9.0	3.1	3.3	5.6	14.5	47.7	21.2	5.4	4.4
1995	123.2	6.5	3.2	6.5	3.7	9.0	35.7	17.3	9.2	4.5
1996	125.7	6.9	2.8	4.3	6.2	8.2	33.3	17.9	6.3	4.5
1997	110.3	4.9	1.8	2.2	3.0	12.7	38.3	15.9	4.4	4.4
1998	118.6	3.3	1.2	2.9	0.8	10.3	30.4	17.0	4.5	4.5
1999	115.4	3.9	1.8	4.6	1.4	11.5	34.9	15.7	6.9	4.5
2000	113.3	4.3	1.5	2.4	1.0	12.7	31.1	17.5	3.5	4.5
Average	114.1	6.1	2.5	3.8	3.9	12.6	39.5	18.0	5.7	4.5

[a] Data were collected at Big Meadows by the National Atmospheric Deposition Program (http://nadp.sws.uiuc.edu) and at White Oak Run and North Fork Dry Run by the SWAS (University of Virginia, Department of Environmental Sciences)

Table V-17. Measured wet deposition fluxes at monitoring sites within SHEN.

Year	Wet Deposition (kg/ha/yr)									
	Ca	Mg	Na	K	H	Cl	SO_4-S	NH_4-N	NO_3-N	Total N
Big Meadows[a]										
1981	1.1	0.5	2.0	0.1	0.3	1.8	6.0	1.4	1.8	3.2
1982	1.5	0.4	2.8	0.4	0.4	1.9	9.7	2.2	3.2	5.4
1983	1.1	0.4	3.7	0.2	0.5	4.6	8.6	2.2	3.0	5.3
1984	1.0	0.3	1.9	0.7	0.3	2.5	8.5	3.3	2.6	6.0
1985	0.9	0.3	1.3	0.1	0.5	1.6	8.2	1.4	2.4	3.8
1986	0.6	0.2	1.0	0.1	0.4	1.1	6.7	1.4	2.3	3.7
1987	0.3	0.1	0.6	0.0	0.1	0.6	1.6	0.3	0.7	1.0
1988	0.7	0.2	1.3	0.1	0.3	1.3	5.4	1.1	2.2	3.2
1989	0.9	0.3	2.6	0.1	0.5	3.1	9.7	2.9	3.7	6.6
1990	0.8	0.3	2.6	0.1	0.4	3.0	7.9	2.4	2.8	5.2
1991	0.6	0.1	1.1	0.2	0.3	1.4	5.9	1.8	2.3	4.1
1992	0.6	0.2	2.8	0.1	0.4	3.0	6.2	1.9	2.4	4.3
1993	0.5	0.1	1.2	0.1	0.4	1.3	7.5	2.3	2.8	5.1
1994	0.9	0.2	1.4	0.1	0.4	1.5	6.4	2.3	2.7	5.0
1995	0.8	0.5	8.7	0.1	0.3	6.6	5.3	2.2	2.7	4.9
1996	1.0	0.3	2.9	0.1	0.5	2.9	7.8	2.8	3.8	6.6
1997	0.6	0.1	1.1	0.1	0.4	1.3	5.9	2.0	2.6	4.6
1998	0.7	0.1	1.4	0.1	0.3	1.6	5.7	2.3	2.5	4.8
1999	1.0	0.3	2.3	0.1	0.3	2.6	6.2	2.1	2.5	4.6
2000	0.6	0.1	0.9	0.1	0.3	1.1	4.7	1.7	2.1	3.9
Average	0.8	0.2	2.2	0.2	0.4	2.2	6.7	2.0	2.6	4.6
White Oak Run[a]										
1980	1.8	0.3	1.3	0.3	0.4	1.9	7.2	1.7	2.8	4.5
1981	1.5	0.3	1.7	0.3	0.4	2.1	6.4	1.1	2.2	3.3
1982	1.2	0.3	1.3	0.3	0.6	1.6	8.6	1.7	3.0	4.7
1983	1.3	0.2	2.2	0.3	0.5	2.2	10.5	2.2	3.2	5.4
1984	1.4	1.3	1.6	0.4	0.5	1.5	10.8	1.9	2.8	4.7
1985	1.3	0.3	2.4	0.6	0.5	2.8	6.9	1.9	2.8	4.7
1986	1.2	0.2	1.9	0.5	0.3	2.8	5.5	1.1	2.0	3.1
1987	1.4	0.2	1.0	0.4	0.7	1.9	10.6	1.8	3.2	5.0
1988	2.1	0.4	1.3	0.8	0.4	2.0	6.2	0.6	2.2	2.8
1989	1.9	0.3	1.1	0.5	0.6	2.2	9.7	0.9	2.8	3.7
1990	1.5	0.3	1.7	0.6	0.4	2.5	5.9	0.9	2.0	2.9
1991	1.6	0.2	0.9	0.4	0.5	1.6	7.5	1.7	2.8	4.4
1992	1.0	0.3	1.8	0.4	0.5	2.5	6.8	1.2	2.5	3.7
1993	1.1	0.2	1.0	0.4	0.5	1.7	6.6	1.0	2.4	3.4
1994	1.0	0.2	0.8	0.4	0.4	1.4	4.9	1.0	2.0	3.1
1995	1.0	0.3	2.3	0.3	0.2	2.8	3.2	0.7	1.5	2.1
1996	1.8	0.4	2.5	0.4	0.5	3.2	5.5	1.5	3.6	5.1
1997	1.2	0.2	1.3	0.5	0.4	1.7	5.1	1.3	1.9	3.2

Table V-17. Continued.

Year	Wet Deposition (kg/ha/yr)									
	Ca	Mg	Na	K	H	Cl	SO_4-S	NH_4-N	NO_3-N	Total N
1998	1.2	0.2	0.8	0.3	0.3	1.4	4.6	1.3	2.3	3.6
1999	1.5	0.3	1.4	0.3	0.4	2.3	5.5	1.1	2.4	3.5
2000	1.4	0.3	0.7	0.4	0.3	1.1	4.7	1.0	2.2	3.2
Average	1.4	0.3	1.5	0.4	0.4	2.1	7.0	1.5	2.6	3.8
North Fork Dry Run[a]										
1987	1.1	0.3	2.0	1.2	0.5	2.5	10.3	3.0	3.3	6.3
1988	1.6	0.4	1.4	0.7	0.4	1.6	7.4	2.2	2.6	4.7
1989	1.5	0.5	1.6	0.9	0.4	2.3	6.2	2.2	3.5	5.7
1990	1.7	0.4	2.4	1.7	0.4	2.8	7.8	2.9	3.0	5.9
1991	1.2	0.2	1.0	1.0	0.4	1.6	7.0	1.9	2.4	4.3
1992	1.1	0.4	2.5	1.2	0.4	3.0	6.3	1.5	2.3	3.8
1993	1.8	0.4	1.4	1.6	0.5	2.1	7.9	1.7	3.1	4.7
1994	1.8	0.4	1.3	1.3	0.4	1.9	7.5	2.0	2.9	4.9
1995	1.6	0.5	3.1	1.1	0.4	4.0	7.0	1.6	3.0	4.6
1996	1.7	0.4	2.1	1.8	0.4	2.8	6.7	1.4	3.1	4.6
1997	1.1	0.2	1.0	0.8	0.4	1.7	6.8	2.0	2.5	4.4
1998	0.8	0.2	1.3	0.2	0.4	1.9	5.8	1.7	2.8	4.5
1999	0.9	0.3	2.1	0.4	0.4	2.8	6.5	1.9	2.5	4.4
2000	1.0	0.2	1.1	0.3	0.3	1.4	5.6	2.0	2.8	4.8
Average	1.4	0.3	1.7	1.0	0.4	2.3	7.1	2.0	2.8	4.8

[a] Data were collected at Big Meadows by the National Atmospheric Deposition Program (http://nadp.sws.uiuc.edu) and at White Oak Run and North Fork Dry Run by the SWAS (University of Virginia, Department of Environmental Sciences)

respectively (Table V-17). Average annual wet S deposition was also similar among sites (6.7 to 7.1 kg S/ha/yr).

Dry deposition fluxes were estimated at Big Meadows by CASTNet for the period 1991 through 1998, although data were incomplete for 1994 (Table V-18). Dry deposition estimates for S and N were slightly lower than the respective wet deposition estimates (about 73% and 70% for S and N, respectively), in agreement with ASTRAP model estimates provided by Shannon (1998) for use in the SAMI assessment (Sullivan et al. 2002a).

Cloud deposition can be substantial in some cases, particularly at high-elevation sites that are immersed in clouds more than 25% of the time (Mohnen 1988a,b; Lovett and Kinsman 1990). The percent of total S deposition contributed by cloud deposition has been estimated to range from near zero for lower-elevation sites (< 1,000 m) to over 50% at higher elevation (Lovett and Kinsman 1990). At SHEN, most of the park lies below 1,000 m elevation. Cloud

Table V-18. Estimated dry deposition fluxes at Big Meadows, based on data and calculations from CASTNet (http://www.epa.gov/castnet/)

Year[a]	Dry deposition (kg/ha/yr)						
	SO_2	SO_4	HNO_3	NO_3	NH_4	Total S	Total N
1991	4.0	0.8	2.6	0.0	0.1	4.8	2.8
1992	5.1	0.8	2.7	0.0	0.1	5.8	2.9
1993	5.3	0.9	3.0	0.0	0.2	6.2	3.2
1995	3.4	0.7	3.3	0.1	0.2	4.1	3.5
1996	3.3	0.7	2.8	0.0	0.1	4.0	3.0
1997	3.5	0.7	3.1	0.0	0.2	4.2	3.3
1998	4.3	0.8	3.3	0.0	0.2	5.1	3.6
Average	4.4	1.3	3.4	0.5	0.7	4.9	3.2

[a] Data were not available for all four quarters for 1994.

deposition is therefore not expected to constitute a sizeable component of total deposition to acid-sensitive watersheds within the park. This assumption is in agreement with measured (Mohren 1988b, Weathers et al. 1988) and modeled (Shannon 1998) values for cloud deposition of S in SHEN.

Estes (1990) collected and analyzed cloud water samples in the North Fork Dry Run watershed in SHEN (1,014 m) during the period 1986-1987. Highly concentrated cloudwater events (those having H^+ plus SO_4^{2-} concentration greater than 400 μeq/L) were more likely to be associated with NW or ESE wind trajectories than with other trajectories, were most common in summer, and were likely to occur in the presence of a stagnant high pressure system. Such highly concentrated acidic cloudwater events tended to be of relatively short duration, typically less than 20 hours long.

Cloud water data had also been collected earlier, during the Cloud Water Project (Weathers et al. 1988) at Loft Mountain in SHEN (~ 1,000 m), yielding similar median concentrations of major ions in cloud water at the North Fork Dry Run and Loft Mountain sites (SO_4^{2-} ≈ 200-300 μeq/L, NO_3^- ≈ 120 μeq/L). Mean concentrations of SO_4^{2-} in cloudwater collected during the Mountain Cloud Chemistry Project (MCCP) at Mt. Mitchell, NC (2,006 m) and Whitetop Mt., VA (1,680 m) were more than double those found at the SHEN sites, and concentrations of NO_3^-, NH_4^+, and H^+ were also considerably higher at the Mt. Mitchell and Whitetop Mt. sites (Estes 1990). Elevations within SHEN are considerably lower than the sites included in the MCCP; many peaks in SHEN are above 900 m elevation, but the highest point in the park is only 1,234 m, at Hawksbill Mountain.

During the period 1995 to 1998, average total S deposition was 10.5 kg/ha/yr and average total N deposition was 8.6 kg/ha/yr at Big Meadows, the only site in SHEN for which both wet and dry deposition estimates are available directly from monitoring station data. The S deposition varies, based on the RADM simulation, decreasing from north to south within the park by less than 12%. East-west differences would be expected to be larger due to elevational changes and orographic effects, but the meteorological model resolution (80-km native prediction interpolated to a 20-km grid) was too coarse to resolve the Shenandoah topography, making it impossible to differentiate within-park east-west variability.

b. Trends in Deposition

Reductions in the S component of acidic deposition have generally followed the recent reductions in SO_2 emissions. Preliminary analysis for the eastern United States indicates that total S deposition, which includes dissolved, particulate, and gaseous forms, declined by an average of 26% between 1989 and 1998 (U.S. EPA 2000a). Of more specific relevance to SHEN, wet deposition of S in the mid-Appalachian area (West Virginia and Virginia, as well as areas to the north), declined by 23% between the periods of 1983-94 and 1995-98 (USGAO 2000). Legislated reductions in SO_2 emissions were largely responsible for these reductions in S deposition, and additional, albeit smaller, reductions can be anticipated though 2010.

NADP wet deposition monitoring data are available for Big Meadows since 1981. Annual average wet deposition has declined at many sites in the eastern United States, including Big Meadows (Figure V-33). Lynch et al. (1996) noted substantial decreases since 1995 in the concentration of SO_4^{2-} in precipitation and in wet S deposition at some NADP stations in and immediately downwind of the Ohio River Valley. These decreases were attributed by Lynch et al. (1996) to implementation of Phase I of the CAAA, Title IV.

Data from the wet deposition monitoring stations at White Oak Run and North Fork Dry Run showed generally declining patterns in wet deposition of S (Figure V-33), total N (Figure V-34), NH_4^+-N (Figure V-35), and NO_3^--N (Figure V-36) throughout the period of record. At each site, however, year-to-year variability was generally high. There is an indication of pronounced consistent variability in wet S deposition among the three sites, despite the substantial year-to-year variation at each site. The overall patterns of annual S deposition values at these sites were generally within 10 to 15% of each other throughout the period of record. At the Big Meadows

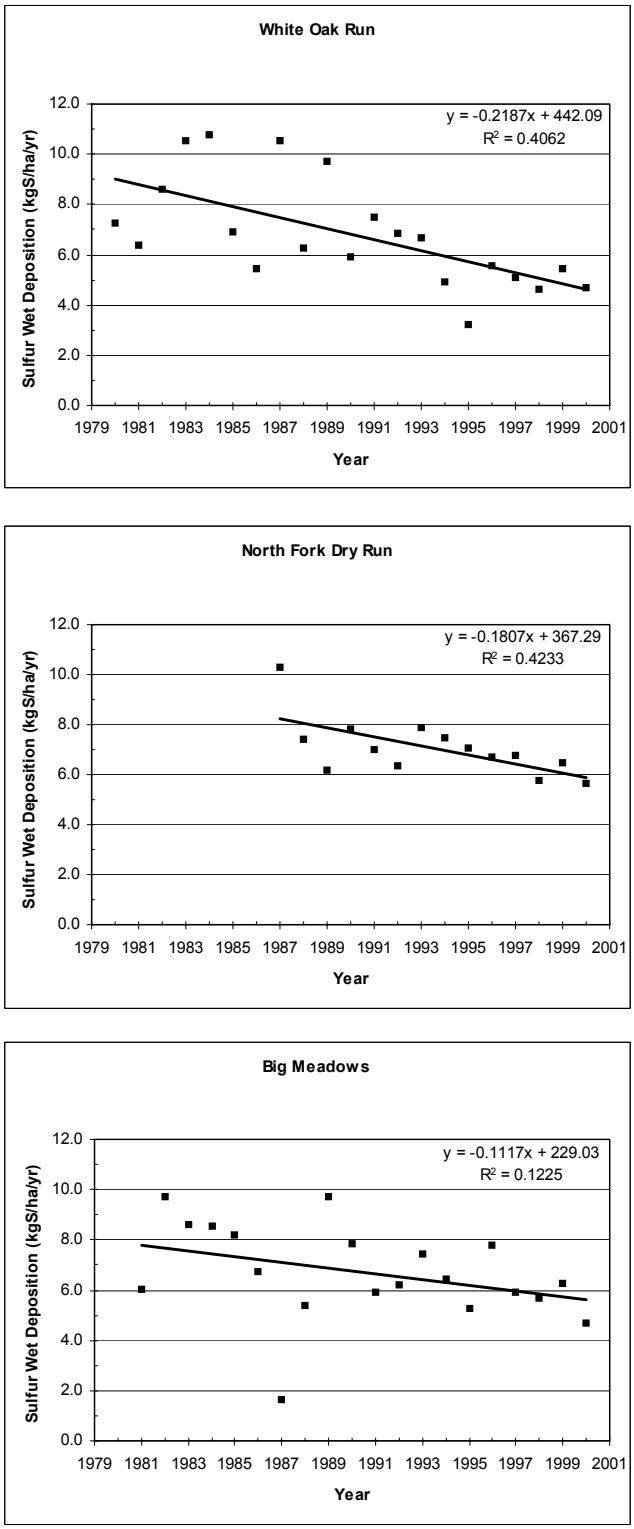

Figure V-33. Wet sulfur deposition for the period of record at three monitoring sites in SHEN. Best-fit regression lines are added. (Data obtained from NADP website and from the University of Virginia.)

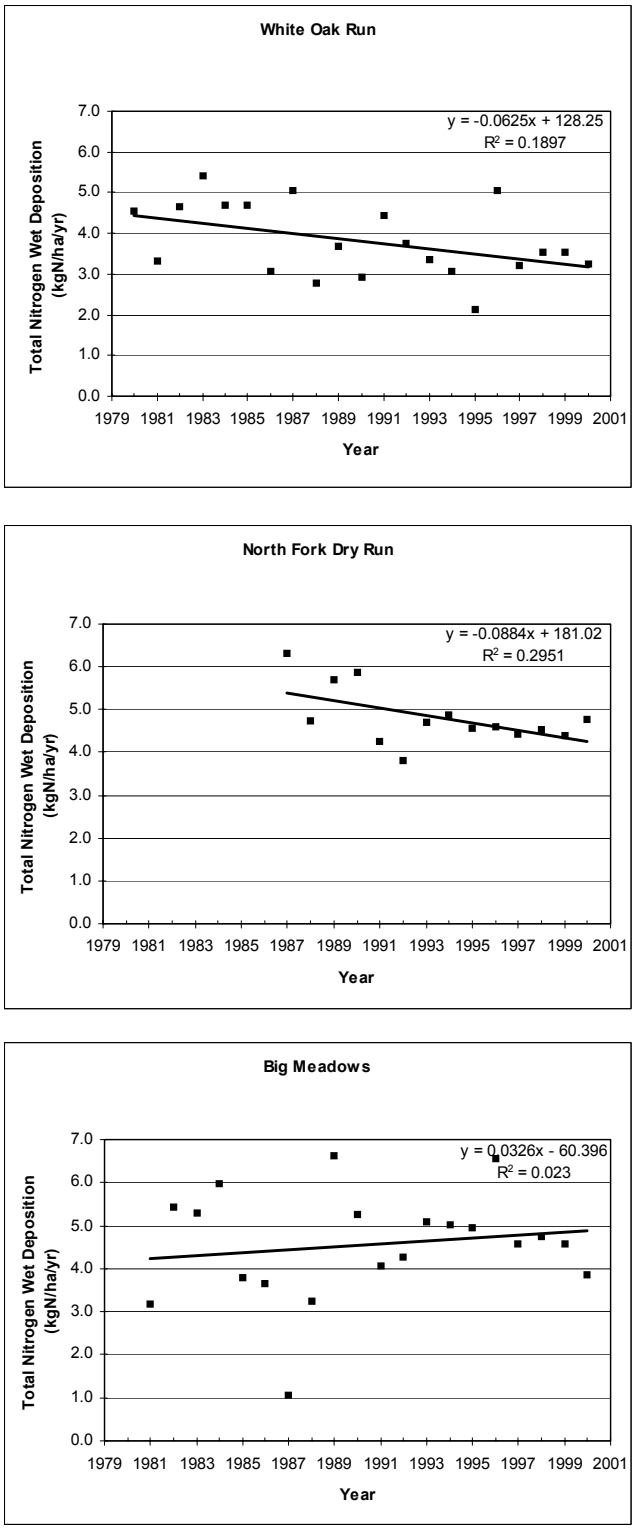

Figure V-34. Wet inorganic nitrogen deposition for the period of record at three monitoring sites in SHEN. Best-fit regression lines are added. (Data obtained from NADP website and from the University of Virginia.)

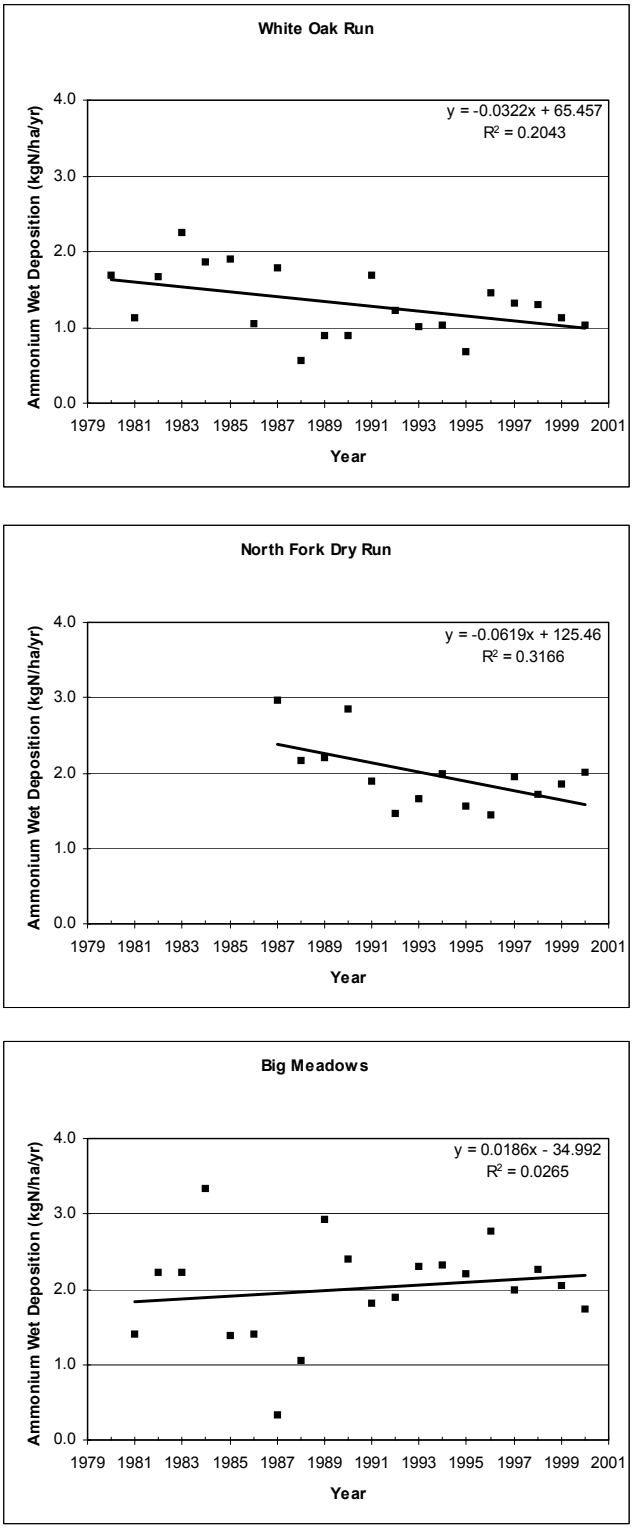

Figure V-35. Wet ammonium deposition for the period of record at three monitoring sites in SHEN. Best-fit regression lines are added. (Data obtained from NADP website and from the University of Virginia.)

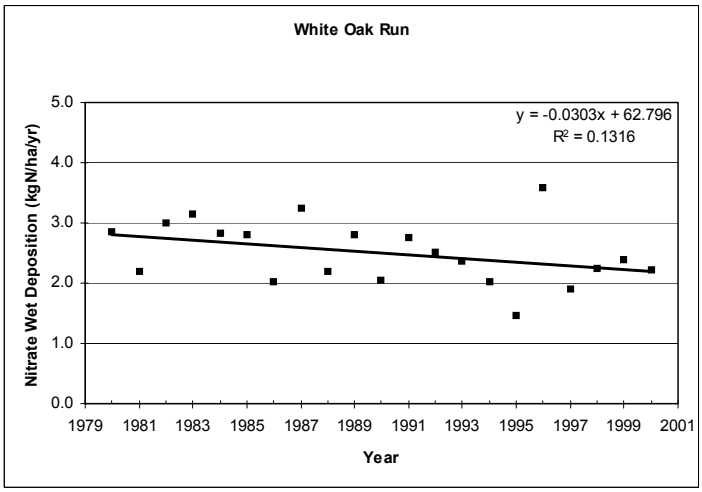

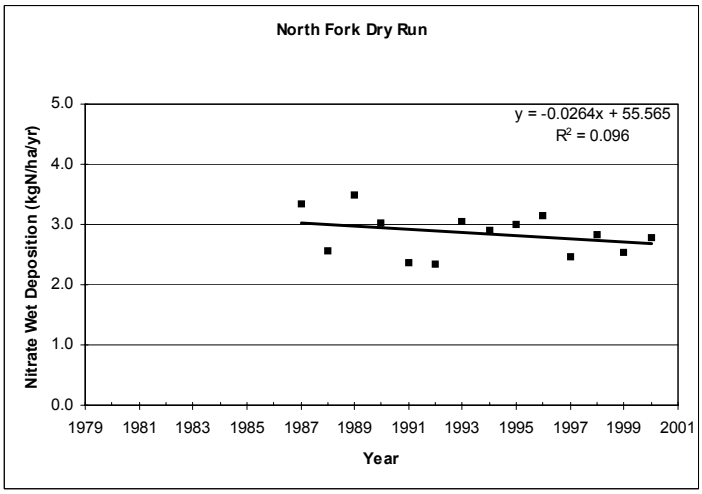

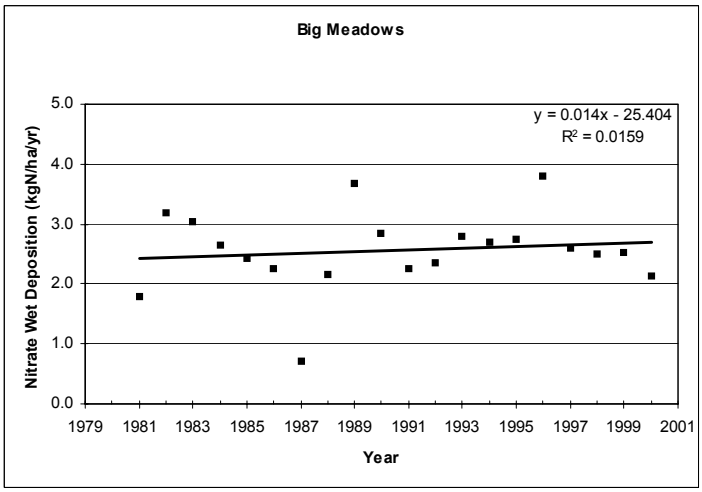

Figure V-36. Wet nitrate deposition for the period of record at three monitoring sites in SHEN. Best-fit regression lines are added. (Data obtained from NADP website and from the University of Virginia.)

monitoring station, S wet deposition data suggested a declining pattern since 1981, but N wet deposition data (total N, NO_3^--N, NH_4^+-N) did not (Figures V-33 through V-36).

Over the 1981 to 2000 period of record, wet N deposition at Big Meadows has varied substantially, generally between about 3 and 7 kg N/ha/yr. There is no indication of large long-term increases or decreases in wet N deposition, although there has been a relatively consistent short-term decline over the last five years at Big Meadows (Figure V-34 and V-36). Additional data will be required to determine whether this apparent downward trend is meaningful.

D. PROJECTED CHANGES IN FUTURE AIR QUALITY AND DEPOSITION

The RADM was developed with grids that are 80-km on a side (Figure V-37). More recently, a 20-km grid covering the northeastern U.S. was created as a one-way nest within the 80-km grid. The 20-km grid was the principal grid used for this assessment. The model was extended or enhanced by adding the capability to represent SO_4^{2-}-NO_3^--NH_4^+-water aerosol composition based on equilibrium thermodynamics by incorporating into RADM a module from the Regional Particulate Model (Binkowski and Shankar 1995). The Extended RADM is described in Appendix C.

RADM is very computationally intensive because it predicts hourly photochemistry. A statistical approach, termed aggregation (Dennis et al. 1990), was developed as part of NAPAP to create annual estimates of acidic deposition without having to model an entire year. Meteorological cases of five-day duration were grouped by large-scale wind flow pattern through cluster analysis and sampled proportionate to their frequency of occurrence across a seven-year period of the early 1980s (Brook et al. 1995a,b). A total of 30 cases constitute the aggregation sample. The precipitation predicted for each cluster was adjusted to the long-term mean precipitation for that cluster to estimate average deposition. The aggregation method produced a climatological average of transport and deposition representative of the transport of the 1980s and the seven-year average precipitation of that period. The precipitation average approximated well the 30-year normal precipitation. Although developed to represent an annual average, the 30 aggregation cases naturally divide into a warm and a cold season. Thus, broad seasonality can be accommodated with the aggregation method which matches well with the seasonally-oriented O_3 control approaches, such as the NO_X SIP Call.

For the Base Case and the scenario projections, the meteorology was held constant, retaining the same climatology of transport, temperature, cloudiness and precipitation. Only the

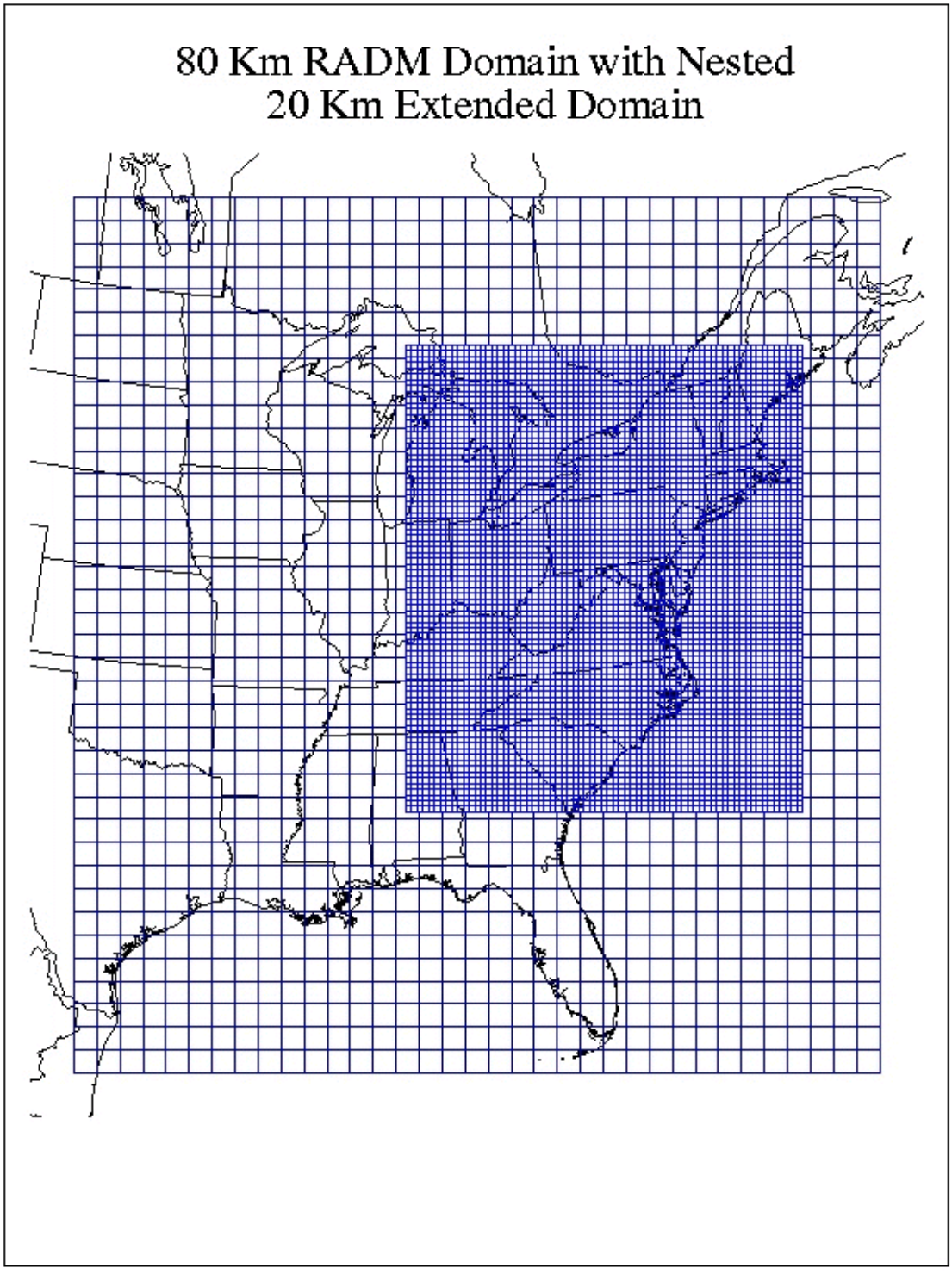

Figure V-37. Representation of the 80-km grid domain of the RADM model, with the nested 20-km grid that was created for this assessment.

emissions were changed for the emissions scenarios. Gridded, hourly emissions were regenerated from the county-level emissions inventory for each of the 30 five-day aggregation cases, using the emissions processing models. The Extended RADM was run in two steps for each of the 30 cases: first the 80-km grid domain and then the 20-km domain nested within it. The 30 cases from each grid domain were aggregated into the corresponding annual (or warm- or cold-season) average for use in the analysis of changes in air quality and deposition metrics associated with the changes in emissions.

The changes in the pollution metrics predicted by the Extended RADM air quality model relative to the 1990 Base Case are given in Table V-19. Each major pollution metric is discussed in turn.

Ozone - The percent change in O_3 concentrations of the upper two-thirds of the O_3 distribution is well illustrated by the changes in the 70th percentile. The percent change in this percentile is consistent with the NO_X emission changes and the corresponding percent changes in NO_x deposition. The projected O_3 change was about one-third of the projected NO_x deposition change, which is consistent with and typical of other regional O_3 modeling results. The growing season SUM06 O_3 exposure metric using a 60 ppb threshold is best represented in its hours-per-day stratification by the Extended RADM with an exposure calculated using a model threshold of 65 ppb O_3 (see Appendix C). The change in the O_3 growing season exposure metric (Exposure above threshold) was projected to change much more than the O_3 concentration. The much larger projected change in exposure above threshold was due to the fact that an increasing number of days/hours during the summer dropped below the threshold. The change in hours above the threshold was large: +7.8%, -27.8%, -49.1%, -58.8%, and -87.6% for 1996, Scenario 1, Scenario 2, Scenario 3, and Scenario 4, respectively. The two factors, the change in O_3 concentration and the change in hours above threshold, together explain the change in the Extended RADM representation of the SUM06 O_3 exposure metric, and that change was dominated by the change in the number of hours above the threshold. For example, in Scenario 2 the O_3 concentration change was -15.7%, the change in hours above threshold was -49.1% and the resulting change in the O_3 exposure metric was -55.5%.

Total sulfur deposition - The estimated changes in annual S deposition were smaller than the estimated changes in annual SO_2 emissions. For example, Scenario 3 had a 90% reduction in EGU SO_2 emissions, which translates into 74% and 77% reduction in total SO_2 emissions for the Top 10 States and Top 5 States, respectively (Table IV-4). The change in median annual SO_2 air

Table V-19. Percent changes in pollutants and pollutant metrics relative to the 1990 Base Case as predicted by the Extended RADM (20-km Grid) model.

Attribute	1996	Scenario 1 2007/10	Scenario 2 2020	Scenario 3 2020	Scenario 4 2020
O_3 - growing season Exposure above threshold	9.9%	-35.4%	-55.5%	-63.2%	-89.7%
O_3 - 70th Percentile	2.0%	-10.0%	-15.7%	-17.1%	-22.4%
O_3 - Hours above threshold (65 ppm)	7.8%	-27.9%	-49.1%	-58.8%	-87.6%
Total sulfur deposition (annual)	-20.2%	-33.2%	-36.7%	-68.7%	-74.9%
Total oxidized nitrogen deposition (annual)	2.7%	-35.2%	-50.3%	-59.0%	-66.8%
Ratio total ox-N/total red-N deposition[a] (where ammonia emissions are kept constant)	2.9 (2.5)	1.9 (1.6)	1.4 (1.3)	1.2 (1.0)	1.0 (0.8)
SO_4+NO_3+NH_4 fine particle air concentrations					
Annual 50th Percentile	-6.9%	-15.7%	-17.5%	-41.7%	-50.4%
Warm Season 50th Percentile	-15.0%	-28.5%	-30.8%	-55.7%	-63.6%
SO_4 fine particle air concentrations					
SO_4 annual 50th Percentile	-10.6%	-21.7%	-23.1%	-54.6%	-61.6%
SO_4 warm season 50th Percentile	-18.0%	-29.5%	-32.0%	-59.1%	-66.4%
SO_2 air concentrations					
SO_2 annual 50th Percentile	-23.2%	-44.5%	-48.8%	-77.1%	-82.6%

[a] Ratio in parenthesis is based on 1990-centered Shenandoah average oxidized and reduced nitrogen deposition estimated from NADP and UVa wet deposition, NADP and CASTNet (ox-N wet-to-dry ratio), and NADP and Extended RADM (red-N wet-to-dry ratio).

concentrations was 77%, consistent with the emissions reduction, while the resulting reduction in S deposition was 69%, about 10% smaller than the air concentration reduction. The S deposition reductions were smaller because of the expected nonlinearity in S wet deposition due to oxidant limitation. The degree of nonlinearity was consistent with estimates made during the NAPAP study.

Total oxidized nitrogen deposition - The projected changes in oxidized nitrogen deposition were somewhat larger than estimated changes in the Top 10 state NO_X emissions. The main reason for this is that the local, top 3 state estimated changes in NO_X emissions were larger than the Top 10 state emission changes and much closer to the change in oxidized nitrogen deposition. The nearby states had a strong influence on projected oxidized nitrogen deposition at SHEN. A quantitatively unimportant effect was the increase in the ratio of particulate NO_3^- partitioned to total NO_3^-. It increased because of the strong reductions in SO_4^{2-}. Particulate NO_3^- dry deposition was an order of magnitude smaller than nitric acid dry deposition; hence, the estimated total rate of oxidized nitrogen dry deposition decreased. However, this effect on the dry deposition rate was offset by the result that the total NO_3^- budget increased, thereby increasing the rate of wet deposition. There was only a small percentage point difference in the projected changes in overall oxidized nitrogen wet and dry deposition.

Inorganic fine particles - The estimated changes in SO_4^{2-} fine particles were smaller than the estimated changes in SO_2 air concentrations. For example, in Scenario 3 the median annual SO_2 air concentrations declined 77%, whereas the median annual SO_4^{2-} air concentrations declined 55%. This was the result of oxidant limitation effects in the aqueous-phase production of SO_4^{2-}. Four of the 5 top source regions affecting SO_4^{2-} air concentrations in SHEN are in the Ohio River Valley (Figure IV-9) where the nonlinearity in SO_4^{2-} production is strongest. The estimated changes in total inorganic fine particles were smaller than even the SO_4^{2-} air concentration changes. The reductions in total inorganic fine particles were influenced toward smaller reductions because of the NO_3^-. Sulfate, and the NH_4^+ associated with it, is currently the largest component of inorganic fine particulate. Major reductions in SO_2 emissions with no reduction in NH_3 emissions would be expected to leave more NH_3 in the atmosphere to bind with nitric acid and form particulate NH_3. Ammonia binds preferentially with sulfuric acid to produce SO_4^{2-}. The eastern U.S. is presently NH_3-limited, the available SO_4^{2-} is not completely neutralized by NH_3, and there is abundant nitric acid. The formation of NO_3^- is determined by "left-over" NH_3 availability. As SO_4^{2-} is reduced, the ratio of particulate NO_3^- to total NO_3^- will increase due to the increase in availability of NH_3, greatly moderating decreases in NO_3^- concentrations and mitigating or offsetting a portion of the SO_4^{2-} reductions.